APPENDIX E

FCT DOCUMENT COVER SHEET [1]

Name/Title of Deliverable/Milestone/Revision No.	Summary Update on the Feasibility of Direct Disposal of SNF in Existing DPCs (Milestone M2SF-18SN010305026)
Work Package Title and Number	SF-18SN01030502 Rev. 1 Direct Disposal of Dual Purpose Canisters – SNL
Work Package WBS Number	WBS 1.08.01.03.05
Responsible Work Package Manager	Ernest Hardin (Name/Signature)
Date Submitted	

Quality Rigor Level for Deliverable/Milestone[2]	☐ QRL-1 ☐ Nuclear Data	☐ QRL-2	☒ QRL-3	☐ QRL-4 Lab- Specific

This deliverable was prepared in accordance with Sandia National Laboratories
(Participant/National Laboratory Name)

QA program which meets the requirements of

☒ DOE Order 414.1 ☐ NQA-1-2000 ☐ Other

This Deliverable was subjected to:

☒ Technical Review	☐ Peer Review
Technical Review (TR)	**Peer Review (PR)**
Review Documentation Provided	**Review Documentation Provided**
☐ Signed TR Report or,	☐ Signed PR Report or,
☐ Signed TR Concurrence Sheet or,	☐ Signed PR Concurrence Sheet or,
☒ Signature of TR Reviewer(s) below	☐ Signature of PR Reviewer(s) below

Name and Signature of Reviewers

Edward Matteo/SNL

NOTE 1: *Appendix E should be filled out and submitted with the deliverable. Or, if the PICS:NE system permits, completely enter all applicable information in the PICS:NE Deliverable Form. The requirement is to ensure that all applicable information is entered either in the PICS:NE system or by using the FCT Document Cover Sheet.*

- *In some cases there may be a milestone where an item is being fabricated, maintenance is being performed on a facility, or a document is being issued through a formal document control process where it specifically calls out a formal review of the document. In these cases, documentation (e.g., inspection report, maintenance request, work planning package documentation or the documented review of the issued document through the document control process) of the completion of the activity, along with the Document Cover Sheet, is sufficient to demonstrate achieving the milestone.*

NOTE 2: *If QRL 1, 2, or 3 is not assigned, then the QRL 4 box must be checked, and the work is understood to be performed using laboratory specific QA requirements. This includes any deliverable developed in conformance with the respective National Laboratory / Participant, DOE or NNSA-approved QA Program.*

Summary Update on the Feasibility of Direct Disposal of SNF in Existing DPCs

Spent Fuel and Waste Disposition

Prepared for
U.S. Department of Energy
Spent Fuel and Waste Science and Technology

Sandia National Laboratories
with contributions from
Oak Ridge National Laboratory

SFWD-SFWST-2018-000511 Rev. 1
October 17, 2018

REVISION HISTORY

Document Number/Revision	Description
Title: *Summary Update on the Feasibility of Direct Disposal of SNF in Existing DPCs (Draft)* SFWD-SFWST-2018-000511 Rev. 0 Deliverable: M2SF-18SN010305026 *FY18 Summary Update on the Feasibility of Direct Disposal of SNF in Existing DPCs* Work Package: SF-18SN01030502 Rev. 1 Direct Disposal of Dual Purpose Canisters – SNL WBS: 1.08.01.03.05	Submitted to the Office of Spent Fuel and Waste Science and Technology, U.S. Department of Energy, for acceptance review. This version was put through programmatic review at Sandia, and is intended for internal use only. Tracking Number: 875810.
Title: *Summary Update on the Feasibility of Direct Disposal of SNF in Existing DPCs* SFWD-SFWST-2018-000511 Rev. 1	Final version that addresses acceptance review comments, and has been through formal R&A for Unlimited, Unclassified Release. SAND2018-11966 R

Notice: This is a technical report that does not take into account the contractual limitations under the Standard Contract for Disposal of Spent Nuclear Fuel and/or High-Level Radioactive Waste (Standard Contract) (10 CFR Part 961). Under the provisions of the Standard Contract, DOE does not consider spent nuclear fuel in canisters to be an acceptable waste form, absent a mutually agreed-to contract amendment. To the extent discussions or recommendations in this presentation conflict with the provisions of the Standard Contract, the Standard Contract provisions prevail.

Sandia National Laboratories

Sandia National Laboratories is a multi-mission laboratory managed and operated by National Technology & Engineering Solutions of Sandia LLC, a wholly owned subsidiary of Honeywell International Inc. for the U.S. Department of Energy's National Nuclear Security Administration under contract DE-NA0003525.

Approved for Unclassified, Unlimited Release

SUMMARY

This report is an update on R&D activities for: 1) injectable fillers that could be used in dual-purpose canisters to prevent postclosure criticality in a geologic repository, and 2) as-loaded DPC data gathering and criticality analysis.

The fillers R&D program, mostly experimental, is now part of a broader R&D program that includes new process modeling and performance assessment of criticality effects and the overall importance of criticality to repository performance (consequence screening). This report covers fillers R&D and as-loaded DPC data gathering, as originally planned.

Literature research and consultation with cement experts in FY18 identified several potentially effective and workable filler materials (Section 5) including aqueous cement slurries, and molten metals, alloys, and low-temperature glasses. Filler attributes were defined and the preliminary lists were compared qualitatively. Further comparative analysis should be done (e.g., cost estimates) after experimental screening has narrowed the list of alternatives. Comparisons between cementitious materials and metals/alloys/glasses will be more meaningful then. Presently much of the effort for fillers is focused on getting experimental screening tests underway.

Preliminary scoping calculations (Section 4) were done to frame the challenges with temperature control during filler emplacement, and the challenges associated with residual moisture in cementitious fillers leading to gas generation due to corrosion and radiolysis, and internal canister pressurization. This line of investigation will lead to future proof-of-concept tests for fillers involving dewatering and direct exposure to gamma and neutron radiation.

Physical models for investigation of filling behavior (void filling and compositional consistency) were substantially advanced in FY18, and mock-ups are available for filling demonstration testing in FY19. Laboratory capability for cement slurry testing was also advanced. All of these testing activities require planning, procurements, and compliance with environment, health and safety requirements extant at the laboratories.

Simulation of DPC conditions during filling has begun, using simulation approaches for computational fluid dynamics and solid-state heat transfer.

An independent expert review of DPC disposal R&D, and fillers in particular (Section 6) was supportive, although alternatives to use of fillers, particularly consequence screening, were also emphasized.

The compilation and analysis of basket configuration and “as-loaded” burnup for loaded DPCs, continued in FY18 building on work done in FY13 through FY17. The unified database of DPC information is essential to support analysis and future decisions on DPC direct disposal.

Fillers investigations are planned to continue through FY19. The planned path forward includes continued testing of cement slurry compositions that have been identified, continued development of mock-up physical models, and filling demonstration tests with surrogate materials. Screening of metals/alloys/glasses for testing will be an important step. Compilation of DPC design data and “as-loaded” fuel data will continue.

Recommendations for additional R&D include identifying additional filler materials (e.g., thermal-setting cements and low-temperature glasses), testing the pourability and self-leveling behavior of certain dry particulate materials, and minimizing costs for exploratory testing using outside contractors and university collaboration.

ACKNOWLEDGEMENTS

This report is a summary of work done by the ORNL team (A.I. Adeniyi, K. Banerjee, N.O. Cetiner, G.G. Davidson, E. Dominguez-Ontiveros, T.M. Evans, E.J. Fountain, S.P. Hamilton, E. Popov, J. Scaglione and V.K. Varma), and the SNL team (E. Basurto, P. Brady, E. Hardin, R. MacKinnon and M. Rigali). Others not mentioned have made significant contributions as well. Compilation, summarization, and production of the document were done by E. Hardin and M. Rigali of Sandia. Thanks are due to Ed Matteo of Sandia for the technical review.

CONTENTS

LIST OF FIGURES

LIST OF TABLES

ACRONYMS

2D	2-dimensional
3D	3-dimensional
AECL	Atomic Energy of Canada, Ltd.
APC	Aluminum phosphate cement
BWR	Boiling water reactor
CAC	Calcium aluminate cement
CANDU	Canadian commercial reactor designator
CPAC	Calcium phosphate aluminate cement
CPC	Calcium phosphate cement
CSAC	Calcium sulfoaluminate cement
DFC	Damage fuel canister
DOE	U.S. Department of Energy
DPC	Dual-purpose canister
FEPs	Features, events and processes
FY	Fiscal year
HA	Hydroxyapatite
IFM	Intermediate flow mixer
JSA	Job Safety Analysis
MIT	Massachusetts Institute of Technology
MKP	Magnesium potassium phosphate cement
MPC	Multi-purpose canister (vendor designation equivalent to DPC)
NRC	Nuclear Regulatory Commission
ONDRAF/NIRAS	Belgian nuclear waste management program
OPC	Ordinary Portland cement
PA	Performance assessment
PWR	Pressurized water reactor
R&D	Research & development
SFWST	Spent Fuel and Waste Science and Technology
SNF	Spent nuclear fuel
SNL	Sandia National Laboratories
TSC	Transport-storage canister
UFD	Used Fuel Disposition (R&D campaign)
UNF-ST&DARDS	Used Nuclear Fuel-Storage, Transportation & Disposal Analysis Resource and Data System
YMP	Yucca Mountain Project

SUMMARY UPDATE ON THE FEASIBILITY OF DIRECT DISPOSAL OF SNF IN EXISTING DPC'S

1. INTRODUCTION

This report is the deliverable M2SF-18SN010305026 *FY18 Summary Update on the Feasibility of Direct Disposal of SNF in Existing DPCs*. It reports on work done throughout fiscal year (FY) 2018, on work planned at the beginning of that FY, consisting of R&D activities for: 1) injectable fillers that could be used in dual-purpose canisters to prevent postclosure criticality in a geologic repository, and 2) as-loaded DPC data gathering and criticality. The work reported here was performed by Sandia National Laboratories and Oak Ridge National Laboratory. Appropriate attribution to source documents is provided in the text, tables, and figures below.

Additional R&D on direct disposal of existing DPCs was planned and funded in mid-FY, and the associated reporting is separate from this milestone. Additional discussion of that new scope and how it implements findings from an independent expert review of the fillers R&D program (Section 10) is provided in the Summary (Section 11).

1.1 Previous Studies of Fillers in Spent Fuel Canisters

Previous work on fillers for spent nuclear fuel (SNF) canisters, including dual-purpose canisters (DPCs) includes

- Swedish program (Oversby and Werme 1995)
- Massachusetts Institute of Technology (MIT) concept development (Forsberg 2000, 2002; Forsberg et al. 2001)
- Yucca Mountain Project (YMP) studies including demonstration testing (Cogar 1996a; Wallin 1996; Massari 1999)
- Atomic Energy of Canada Ltd. (AECL) demonstration (Forsberg 1997)
- Filler studies by the Belgian program (ONDRAF/NIRAS 2001)
- Filler selection analysis for the Spanish program (Puig et al. 2008a)
- DPC fillers study for the Used Fuel Disposition (UFD) R&D campaign of the U.S. Department of Energy (Jubin et al. 2014)

The work described by this report follows on these previous studies, most of which evaluated the use of granular solids (MIT, Belgium, YMP, AECL, UFD) or molten metal fillers (YMP, UFD). Use of cementitious fillers was also examined by the UFD campaign in the context of spent fuel transportation (Maheras et al. 2012).

This report addresses filler attributes (i.e., possible requirements), assumptions established for analysis, filler material alternatives, scoping analyses, testing preparations, and a long-range perspective on R&D activities leading to filler demonstration and a safety basis for implementation.

A key assumption for this work is that access to DPC internal void volume is limited to the original vent/drain ports, or new ports created in similar fashion (e.g., by drilling through the canister shell). Cutting canister lids off, or other modifications to expose the fuel assemblies, are considered out of scope. This is primarily because filling of open canisters (prior to installing lids) has already been studied and demonstrated at full scale. The AECL waste package development program demonstrated filling of fuel with silicate particles and fine sand (Forsberg 1997), while the YMP demonstrated filling of a pressurized water reactor (PWR) fuel assembly with steel shot (Cogar 1996a). Whereas these demonstrations used dry particulate fillers, emplacement of liquid fillers with similarly exposed fuel would likely present no additional problems. If the DPC lids are cut off it is likely that virtually any filler material could be emplaced. Some questions would remain, for example, emplacement of dry particulate fillers could require that the lids are cut off in a dry facility.

Fillers R&D has therefore focused on materials that can be emplaced as liquids which then solidify. Two major approaches have been identified: 1) molten metal fillers introduced at higher temperature, and 2) liquids such as resins or cement slurries that solidify at much lower temperature.

1.2 DPC Construction Details

Canister shells are generally made from stainless steel sheet (typically grade 304L) of 0.5” or 0.625” thickness, which is cold-rolled and welded to form cylinders. A base plate is welded on the bottom, and fixtures are installed for handling the canister during fabrication.

A fuel basket is fabricated and lowered into the shell, and permanently attached. The basket provides structural support, heat transfer, and criticality control for the fuel (Greene et al. 2013). There are two general types of baskets:

- Tube-and-plate type with a square, longitudinal, metal fuel tube holding each fuel assembly (Figure 1). The tubes are held in place by transverse spacer plates, which in turn are held together in assembled position by support rods that run the length of the basket. Fuel tubes are typically thin-walled stainless steel, and spacer plates may be stainless, aluminum, or plated steel (to reduce cost but prevent exposure of steel to the fuel pool). Many spacer plates are typically used (Figure 2) and they may be of different materials within the same basket, e.g., aluminum plates may be used as thermal shunts, and steel plates for strength.
- Egg-crate type baskets use longitudinal plates in a rectilinear array, forming square cells to receive fuel assemblies (Figures 1 and 3). The longitudinal plates may be stainless or aluminum-B_4C composite such as Metamic® (Figure 4). The egg-crate baskets are rigid and self-supporting once the plates are attached together to form a grid.

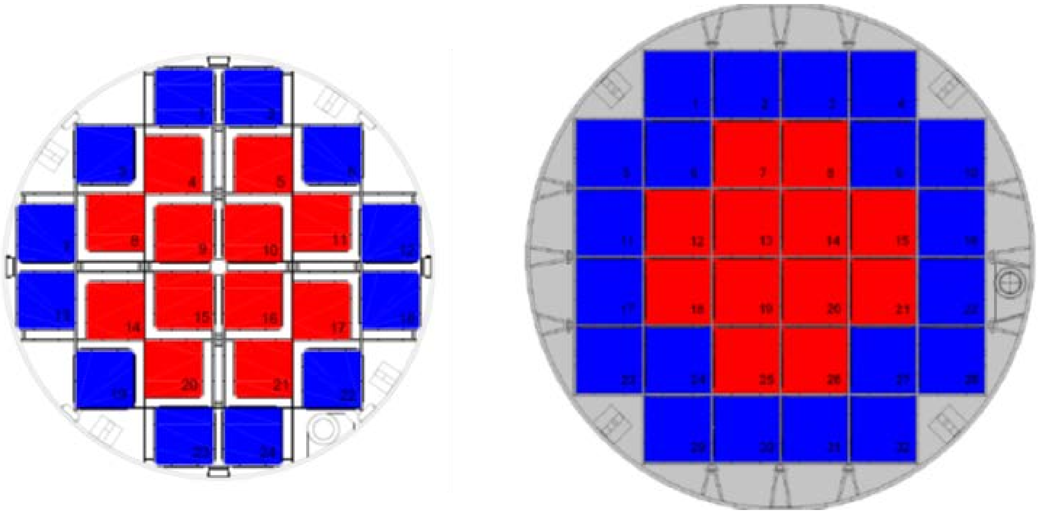

Figure 1. Basket arrangements for a fuel tube design (MPC-24, left) and an egg-crate design (MPC-32, right) (from Greene et al. 2013).

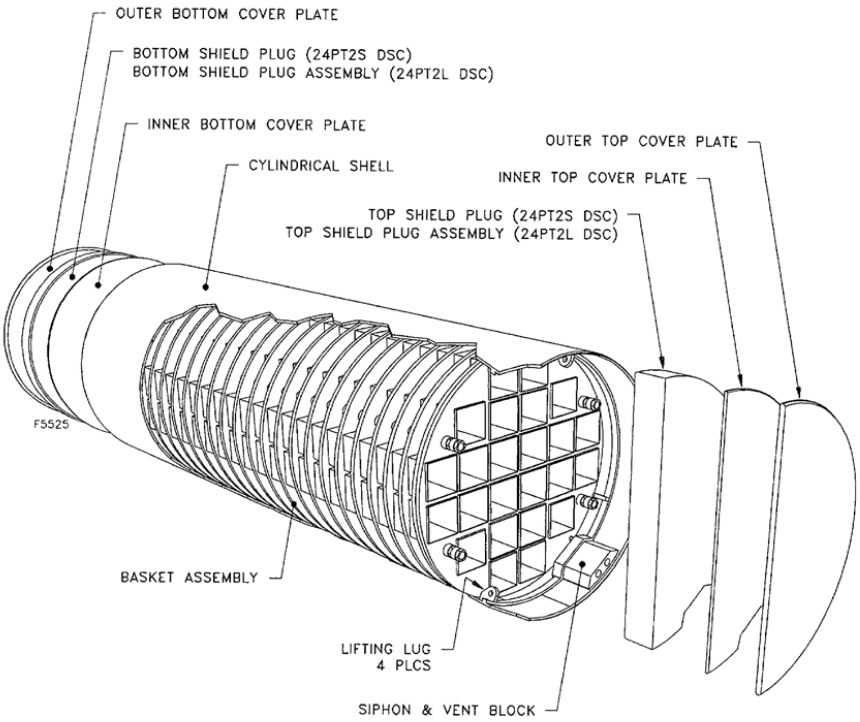

Figure 2. Cutaway of NUHOMS® 24-PT2 basket, shell, and lids (from Greene et al. 2013).

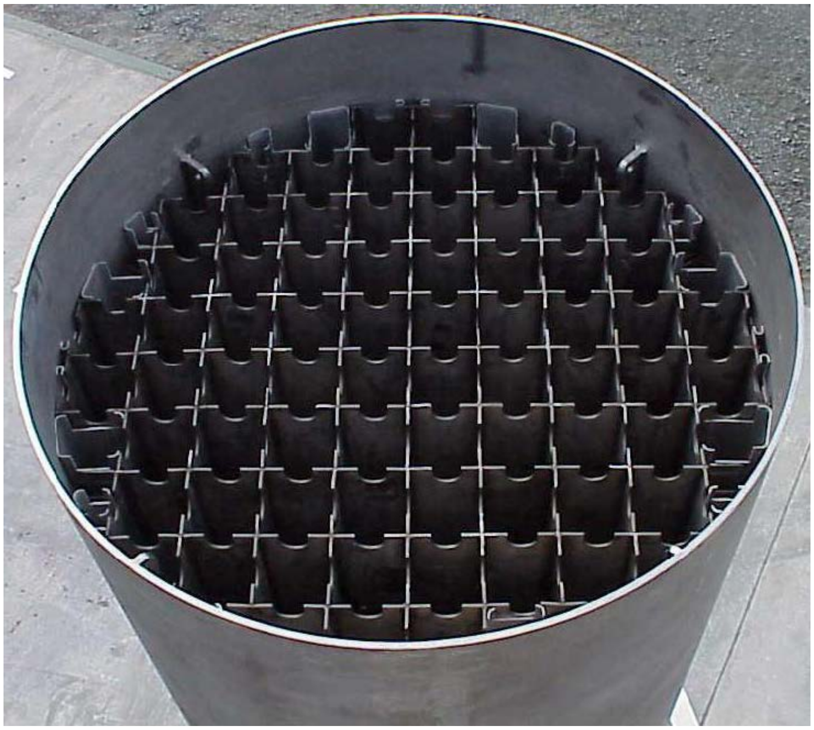

Figure 3. Top view of MPC-68 shell and basket (from Greene et al. 2013).

Figure 4. Metamic HT® basket for MPC-89 canister (from Greene et al. 2013).

Neutron absorbing material is typically added (or flux trap geometry maintained) between each pair of adjacent fuel assemblies. Recent DPC designs rely more on neutron absorbing plates and less on flux traps, which gives a more compact basket that increases the fuel capacity. The neutron absorbing material is generally ceramic B_4C in particle form, which is hot-rolled with aluminum to form sheet that can be cut and formed (e.g., Boral®). Sheets of aluminum-based neutron absorbing material are typically attached to the walls of the basket cells by thin cover sheets of stainless steel that are tack-welded in place. The welds in this case are intermittent and do not seal the aluminum from moisture if it exists in the canister environment. The Metamic HT® basket (Figure 4) is a departure from this type in which the egg-crate structure is fabricated almost entirely from aluminum-B_4C composite.

The empty, open canister is placed into a shielded transfer cask, open at the top, which is then submerged in the fuel pool. Fuel assemblies are loaded one at a time. The shield plug is then placed on the top, and the transfer cask with DPC is hoisted from the pool. The shield plug is welded, and the canister is dewatered. This is accomplished using a drain tube (runs to the bottom of the fuel cavity) and a top vent. Bulk water is removed by suction or applied gas pressure, and final dewatering is performed by circulating dry inert gas as the canister heats up from fuel heating. Every basket design has features that allow water to drain from the fuel toward the drain tube. These take the form of limber holes (Figure 2) or standoffs between the basket and the base plate. Similar provisions are made to allow gas and water vapor movement during final dewatering. After dewatering, the drain and vent ports are covered and welded. During all of these operations radiation protection is provided by the transfer cask and the shield plug.

The remaining steps in DPC deployment for fuel storage and transportation are discussed in other sources (Greene et al. 2013; Raddatz & Waters 1996; EPRI 2009).

2. FILLER PERFORMANCE CRITERIA

Desirable attributes for filler materials and the methods used for emplacement are developed here (Table 1) starting from a previous study (Maheras et al. 2012). These attributes are not inflexible requirements because tradeoffs are possible, so they may be prioritized or adjusted for specific fillers. For example, the capacity to incorporate neutron absorbers may be needed only for materials that contain significant fractions of hydrogen or other neutron moderating elements.

Table 1. Desired attributes for filler materials (adapted from Maheras et al. 2012)

Criticality Avoidance	• Provide moderator displacement • Neutron absorption capability if needed • Minimize neutron moderation • Provide isotopic dilution of fissile radionuclides • Capacity to fill greater than 60% of the canister free volume (e.g., complete filling with less than 40% porosity) • Fill material does not compact by more than 10% of its initial volume
Heat Transfer Properties	• Promote heat transfer from the fuel during handling and after disposal
Stability Properties	• Thermal stability and expansivity • Chemical stability (e.g., low solubility, low reactivity) • Radiation stability • Chemically compatible with cladding, fuel, neutron absorbers, fuel baskets, and other materials within canister • Limited gas generation (radiolytic, or on contact with ground water)
Homogeneity and Rheological Properties	• Homogeneous and consistent batches • Good rheological properties (e.g., setting time, viscosity) to ensure proper filling • Wetting behavior for fuel and canister materials
Remediation	• Allows for safe recovery of fuel from a canister (e.g., after unsuccessful filling)
Material Availability and Cost	• Low to moderate cost • Material available in required purity
Weight and Radiation Shielding	• Fill material doesn't add excessively to canister weight • Good radiation shielding properties
Operational Considerations	• Easy to emplace • Able to place in the canister without damaging fuel or canister (flow characteristics and pressure) • Fill material does not adversely react to canister handling and emplacement in the repository

The attributes in Table 1 are compared to other previous studies (Oversby and Werme 1995; Puig et al. 2008a) in the following paragraphs.

An early study for the Swedish disposal R&D program (Oversby and Werme 1995; summarized by Jubin et al. 2014) suggested a three-tiered approach to filler attributes: 1) those that ensure void filling and long-term stability, 2) other desirable properties, and 3) undesirable properties. The fill material should be placed in the canister in a way that does not damage the fuel, and results in a residual void volume of less than 40% of the original void volume (i.e., with small-scale intergranular porosity). Virtually the entire DPC volume should be filled, with less than 10% volume compaction after emplacement, since a relatively small region can achieve criticality when flooded with water (with degraded components). These void volume (<40% as emplaced) and compaction (<10% of initial volume) limits were derived from criticality simulations of packages containing 12 fresh (unirradiated) boiling-water reactor (BWR) fuel assemblies, attributed to Risenmark (1993). As pointed out by Puig et al. (2008a) initial fuel enrichment is higher at present than the 3.6% used in these original calculations.

The Swedish effort further proposed that filler material should have solubility less than 100 mg/L at 50°C in pure water and in the water of the anticipated repository environment (Jubin et al. 2014). Desirable properties were also identified (in no special order):

- Chemical compatibility with the disposal system
- Homogeneous properties and consistency between batches
- Well-understood long-term durability
- Favorable rheological properties for emplacement in the canister
- The material contains a neutron-absorbing material or has the capacity to incorporate one
- Potential to attenuate radionuclides released from spent fuel
- Potential to suppress the generation of hydrogen
- Reasonable cost (in the context of system cost)
- Low density to limit total canister weight

And undesirable properties were identified, including

- Limited availability
- Potential to enhance corrosion of the canister, fuel cladding, or the fuel itself
- Generates gas when altered (as by radiolysis) or reacted with water or other substances
- Contains water
- Affinity for absorbing air (which could interfere with liquid flow completely filling a canister)

Puig et al. (2008a) reviewed filler material choices for spent fuel waste packages, identifying five categories of selection criteria: 1) criticality avoidance, 2) general desirable properties, 3) general undesirable properties, 4) performance improvement features, and 5) attributes not directly related to repository performance but potentially important. The fillers discussion reiterated the 40% maximum void space and the 10% maximum compaction criteria which was based on a calculation that criticality could result from a 40-cm high unfilled region (attributed to Agrenius 1993). They identified a fuel cladding temperature limit of 350°C.

Thermal, radiation, and chemical stability criteria were similar to those listed above (Table 1). Criteria for disassembly and fuel retrieval (from a filled canister) were included. The presence of air in the filler was associated with formation of nitric acid by radiolysis, possibly contributing to stress corrosion cracking. The Spanish waste program is considering the use of clay-based buffers, so compatibility with buffer function (low hydraulic conductivity, diffusion resistance) was also identified as a filler attribute. Sorption capacity of fillers for released radionuclides, mechanical strength to maintain configuration, chemical durability (especially natural analogs), control of hydrogen generation, radiation shielding, low weight, and low cost were also identified.

Finally, filler studies for the Yucca Mountain Project (Cogar 1996a; Wallin 1996; and Massari 1999) considered a range of materials but focused on solid particulates (steel shot, glass or ceramic beads possibly containing depleted uranium) that could be loaded before final closure of the canister. This included a full-scale, single-assembly demonstration of loading steel shot. Requirements identified at that time included the capability "...of unloading a damaged waste package after the occurrence of a design basis event" (Massari et al. 1999). DPC direct disposal at Yucca Mountain (with and without fillers) has been considered (BSC 2003; Kessler et al. 2008) and important aspects of engineering feasibility including postclosure criticality control have been identified (Hardin et al. 2015).

Filler criteria are discussed below (Section 5) in the context of selection materials for testing.

3. ASSUMPTIONS

Assumptions of various types were documented previously for investigation of feasibility of direct disposal of DPCs (Hardin and Howard 2013). This section updates that list for the purpose of identifying any constraints on, or conflicts with, potential filler strategies.

3.1 Assumptions from Previous Direct Disposal Analysis

3.1.1 DPC Characteristics

a) DPCs contain commercial UNF. Average burnup for existing SNF in dry storage is nominally 40 GW-d/MT, with a reasonable-bound value of 60 GW-d/MT for future DPCs.

Discussion: These values (from Carter et al. 2012) provide representative and bounding values (5% enrichment and 60 GW-d/MTU burnup) for criticality, thermal, and radiolysis studies with fillers. Filler emplacement may not be sensitive to burnup, but these studies will depend on burnup and cooling time.

b) The capacity of DPCs is typically 32 PWR assemblies or 68 BWR assemblies. Larger DPCs are available (Greene et al. 2013) from NAC International (Magnastor® 37/87 system, nominally 37-PWR or 87-BWR), Holtec International (MPC-37/89, nominally 37-PWR or 89-BWR), and Transnuclear (NUHOMS® 37 series).

Discussion: The 37-PWR (89-BWR) is current, and along with the 32-PWR size, represents the type of DPCs for which fillers could be most beneficial.

c) Storage-only canisters can be included in the evaluations.

Discussion: Storage-only canister based systems include the MSB (24-PWR, Energy Solutions) and the NUHOMS® 24PS, -24PL, -24PHBS, -24PHBL, -52B and -07P (Transnuclear). These canisters currently exist at the Idaho National Laboratory, and at the Calvert Cliffs, Surry, Oconee, Arkansas Nuclear One, Palisades, Davis-Besse, Point Beach, Susquehanna, and H.B. Robinson nuclear power plants. These are sealed canisters, separate from non-canistered cask systems with bolted closures.

3.1.2 Potential DPC Modifications

d) Liquid fillers can be introduced through the existing drain tube, or new vents, ports, or drain tubes can be installed.

Discussion: This assumption is intended to remove uncertainty in filler selection, as to whether there would be adequate rate of filler flow through the existing drain tubes. The assumption may be unnecessary, because a liquid suitable for penetrating DPC void spaces (low viscosity, self-leveling, delayed setting time) might not produce much restriction in the filling tube.

3.1.3 Disposal Concepts

e) Surface decay storage of DPCs and storage-only canisters for up to 100 years (out-of-reactor) can be assumed in disposal feasibility evaluations. Further, heat generation is assumed to be that typical for 50-year old fuel.

Discussion: Typical SNF with age of 50 to 100 years out-of-reactor can be assumed for thermal analysis of filled canisters.

f) Underground handling and transport of DPCs will be shielded.

Discussion: Shielded transporters and handling equipment are available so that fillers will not be relied upon entirely for worker shielding.

3.1.4 Criticality Analysis

g) Analysis of postclosure criticality will include full burnup credit (i.e., actinides and fission products) and assembly-specific or cask-specific characteristics.

Discussion: Past studies have identified situations where burnup credit and detailed modeling (principal isotopes, BSC 2003; more complete isotopics, EPRI 2008) is needed in DPC disposal analysis. Burnup credit analysis may allow some DPCs to be disposed of directly without fillers for criticality control.

h) Consequence analysis may also be used to include or exclude postclosure criticality.

Discussion: Postclosure criticality consequence analysis has been described previously (DOE 2003, Section 3.7) and the impact on radionuclide inventory (part of a repository source term) was found to be negligible (Rechard et al. 1996). The consequences of one or more criticality events in a repository could be insignificant if criticality is an unlikely event. Use of consequence analysis may be further limited if regulatory guidance pertains, such as that at 60.131(h): "…criticality is not possible unless at least two unlikely, independent, and concurrent or sequential changes have occurred…" Hence, fillers should be designed such that postclosure criticality is very unlikely or at least unlikely in the regulatory sense.

3.1.5 Surface Facilities

i) DPCs will be sealed at the power plants or at a centralized storage facility and fuel will not be removed at the repository. However, opening and subsequent re-sealing of de-watering ports is permissible.

Discussion: Opening and re-sealing of dewatering ports, in order to pump in filler material, is the primary approach. Drilling new ports or augmenting existing ones may also be considered.

j) DPC inspection to verify filler emplacement can be done remotely in a hot cell, and detected non-conformances can be corrected or mitigated.

Discussion: The ease of inspection and mitigation of defects should be a factor in filler selection.

3.2 DPCs Targeted for Filler R&D

The objective for DPC fillers is to provide criticality control by means of moderator displacement, with the possibility of added neutron absorption, over repository performance time frames. Criticality analysis of degraded DPCs flooded with groundwater has been performed for more than 600 as-loaded DPCs (Section 9). Two simplified configurations were used to assess DPC reactivity after flooding in a repository:

- Complete loss of neutron absorbing components (and replacement by water in the model) due to unspecified chemical degradation and transport processes, and flooding with fresh water. Aluminum-based neutron absorbing materials are expected to corrode on exposure to groundwater, and not to perform their function over any postclosure timeframe.

- Complete loss of the internal basket structure (including neutron absorbers) with elimination of assembly-to-assembly spacing, but retaining edge-to-edge arrangement of fuel assemblies, and flooding with fresh water.

Both configurations were analyzed for most DPCs, however, only the second configuration was used for DPCs with plated carbon steel structural components. DPCs were analyzed using as-loaded SNF inventory, including both PWR and BWR fuel types, and several basket design variants. The criterion for subcriticality ($k_{eff} < 0.98$) was applied up to 13,000 years from loading. The results show that some of the existing PWR DPCs, and most of the existing BWR DPCs would remain subcritical when flooded with fresh water. The reader is referred to previous publications for details of these analyses, which include responses for flooding with both fresh and saline groundwater compositions (Liljenfeldt et al. 2016; Hardin et al. 2015).

PWR DPCs can be divided into two broad categories, those with flux traps and those without. A majority of the PWR DPCs analyzed with flux trap designs would remain subcritical, while those without flux traps would not. Analysis of more recent PWR DPC designs with egg-crate baskets constructed mostly from aluminum-based neutron absorbing materials, is ongoing. In summary, filler implementation for postclosure criticality control would be targeted to PWR DPCs without flux traps, including modern designs with egg-crate baskets made from aluminum-based structural materials.

3.3 Spent Fuel Condition at Disposal

Fuel cladding integrity may be important for filler radiolysis calculations since the higher energy and shorter range of alpha emanation (compared with gamma) ensures more radiolytic activity per disintegration.

A previous cladding integrity analysis (BSC 2005) concluded that less than 2% of the fuel, including all of the stainless-steel clad fuel, received at a repository would be failed (perforated). All failed fuel was assumed to axially split after waste package breach in an oxidative environment.

A recent industry survey (EIA 2012) describes spent fuel status through June, 2013. Approximately 2% of the ~245,000 discharged assemblies were reported as failed, with known damaged fuel packaged in damage fuel containers (DFCs). The extent of damage for much of this fuel (especially that which is not packaged in DFCs) is not explicitly known. DFCs typically use very fine mesh screen at the top and bottom, which may prevent filler penetration of the void spaces within. Additional investigation could be needed to ensure proper filling of the DPCs that contain failed assemblies in DFCs.

4. SCOPING ANALYSIS OF CANISTER ENVIRONMENT FOR FILLER PERFORMANCE

Filler material loaded into DPCs will immediately encounter gamma and neutron radiation, and elevated temperature. For cement slurry fillers, DPCs would subsequently heat up (assuming filler is at ambient temperature or cooled, before loading) and pressure would build up from thermal expansion of the filler, evaporation of moisture, and any cement expansion on cure. Pressure would be relieved at the vent, and the rate of venting would depend on the permeable flow characteristics of the filler. For scoping discussions the fuel temperature limit is assumed to be 150°C, which would require some thermal aging of DPCs, although higher limits may be possible.

For molten-metal fillers the DPCs would be pre-heated externally to above the filler melting temperature. This temperature would be approximately 200°C, or higher if needed to ensure filler flow properties and complete filling. Such a temperature is within the temperature limits for the canister and the fuel (NRC 2003). Note that if the entire canister is heated, the fuel temperature will increase further from decay heating. However, calculations show that the temperature differential between fuel and canister wall (when the fuel is the only source of heating) is less than 100 C° (Section 4.2).

4.1 Bounding Transient Temperature Response During Cement Curing

To investigate short-term temperature rise for cement fillers that could be sensitive to temperature during cure, a numerical case was implemented in FLAC (Itasca 2011). The model is a 2D cross-section through a fuel rod and surrounding cement, with adiabatic boundaries. Thermal properties were extracted from literature (UO_2, Zircaloy properties from IAEA 2008) or assumed in the case of cement (conductivity 1.5 W/m-K, specific heat 1,300 J/kg-K, density 1.97×10^3 kg/m^3). Heat generation was assigned to fuel rods such that a 21-PWR waste package with 17×17 assemblies would have total output of 10 kW. Heat of reaction in the cement was set to 10 kW/m^3 for the duration of the simulation. Initial temperature of the fuel was 150ºC, while the cement was introduced at 25°C. These inputs can be modified (for example, the heat output of a DPC at disposal could be as high as 18 kW) for comparison to other analyses.

The simulation shows that temperature rise is not limited by conductivity (short distances are involved), and that temperature in the cement rises by about 0.0013 K/sec (Figures 5 through 7). Thus, a 25 C° temperature rise would occur in about 5 hours, dominated by heat capacity.

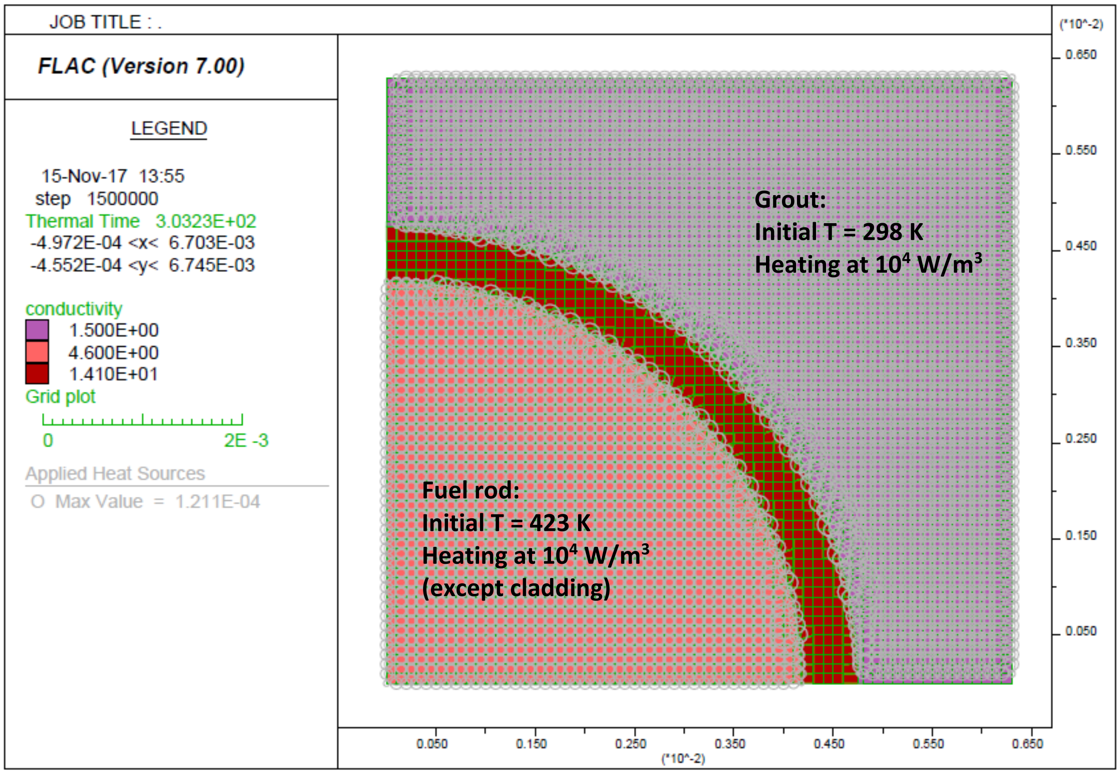

Figure 5. Fuel rod-scale adiabatic model for short-term temperature history (from SNL 2017).

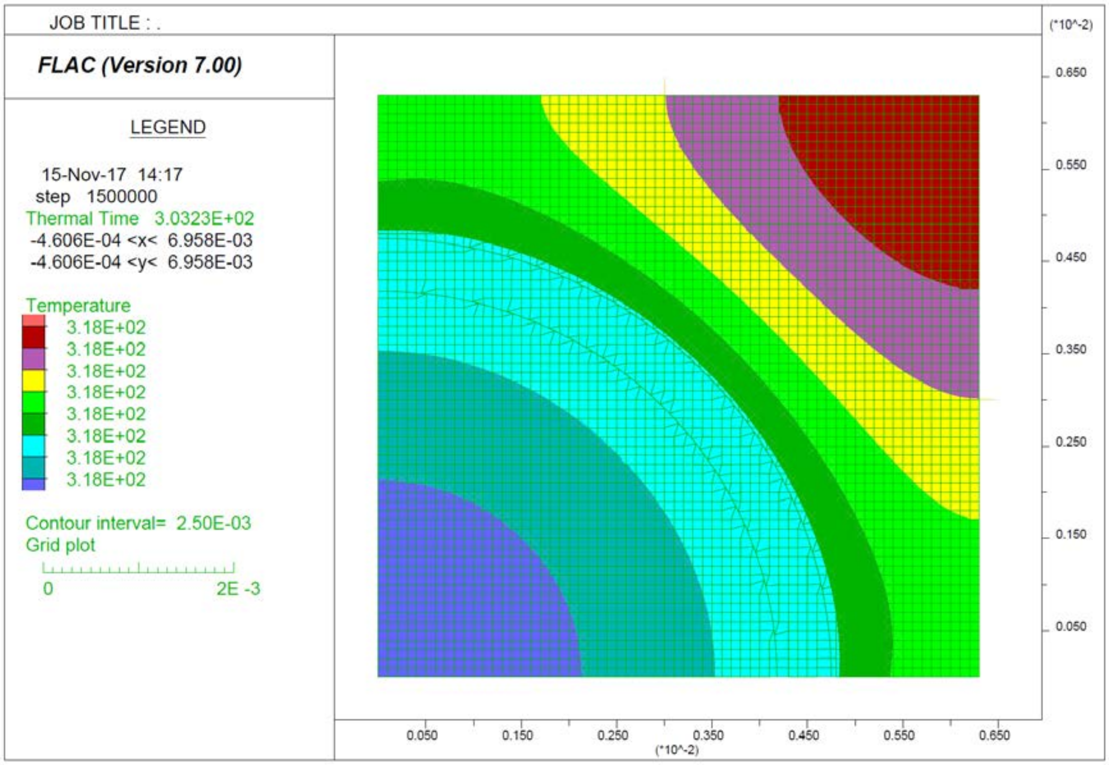

Figure 6. Rod-scale temperature showing equilibration at 300 seconds (from SNL 2017).

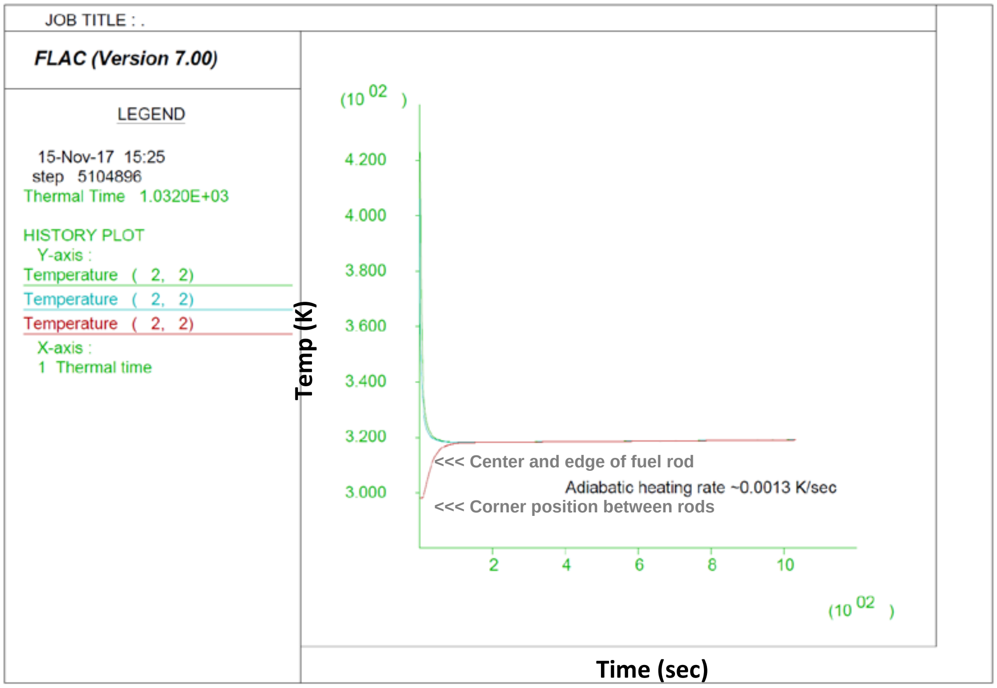

Figure 7. Temperature histories for outer edge of cladding, and corner position between rods (from SNL 2017).

To investigate longer-term temperature rise, and the effect of varying thermal conductivity, additional simulations are needed for an entire canister.

4.2 Canister-Scale Steady-State Temperature Analysis with Helium and Solid Fillers

The following material is excerpted from: *Thermal Analysis of DPC Fillers – Phase I*, by Kevin Robb of Oak Ridge National Laboratory (deliverable M4SF-18OR010305016, issued as report ORNL/SPR-2018/799). Minor edits have been included for clarity, and some discussion of work in progress has been omitted. The reader is referred to the source document for more detail.

The current effort is a phase I analysis of the thermal considerations of adding filling material to a DPC (SNL 2017). Several filler materials are under investigation, ranging from cements to metals. These filler materials, in substitution of the standard helium backfill, will impact the temperature of the internal structures and SNF assemblies.

A DPC sized to contain 32 PWR SNF assemblies was considered in the current analysis. The COBRA-SFS (Coolant Boiling in Rod Arrays-Spent Fuel Storage) code was used to model the DPC and perform the thermal analysis. Different filler materials were simulated by varying the thermal conductivity of the typical void space within the DPC. The impact of the filler material on the peak temperatures in the DPC and temperature gradients was assessed. The following sections describe the simulation setup, results, and potential areas for future phases of thermal analysis.

COBRA-SFS Overview

COBRA-SFS is a computer program that performs thermal-hydraulic analyses of multi-assembly SNF storage and transportation systems (Michener et al. 2015). It uses a lumped-parameter, finite difference approach to predict flow and temperature distributions in SNF storage systems and fuel assemblies under forced and natural convection heat transfer conditions, both steady state and transient. COBRA-SFS is developed for single-phase analysis problems that may include 2D radiative and 3D conductive heat transfer. It has been used to analyze various single- and multi-assembly SNF storage systems containing unconsolidated and consolidated fuel with a variety of fill media.

Model Geometry and Material Properties

The DPC chosen for analysis accommodates 32 PWR assemblies in an egg-crate-type basket. Heat transfer across the assemblies, gas/filler space, and other DPC structures is modeled. Axially, the DPC is divided into three regions: basket, upper plenum, and lower plenum:

- **Basket region** – This region spans from the bottom to the top of the SNF assemblies. It includes the 32 SNF assemblies, basket structure, gas/filler spaces, and the canister and overpack walls. The basket region is modeled in detail with each fuel pin and every subchannel (i.e., open space between fuel pins) represented. Each basket location contains a 17×17 SNF assembly and each assembly contains 25 non-fueled rods (guide tubes). In total, there are 9,248 rods and 10,368 subchannels modeled within the basket. The basket structure is modeled with 441 solid-conduction nodes, termed “slabs” in COBRA-SFS. Lateral discretization of the basket structure is illustrated in Figure 8. Each assembly location contains neutron absorbers on 0, 1, or 2 sides. Around the periphery of the basket there are open spaces (indicated by white in Figure 8) filled with gas or filler material. The DPC and overpack walls are discretized into five concentric cylindrical rings using a total of 112 slabs to represent an inner 50.8 mm stainless steel wall and an outer 101.6 mm outer carbon steel wall. Axially, the basket region is 4.53 m tall and is uniformly discretized into 44 axial levels. Heat is transferred axially and laterally within the basket region. If the DPC is filled with gas, thermal radiation is evaluated between fuel pins, from fuel pins to basket walls, and from basket walls to the DPC walls. The overpack outer surface is 2.02 m in diameter and has surface area of 28.7 m^2.

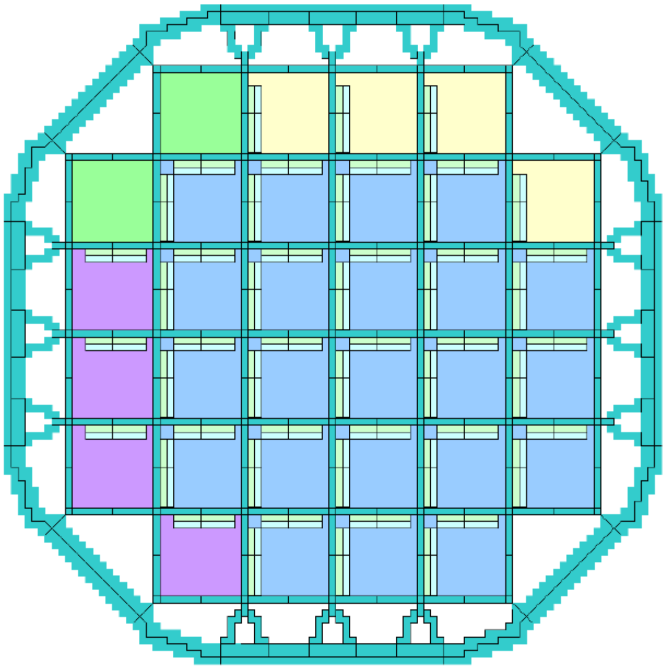

Figure 8. Basket mesh for COBRA-SFS modeling of the DPC canister (not to scale, node thicknesses exaggerated to show detail; from Robb 2018).

- **Top and bottom plenum regions –** These regions are modeled as 1D arrays of materials of various thickness. COBRA-SFS calculates the heat conduction through the layers of materials to the outer surface. The top plenum includes the gas space above the basket, then an inner lid of stainless steel, a gas gap (air), and the structural lid of carbon steel. The bottom plenum includes the gas gap below the basket and extends through the inner and outer walls discussed above. The outer surfaces of the upper and lower plenums are modeled to have a surface area of 3.2 m^2.

Thermal conductivity of the various DPC materials is summarized in Table 2, and helium properties are provided in Table 3 for use with the cases in which DPCs are backfilled only with helium.

Table 2. Thermal conductivity for DPC materials (from Robb 2018).

Material	Thermal conductivity (W/m-K)
304 SS	19.6
1100 Al	213.0
A36 CS	40.0
XM-19 SS	16.1
Neutron absorber	76.8

Table 3. Helium properties (from Robb 2018).

Temp. (°C)	Enthalpy (kJ/kg)	Thermal conductivity (W/m-K)	Specific heat (kJ/kg °C)	Specific volume (m^3/kg)	Viscosity (Pa-sec)
−17.8	43.0	0.135	5.19	0.739	1.69E-05
93.3	149.6	0.168	5.19	1.060	2.20E-05
204.4	256.2	0.199	5.19	1.382	2.65E-05
315.6	362.9	0.223	5.19	1.704	3.01E-05
426.7	469.5	0.239	5.19	2.025	3.40E-05

Thermal Boundary Conditions and Sources

For the Phase I thermal analysis, the DPC has been modeled independently from the details of emplacement, by applying a specified temperature to the external surfaces of the outer layer of the overpack wall. Conditions in the near field and far field of a geologic repository control in-package temperature, but are beyond the scope of this analysis.

The external surface of the overpack was set to 100°C with no insolation. With temperature-independent properties and constant decay heat, the temperature rise between the external surface and the hottest fuel remained constant and independent of the boundary temperature. This result can be used with any value of the external surface temperature to estimate the peak cladding temperature.

The total decay heat of the package was assumed to be 1.7, 3.4, 6.8, or 10.0 kW. The area-averaged heat rejection rate at the package external walls was respectively 48.5, 96.9, 193.9, or 285 W/m^2. These values could be used to determine the package surface temperature for a particular emplacement arrangement and near-field/far-field conditions.

Each of the 32 assemblies was modeled to have the same total decay heat, and the same axial heat generation profile (peaking factor 1.11, see Robb 2018).

Modeling Fillers

To simulate the filler material, thermal conductivity of the void space (occupied by helium) within the DPC were altered. For steady-state analyses, this is the only material property that affects analysis results. Future thermal analyses that simulate the transient filling and solidification of the filler material will also need to model the density, specific heat, and enthalpy changes.

For this analysis a range of temperature-independent filler thermal conductivity values was considered. Helium has thermal conductivity on the order of 0.17 W/m-K. Cements have thermal conductivity on the order of 0.7 to 1.4 W/m-K. Metallic fillers have thermal conductivity on the order of 40 to 100 W/m-K. Recirculation of filler material and heat transfer by thermal radiation were prohibited. Filler material was assumed to fully fill the DPC void space including within assemblies (i.e., subchannels). Future analysis may take into account the possibility of small gaps between the filler and structures/assemblies due to differential thermal expansion or incomplete filling.

Steady-State Thermal Analysis Results

Two cases, vertical and horizontal, were simulated with helium as backfill gas and including thermal radiation. For the vertical case, internal recirculation of the helium occurred. With 3.4 kW of decay heat, the peak cladding temperature was 128.9°C. This equates to a rise of 28.9°C between the package wall and the hottest location inside the DPC. For the horizontal case, internal recirculation of the helium was inhibited. With 3.4 kW of decay heat, the peak cladding temperature was 160.2°C, which equates to a rise of 60.2°C.

Peak cladding temperature results for various decay heat levels and filler thermal conductivity values are presented in Table 4. As expected, replacing the helium with a higher thermal conductivity filler decreases temperatures within the basket. As the decay heat is readily conducted out of the basket for high-conductivity fillers, non-uniform loading of decay heat in a DPC would have a minor effect on peak internal temperatures.

Table 4. DPC peak cladding temperature (package surface held at 100°C; from Robb 2018).

Filler Thermal Conductivity (W/m-K)	**Total Package Decay Heat (kW)**			
	1.7	**3.4**	**6.8**	**10.0**
0.168	138.2	159.5	236.8	na
0.8	119.0	137.6	174.1	208.9
1.4	na	124.6	na	na
10	102.6	105.2	110.5	115.4
50	na	102.1	na	na
100	100.9	101.7	103.5	na
na = not analyzed				

The rise in temperature between the package wall and the hottest cladding (i.e., highest temperature within the DPC) is summarized in Table 4. Compared to helium, a filler with a thermal conductivity representative of cements decreases the peak internal temperature by approximately half. For metallic fillers, the peak temperature within the DPC is only a couple degrees hotter than that of the DPC external surface. The sensitivity of the temperature difference to the total package decay heat decreases with increasing filler thermal conductivity.

The axial temperature profile along a central basket structure is illustrated in Figure 9. With increasing filler thermal conductivity, the axial temperature gradient decreases as well as the radial gradient.

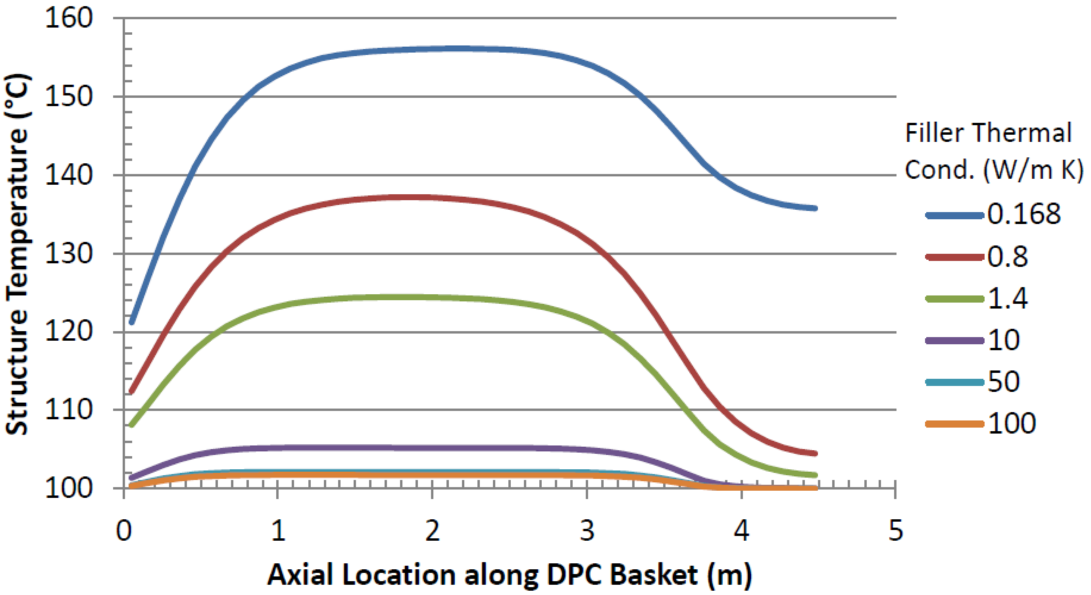

Figure 9. Temperature profile along basket centerline with 3.4 kW package decay heat (from Robb 2018).

4.3 Canister Pressure Limit

Previous waste package design work used nuclear containment boundary requirements for pressure vessels (DOE 2008; ASME BPVC Section III - *Rules for Construction of Nuclear Facility Components, Division 1- Metallic Components, Subsection NB Class 1 Components*). Components designed to these specifications can serve as part of the fluid-retaining pressure boundary of a reactor coolant system. It is typically used for reactor pressure vessels and piping, generally with a safety factor of 1.5 to yield, and 3.5 to ultimate tensile strength. Of course, this approach is scoping only because it does not take into account the stress condition at the canister ends, particularly at the end welds.

Using best-available public information on DPC construction (Greene et al. 2013) shell thicknesses and diameters (overall) for typical DPCs are given in Table 5.

Table 5. Shell thicknesses and diameters for typical canisters (from SNL 2017).

Vendor	Canister Type	Shell Thickness (in)	Overall Diameter (in)
Holtec	MPC-24/ MPC-32/MPC-68	0.5	68.5
	MPC-37/MPC-89	0.5	75.5
NAC	MPC (CY style)	0.625	70.64
	UMS® TSCs	0.625	67.1
	Magnastor®	0.5	71
Transnuclear	NUHOMS® 24-PWR versions	0.625	67.19
	24-PTH, 32-PWR and 37-PWR versions	0.5	67.19
	32-PTH versions	0.63	69.75
FuelSolutions	VSC 24 PWR	1.0	62.5
	W74 64-BWR	0.625	66

The ratio of diameter to 2× wall thickness describes the effect of internal pressure on hoop stresses, and this ratio is approximately 70 for DPCs. With yield stress of 215 MPa (www.asm.matweb.com) and a safety factor of 1.5 to yield, the maximum internal pressure would be 2 MPa. Ultimate tensile strength (test specimens) is reported at 505 MPa, so there is margin for additional loading. Further, the maximum elongation at rupture is 70%, which would not be achieved in a waste package setting, but would ensure that a DPC shell in yield would readily expand against the disposal overpack imparting additional strength, possibly without canister breach. Note that this discussion does not account for residual stress (DPC shells are cold-rolled and welded without stress relief), nor does it account for end effects particularly shears and moments produced at the top and bottom welds, or metallurgical damage to the DPC during storage. However, it does show that SS304 (nearly universal in DPC shell construction) can maintain containment integrity inside a more robust overpack, in response to internal pressure on the order of 1 MPa or greater. This pressure is much less than the H_2 pressure needed for hydrogen to react with iron (Grundfelt and Crawford 2014) and by extension, with other species present as well.

DPCs are designed and analyzed to withstand stresses due to pressurization with He following loading. Design pressures vary with canister type. However, larger canisters with higher heat output have higher pressures to improve internal heat transfer. Maximum canister pressure is calculated based on stresses incurred during off-normal and accident conditions. Using best-available public information on DPC construction, typical design and maximum canister pressures are shown in Table 6.

Table 6. Internal pressure values used in licensing of some DPCs (from SNL 2017).

Vendor	Canister Type	SNF capacity	Design Pressure (psig)	Max. Pressure (psig)
BNFL	W74	64-BWR	10	30
	VSC	24-PWR	0	1.5
Holtec	HI-STORM 100®	24-PWR/32-PWR/68-BWR	100	200
	HI-STAR 100®	24-PWR/32-PWR/68-BWR/80-BWR	100	125
NAC	MPC	26-36	0	18
	UMS	24-PWR/56-BWR	0	15
	MAGNASTOR®	37-PWR/87-BWR	110	250

4.4 Gas Generation from Radiolysis and Alpha Production

The radiation dose to filler materials can be estimated for scoping purposes, using the 400 Gy/hr gamma dose rate calculated for PWR fuel assemblies with 45 GW-day/MTU burnup and 20-year age out-of-reactor (R. Cumberland/ORNL, verbal communication). Assuming this gamma flux originates entirely from fission products with 30-yr half-life, the total dose can be estimated by integrating the exponential decay equation

$$\frac{\partial N}{\partial t} = -\lambda N_0 e^{-\lambda t}$$

over many half-lives. The result calculated for fillers installed in DPCs containing fuel with 50-year age, shows that the total dose to filler materials is on the order of 50 MGy. This precludes the use of many organic polymers as shown in the summary table from Nordion (Table 7).

Table 7. Gamma radiation dose tolerance for organic polymers.

Polymer	Tolerance (kGy)	Comments
Thermoplastics		
Aromatic Polyamide (Nylons)/Polyimide	10,000	High heat/strength grade.
Polyimides	10,000	
Polystyrene	10,000	All styrenes are stabilized by benzene ring structure.
Polysulfone	10,000	Amber color before irradiation.
Polyurethane	10,000	Excellent clarity and chemical resistance to stress-cracking. Drying is essential.
Thermosets		
Allyl Diglycol Carbonate (Polyester)	5,000-10,000	All thermosets as a class are highly resistant.
Phenolics	50,000	
Polyesters	100,000	

Excerpted from: http://www.nordion.com/wp-content/uploads/2014/10/GT_Gamma_Compatible_Materials.pdf

In a gas-filled canister penetrating gamma and neutron radiation from the fuel interacts with the basket and the canister, but not the filler (e.g., helium gas) which absorbs negligible amounts of radiation. In a canister with solid filler, significant energy would be absorbed. The principal effect is that chemical bonds are broken by gamma energy, forming reactive chemical species and hydrogen gas. The flux of neutrons produced by spontaneous fission and (α,n) events decreases in the first few hundred years from decay of ^{238}Pu, ^{241}Pu and ^{241}Am, ^{242}Cm and ^{244}Cm (Hsue et al. 1979). Whereas this discussion focuses on the production of hydrogen from gamma radiolysis of water during the first few hundred years, neutrons from (α,n) reactions could also be relatively important especially over very long time frames.

The potential for radiolytic production of H_2 is high, as shown by the following scoping calculation. If the initial H_2O inventory in a filled canister is 1 m^3, exposed to a gamma dose of 50 MGy, roughly 2,500 moles of H_2 could be produced:

$$\begin{aligned} N_{H2} &= \text{Dose per Unit Mass} \times H_2O\ \text{Mass} \times G_{H2} \\ &= 50\times10^6\ \text{J/kg} \times 10^3\ \text{kg}\ H_2O \times 3\times10^{16}\ \text{molecules}\ H_2/\text{J} \div N_{\text{Avogadro}} \\ &= 2.5\times10^3\ \text{moles}\ H_2 \end{aligned}$$

Where the value for radiolysis constant G_{H2} is taken from experiments at saturated aqueous conditions, near-neutral pH, and 25°C reported by Elliott et al. (1990, Figure 1). The same dose could also produce a similar quantity of gaseous O_2, although oxygen radicals are often assumed to form H_2O_2.

For an internal pressure of 1 MPa, 10% of the total DPC interstitial volume of 6 m^3 at pressure would represent about 250 moles of gas, which is an order of magnitude less than the potential H_2

production. Thus, there is the potential for damaging H_2 gas pressure depending on the availability of moisture and the efficiency of radiolysis.

Another possible source of gas generation is the neutron capture reaction

$$n + {}^{10}B \rightarrow {}^{7}Li + \alpha$$

where the α particle becomes a helium atom after redox reaction in the solid matrix. Model calculations of gamma and neutron radiolysis are needed to estimate the rate of radiolysis inside the canister, particularly of H_2O producing H_2 gas, H_2O_2, and other products, and neutron capture by ${}^{10}B$.

Strategies for reducing H_2 gas generation include minimizing moisture availability, recombination, permeation, and getters. The cement could be approximately 10 to 50% water by weight initially, because many existing cement recipes contain this much, and water is used to achieve self-leveling flow properties and retarded set in cement slurries. Hence the amount of water present in a DPC will be on the order of 1 m^3. Only a small amount of the initial water is likely to be taken up as bound water in cement mineral structures, with much of it creating micro-pores between and around insoluble grains. Some of this water could be removed by venting and self-heating after cure, before the DPC is resealed. This will depend on the permeability and curing rate of the cement, and the maximum temperature, and will be a focus of laboratory testing.

A recombination strategy could work by using catalysts to react stoichiometric proportions of H_2 and O_2 gases (Hariprakash et al. 2001) similar to the catalytic plugs used in sealed lead-acid batteries. The rate of gas production by electrolysis during battery charging is readily calculated and comparable to the rate from radiolysis in DPCs containing water. Other catalysts are available for converting H_2O_2 to water and oxygen gas (granular MnO_2 or TiO_2) although this reaction may occur fast enough in response to gamma radiation (McDonell 1954) or in the presence of stainless steel (Russo et al. 2013) without added solid catalysts. Hence, recombination strategies could be viable and would not necessarily need to last more than a few hundred years during which the gamma flux is greatest.

Hydrogen permeation refers to slow flow of hydrogen into and through solid materials. It occurs by splitting of H_2 and migration of monatomic H into the surface of a metallic solid, with internal storage, and recombination as H_2 on the downgradient surface. The process can be measured but is slow, possibly 1 to 2 orders of magnitude slower than needed to disperse radiolytic hydrogen generated in a few hundred years.

Getters in gaseous systems are solid materials such as Ti or Mg metals that absorb H_2 or other gases without significant change in solid volume. With treatments such as activation by heating, materials such as Mg can be made to take up on the order of 5% H_2 by weight. For the 2,500 moles of H_2 estimated above, approximately 100 kg of Mg (or more) would be needed. Getters such as Mg and Ti foils that work in vacuum systems would need to be formulated to work in a moisture environment. Organic getters are also used, but would be subject to radiolytic breakdown.

The foregoing discussion focuses on gamma radiolysis of water, but there is also a possibility for direct exposure of UO_2 to the filler moisture environment, with alpha radiolysis of water and other species. A small fraction of SNF rods are likely to have defective cladding (see assumptions). Hence alpha radiolysis must be assumed in the vicinity of some of the fuel.

Finally, for DPCs containing plates of aluminum-based material as neutron absorbing material (mainly Boral® or Metamic®) the reaction of aluminum and water could produce approximately 48 kmoles of H_2 represented stoichiometrically by the reaction:

$$2 \cdot Al(s) + 3 \cdot H_2O \rightarrow Al_2O_3(s) + 3 \cdot H_2(g)$$

giving an estimate for the amount of H_2 produced (assume 52 plates for a 32-PWR assembly canister):

$$\begin{aligned} N_{H2} &= (\#\text{ plates})(\text{area} \times \text{thickness})(\text{Al density/MW}) \times (1.5 \text{ mol } H_2/\text{mol Al}) \\ &= 52 \times (0.2 \text{ m} \times 4 \text{ m}) \times 0.006 \text{ m} \times (3{,}000 \text{ kg/m}^3 / 0.023 \text{ kg/mol Al}) \times 1.5 \\ &= 5 \times 10^4 \text{ mol } H_2 \end{aligned}$$

Similarly, stainless steel corrosion could yield on the order of 1 mole/yr of H_2 for 100 nm/yr corrosion rate, depending on availability of moisture or oxidants (H_2O or H_2O_2). Note that if neutron absorber plates and other basket and canister materials do not degrade significantly prior to canister breach from other causes, then gas production from metal corrosion will not be important.

4.5 Thermal Expansion/Contraction

Cooling of DPCs after filling may cause differential thermal contraction among different materials present in the DPCs. For example, the difference in linear thermal expansion coefficients for stainless steel, and a filler that is mostly tin, is on the order of 10^{-5} C^{-1}, which would induce void space on cooling (150 C° × 10^{-5} × 3 = 0.45%). If the filler bonds to the fuel and basket surfaces on freezing, then thermal contraction will also induce small tensile loads that would be at least partially relieved by creep.

Linear thermal expansion of SS304 (17.3×10^{-6} C^{-1}) is greater than for cement and concrete (10^{-5} C^{o-1} as an analog for filler cement), so the shell would not be stressed during cement curing and temperature increase. However, after some years of heating and final cure of the cement, gradual contraction of the shell could induce tensile stress on the order of 180 MPa, as shown by the following scoping calculation:

$$\varepsilon = \Delta T \times (\alpha_{SS304} - \alpha_{Filler}) = 125 \text{ C}^o \times (17.3 \times 10^{-6} \text{ C}^{-1} - 10^{-5} \text{ C}^{-1}) \approx 0.09\% \text{ tensile strain}$$

acting in stainless steel with Young's modulus of 200 GPa. This assumes no inelastic deformation of the filler, and no void space between the filler and the internal surfaces of the canister. The calculated tensile strain would develop gradually, and is less than the yield strength of the canister shell (but does not include possible pressurization from radiolytic gas generation). Thermal expansivity during cure and eventual cooldown needs to be measured for filler materials.

5. FILLER MATERIAL SELECTION

This section reviews available fillers and makes preliminary selections for testing, in two groups: slurry cements (typically water based), and low-temperature molten materials (e.g., molten metals). In addition, a preliminary investigation of dry particulate fillers is described.

The selection produces lists of candidate materials in each group, for laboratory and possibly scale-model testing. Selection criteria are identified, and advantages and disadvantages are indicated qualitatively. This selection process can be revisited at any time, for example if undesirable attributes are discovered for certain materials, or additional materials become available.

5.1 Previous Filler Studies

Maheras et al. (2012) reviewed filler material analyses done initially by the U.S. Department of Energy (DOE; Fish et al. 1982; Forsberg 1997, 2000; Forsberg et al. 1995; Pope et al. 1996; Wynhoff et al. 1982), Allied-General Nuclear Services (Anderson 1981), the Canadian Nuclear Fuel Waste Management Program (Johnson et al. 1994; Shelson 1983; Teper 1987a,b), the Belgian waste management program (Bennett and Gens 2008), Spain (Puig et al. 2008a,b), Sweden (Oversby and Werme 1995; Puig et al. 2008a,b), and more filler studies done later by the U.S. DOE Yucca Mountain Project (Arthur 2000; Cogar 1996a,b; Mobasheran 1999; Montierth 2000; Moscalu et al. 2000; Radulescu 2001; Wallin 1996). Fillers considered by these programs include oxides/silicates, injected metal alloys, organic binders, sands, air/gases, glass, graphite, boron carbide, cements, glass beads, bauxite, depleted uranium compounds, metallic shot, zeolites, phosphate minerals, and clays. Although a wide variety of filler materials has been identified, there is only sparse information available about injection or emplacement of the materials into fuel canisters (Maheras et al. 2012).

A range of water-based slurry cements is developed below that represents previous work on such cements, and adds some new compositions. Past work has emphasized dry particulate fillers, for example Oversby and Werme (1995) considered glass beads, lead shot, copper spheres, sand, olivine, hematite, magnetite, crushed rock, bentonite clay, other clays, and concrete. Dry particulate fillers would need to be emplaced in DPCs after dewatering but before they are initially sealed. Alternatively, the lids could be cut off from existing, loaded DPCs, followed by dewatering (if lids are cut off underwater), filling, and re-sealing. Of the dry filler materials identified by previous studies, glass beads were a favorable type because they can be made to contain one or more burnable poisons and have other positive features. Copper and magnetite particles were also identified as advantageous if these substances are stable in the host rock chemical environment.

Importantly, the fillers work described in this report is predicated on the possibility of pumping fillers into existing DPCs through the dewatering and vent ports, with the possibility that additional ports could be drilled in the canister wall if needed. This approach would realize the full potential cost savings associated with not re-packaging the current fleet of existing DPCs.

5.2 Filler Selection for Testing

The discussion below focuses on fillers that can be injected into DPCs as slurries or molten metals, to form a monolith after curing or cooling. We avoid dry powders, grains, and beads (Teper 1987a,b) which might be difficult to inject into interstices, and typically do not react together to form a monolith. (Scoping investigation of dry particulate filler performance is discussed below.)

Criteria for qualitative comparison of cement or molten metal alternatives include the following:

- **Injectability** – The ease of handling, mixing, pumping, and emplacement of filler material. Candidate fillers must be injected through one or more ports with inner diameters of roughly 10 to 20 mm. The ease of maintaining filling rate and temperature conditions to control solidification. Injectable so that ~6,000 liters can be pumped into a canister and flow into all interstices, before setting as a monolithic pour.
- **Void Filling** – Self-leveling, and readily penetrates DPC interstices with apertures as small as ~1 mm. While filling small voids, it also acts as a carrier and binder for boron carbide powder, or other chemically inert particulate.
- **Long-Term Chemical Stability** – Forms a long-lasting solid with expected longevity of thousands of years in groundwater, and natural analog evidence. Filler has low permeability to groundwater after package breach, which can slow its degradation. Filler may delay degradation of basket components such as neutron absorber plates, by limiting moisture availability.
- **Retrievability/Recoverability** – Can be removed from filled canisters for safety reasons, or to recover economic value in spent fuel. Retrievability may be a second-order concern, because if entire waste packages can be retrieved then they can generally be processed by various methods to separate spent fuel constituents.
- **Material Compatibility** – Chemically inert or reacts very slowly with DPC internal components, especially Zircaloy cladding and aluminum-based neutron absorber or structural materials. Stable to groundwater and chloride brine (permits use in a salt repository) after set and during aging at temperature. Controllable shrinking/expanding behavior during initial set and subsequent gradual cooling (limits stresses and maintains low permeability). Filler readily bonds to metal surfaces of the fuel and canister internals (promotes void filling and durability).
- **Moderator Displacement** – Capability to eliminate water and other neutron moderators from the canister.
- **Gas Generation** – Gas generation by chemical reactions or as a result of radiolysis, is limited or can be controlled so as to avoid initiating canister rupture. Resists radiolysis from gamma and neutron radiation. Filler has low water content (to control porosity and to limit radiolytic gas generation).
- **Solidification Temperature** – The conditions of emplacement, particularly temperature, are consistent with maintaining the integrity of both the filler and the spent fuel. Solidifies in a temperature environment of ~150°C (a nominal temperature for spent fuel rods after some aging). Controllable heat of fusion or reaction (e.g., on the order of roughly 10 W per liter or less, during set) to limit contribution to the peak temperature. Thermal conductivity before and after set is sufficient to dissipate heat of fusion and waste heat, so the filled canister temperature stabilizes at an acceptable and predictable level.
- **Toxicity** – Filler material does not include large amounts of constituents that are known toxins (e.g., regulated metals).
- **Radionuclide Sequestration** – Certain chemical affinities may exist between fillers or their weathering products, and long-lived radionuclides important to repository performance assessment (PA). Examples include actinides and phosphates, and iodine and bismuth solids.

- **Material Cost –** Filler material cost is reasonable (e.g., commensurate with selection of filling vs. other approaches to fuel preparation such as re-packaging).

5.2.1 Slurry Cements

Because the DPC filler must physically stabilize the fuel elements, basket structure, and neutron poisons in place to prevent criticality for at least several thousand years, the DPC filler must be made of a material that can maintain structural integrity for thousands of years, first in the unbreached canister environment, then in contact with groundwater. Consideration of high-solids cements is motivated by geologic and archaeological observations that certain materials are stable in nature and that natural analogues exist. For example, pozzolanic cements used by the Romans still maintain structural integrity today. The ancient Greeks also used pozzolanic cements hundreds of years before that. A DPC filled with cement might therefore be expected to maintain some structural integrity for a few thousand years. Analogous arguments could not be made for DPCs filled with recently developed man-made materials such as organic polymers.

The term 'slurry cements' identifies formulations that contain relatively insoluble solid constituents such as silica, alumina, etc., in significant amounts, but which can serve as injectable grout. Some constituents of slurries may be soluble (e.g., CaO) but not all, as would be the case if liquids were mixed to form insoluble precipitate. Such chemical solution grouts have special properties such as rapid setting, adhesion, expansivity, and light weight, and they have applications where more conventional slurry cements do not perform well.

The following discussion describes the types of cements ("families") that are considered for testing as slurry cement fillers, and plans for laboratory work that is now underway.

Ordinary Portland Cement

Milestone (2006) reviewed radionuclide immobilization in cements and emphasized their inexpensiveness, availability, ease of preparation and "ability to penetrate complex waste forms". Moreover, cements are radiation-stable and, because of their alterable composition, provide operational flexibility.

Ordinary Portland cement (OPC) is a sintered mixture of calcium silicates, gypsum, and minor fillers. OPC has also been blended with fly ash, blast furnace slag, and volcanic ash (pozzolans). Two obstacles to using OPC are the high temperatures caused by its exothermic reaction with water, and high pH (> 12) in the water in contact with the cement. Including blast furnace slag and fly ash decreases the temperature swing, and attendant thermal stresses, and lowers the pH slightly. The high pH of OPC fluids would be detrimental to DPC performance because it would favor corrosion of aluminum metal in the Boral® neutron absorber, and because most of the radionuclides in the fuel sorb sparingly and are highly soluble under high pH conditions. Little radionuclide retardation would occur in an OPC filler once fuel elements were exposed to water.

Predicting the long-term stability of OPC is problematic because it is a metastable mixture of phases that transform to more thermodynamically stable assemblages through largely uncertain kinetic pathways. Carbonation, the formation of calcite and a reduction in solution pH, occurs rapidly and predictably near and on OPC surfaces, but the long-term reaction of calcium silicates in OPC is less clear.

Many pre-mixed 1-part formulations are available for self-leveling cement applications, such as flooring underlayment, embossing, etc. Most of these contain sand and Portland cement, modified with a polymer plasticizer. They have setting time on the order of 30 minutes or less. These cements can be pumped, but this is not typically an objective. Importantly, the slurry pH and cured cement pH are too alkaline for DPC filler application (pH > 11).

Low-pH OPC grout is a niche application where metal corrosion, or other chemical interactions such as radionuclide sequestration, are objectives. Low-pH formulations have been developed for nuclear waste repository applications to enhance stability and durability, reduce corrosion of engineered barriers, and limit complexation of dissolved radionuclides at high pH. A review by Holt (2008) reports that low-pH injection grout for fractured rock, can be formulated with any class of cement, and silica fume content >20% of the dry powder weight. The slurry pH can be decreased to pH 11, and possibly lower through mix design. Water:binder ratios between 0.4 and 2.0 (binder includes cement and silica, not aggregates or fillers such as fly ash) have been found effective. Silica fume in large proportions apparently delays setting time, although possibly not initial setting that would be important for DPC filler applications. Increased mixing water is widely known to increase porosity and decrease strength, while improving flow properties. Addition of silica fume may recover some of that strength. The author notes that high-silica OPC-based grout has exhibited adverse shrinkage in response to drying.

A recent experimental study investigated cements for grouting deep boreholes for disposal of nuclear waste (Collier et al. 2015). They used Class G oil well cement (median particle size 16.5 μm) partially replaced by silica fume (median 17 μm). Polycarboxylate poly-ether plasticizer Sika Viscocrete 3110® functioned at temperatures well above 100°C, while a sulfonate-based organic plasticizer degraded at 90°C (Collier et al. 2015). The Viscocrete admixture functioned as both a plasticizer and set retarder. It produced an initial increase of consistency for a few minutes, followed by approximately 2 hours of consistency *decrease* to 0 Bc (consistency units; corresponding to a very low viscosity). This condition was maintained, for example, for more than 3 hours at 120°C with plasticizer addition of 2% (weight of binder, i.e., silica and cement dry powders). Setting time (determined by a needle penetration method such as ASTM C403) was at least 4 hr for plasticizer loading of 1% or greater. Superplasticizer loading and temperature of setting did not appear to affect final strength.

Following these studies, and recognizing that a generic OPC design cannot nearly represent the range of variation of available Portland-based cement formulations, a simple formulation is recommended here combining Class G oil well cement (for elevated temperature conditions), silica fume, polycarboxylate plasticizer (e.g., Viscocrete 3110®), and Class F fly ash filler. The initial binder:filler and water:binder weight ratios should both be 1:1, and the ratios should be independently varied up and down in increments of 30%. The initial plasticizer concentration should be 2%, which can be decreased to 1% when a promising recipe is found.

Sources for Class G cement include GCC Rio Grande (Tijeras, NM, 505/281-3311). Silica fume that conforms to ASTM C1240 (*Standard Specification for Silica Fume Used in Cementitious Mixtures*) is available from Sika Corp. as Sikacrete-950DP® (201/933-8800, usa.sika.com). Plasticizer Sika ViscoCrete 3110® is available as an aqueous liquid, from the same source. Larger particle sizes can be obtained as precipitated amorphous silica from PPG Silica Products (www.ppgsilica.com), or ground silica that is typically quartz with increased inhalation hazard (not recommended). Sourcing for Class F fly ash is discussed above.

Chemically Bonded Phosphate Cements

Chemically bonded ceramics have ionic or covalent bonds instead of hydrogen bonding and van der Waals bonds that are active in Portland cement (Wagh 2016). So-called ceramic cements are ceramic because of chemical bonding, and cements because they are mixed and set at low temperature. Phosphate ceramics are inorganic, nontoxic, have neutral pH, and are insoluble (at near-neutral pH). They are made from low-cost naturally occurring materials, and they are self-bonding, i.e., a second layer will bond to the previous one. Encapsulation of radioactive waste in the U.S. and other countries is a major application of chemically bonded phosphate cement (Wagh 2016).

Phosphate cements are typically grouped with acid-base cements, because they involve reaction of a soluble source of metal cations (e.g., MgO or ZnO) and an acidic phosphate salt. Calcium is quite soluble as CaO leading to very fast reaction times, so Ca-phosphate formulations rely on other Ca compounds such as phosphates, aluminates, or carbonates. The following discussion focuses on cements that have been previously studied (and which in some cases are commercially available). These include phosphate cements with Mg and Ca, Al, and Ca-aluminate-phosphate cement, all of which are considered chemically bonded. The discussion also covers Ca-aluminate and Ca-sulfoaluminate cements, which are considered hydraulic cements.

Mg-K-Phosphate (MKP) Cement

Mg-K-phosphate (MKP) cements are less exothermic than OPC and result in lower pH (4 to 8). Ceramicrete® is a MKP cement developed at Argonne National Laboratories (Singh et al. 1997) for stabilizing waste streams (Covill et al. 2011; Stefanko et al. 2011). The Ceramicrete synthesis reaction is:

$$MgO + KH_2PO_4 + 5H_2O \rightarrow MgKPO_4 \cdot 6H_2O$$

Not all of the particulate MgO is reacted once the cement sets (~ 2 hours). The only clear natural analogue for Mg-phosphate cements comes from ancient middens where the mineral struvite is found. These cements develop high strength, are resistant to temperature swings and road salt, and maintain bond strength better than other construction materials (Wagh 2016). They tend to cure more slowly than other chemically bonded cement types and can therefore be used more readily in large monolithic pours.

The starting mix should be 0.9:2:3.1:5 parts (w/w) MgO, H_2O, KH_2PO_4, and Class F fly ash. These ratios yield equimolar portions of MgO and KH_2PO_4 which is stoichiometric, but the ratios are typically simplified to 1:2:3:5 for $MgKPO_4$ (MKP) cement, producing a slight molar excess of MgO. Note that Mg is a minor constituent of fly ash (~1% MgO by weight in oxide analysis).

Boric acid has been extensively tested as a retarder (Wagh 2016). NaCl was also suggested (Sugama 2016) but could facilitate corrosion in a DPC. Fluidity may be increased by increasing water (and setting time might be extended). Plasticizer admixtures (a few percent) when they are effective, are known to increase cement fluidity, and inhibit settling of fine aggregates, without additional water.

Increasing the fly ash filler, or possibly adding another filler such as quartz sand which is inert, will be necessary to slow setting time. This occurs for two reasons: 1) the heat capacitance of additional filler slows the temperature rise and the resulting thermal acceleration of the binder reaction, and 2) introducing more relatively inert surface area may tend to decrease the availability of the acid solution for reaction with MgO. Reported setting times of 30 to 60 minutes for MKP cement include the effect of fly ash at the proportion given in Table 8. Significantly longer setting time will be needed for DCP filler application.

Alumina may also be effective for retarding set, replacing all or part of the fly ash. Powdered alumina is relatively unreactive, so fine particle size can be used without causing setting reactions (except elevated temperature approaching 150°C). Use of "reactive" grade Al_2O_3 could greatly increase its surface area compared to MgO, so that even weak affinity with PO_4 species in solution would tend to compete with formation of MKP.

Thermal activation is especially important because MKP cement binder will have completely set when its temperature reaches approximately 50°C, and the binder reaction is exothermic (Wagh 2018, personal communication). It may be impractical to maintain $T < 50°C$ everywhere inside a loaded DPC for the ~2 hours that it could take to fill the canister with cement. Note that KH_2PO_4 dissolution in water is mildly endothermic, and when the mix temperature returns to ambient, mixing can be taken as complete.

The crystalline species actually produced during set is $MgKPO_4 \cdot 6H_2O$, which dehydrates to $MgKPO_4$ when the temperature is raised to approximately 100°C or greater. Disintegration of the solidified grout does not occur on dehydration (Wagh 2018, personal communication). Thus, an intact low-water grout filler could be obtained in a DPC by dewatering the cured cement, during heating >100°C. Final porosity will be strongly affected by the amount of water in the initial mix, and could be on the order of 25%. The pore structure created by dewatering the MKP hydrate is reported to be fine with micron-scale pores that tend to be connected (Wagh 2018, personal communication). The cured cement may therefore have limited permeability due to connected, but fine pores (e.g., < 1 md). Measurement is discussed with other follow-on testing (Section 4.3).

Table 8. Information on candidate cement slurry filler materials (from Hardin and Brady 2018).

Material	Starting Recipe for Screening	Notes on Variants
Al-Phosphate Cement (APC)	Based on Wagh (2016) deep/geothermal cement: Calcined alumina (Al_2O_3, e.g., 10-50 μm) 49% Aluminum hydroxide ($Al(OH)_3$ nucleant) 1% Class F fly ash 50% 50% H_3PO_4 solution ~45 mL/100 g dry alumina Water Sufficient for slurry; not more than ~50 mL per 100 g fly ash	• Vary fly ash from 0 to 75% of powders, in steps of 25%. • Vary $Al(OH)_3$ content: 0 and 3% to test for effect. • Increase water in steps of 15% of initial amount, only as needed to achieve fluidity and setting behavior. • Add plasticizer at 1% and 3% as needed to achieve fluidity and setting behavior, while decreasing water. • Samples must be heated to 150°C for hours to cure. This can be attempted at ambient pressure in an oven, but boiling may prevent proper cure. • Curing may need to be done in a pressure vessel placed in the oven, exposing samples to a steam environment at 150°C (5 atm pressure). • Check curing time by extending cure to 7 days for representative samples. • Calorimetry will not be effective by the method described (insulated cup). • Aluminum hydrophosphate will form as a possible precipitate during cure as $T \rightarrow 100°C$. This should be investigated by direct observation. • If a retarder is needed, which is unlikely, 1 to 3% boric acid has been recommended (see text).
Mg-K-Phosphate (MKP) Cement	Typical Ceramicrete® recipe (Wagh 2018, personal communication): MgO, calcined (w/w of dry powders) 10% KH_2PO_4 powder 34% Class F fly ash (reactive) 55% Water 22% of total dry powders Boric acid retarder ≥ 0.5%	• This Ceramicrete® recipe is self-consolidating (flows into complex forms) and may also be self-leveling. • Recipe is stoichiometric for $MgO + KH_2PO_4 + 5H_2O \rightarrow MgKPO_4 \cdot 6H_2O \rightarrow MgKPO_4 + 6H_2O$. • Much of the MgO is unreacted, but the fly ash forms PO_4 compounds. • MgO is calcined to reduce reactive surface area, to limit the setting rate. (Increasing MgO surface area cannot be used to neutralize slurry pH.) • Increase boric acid in 1% increments if needed, but there may be little additional retarder effect at >3%. • Increase water in small increments (e.g., 3% of dry powders) as needed for fluidity. • Add plasticizer (see text) at 1% and 3% if needed, decreasing water, to prevent bleed and control final porosity.

Material	Starting Recipe for Screening	Notes on Variants
Calcium-Phosphate Cement (CPC)	Typical bone cement binder recipe (Wagh, 2018 personal communication) with aggregates: Binder TTCP 73%, DCPA 27% 40% Class F fly ash 60% Water (sufficient to produce slurry) Citric acid retarder 4%	• Binder proportions should be stoichiometric for hydroxyapatite (Ca/P = 1.67). • Vary citric acid retarder from 0 to 6% in steps of 2% following Sugama (2006) work with CAPC. • Note that citric acid may not be effective and a different retarder may be needed. • Vary fly ash from 30 to 90% to retard set. • Water requirement will be at least 10% of total weight; increase in steps of 3% to increase fluidity and retard set.
Ca-Aluminate-Phosphate Cement (CAPC)	Haliburton ThermaLock® (according to instructions)	• Pre-mixed dry cement product; mix according to instructions. • Refer to Sugama (2006) for composition and potential variations, if pre-mixed composition does not suffice.
Ca-Aluminate Cement (CAC)	Deferred because of potential setting time, heat generation, and alkaline corrosivity issues.	
Ca-Sulfo-aluminate Cement (CSAC)	Deferred because of potential setting time, heat generation, alkaline corrosivity, and microbial activity issues.	
Generic OPC Grout	Cement recipe reported by Collier et al. (2015): Class G oil well cement 38% Silica fume (submicron) 10% Class F fly ash 50% ViscoCrete 3011® liquid (mix first with water) 2% Water100% of binder (cement, fume, plasticizer)	• Viscosity may increase in the first few minutes, then decrease steadily for ~2 hours, due to the plasticizer. • Vary fly ash up/down from reference by 30% of initial amount. • Vary water up and down by 30% of initial amount. • Vary silica fume up and down by 50% of initial amount (goal is slurry pH ≤ 10), • Decrease plasticizer to 1% after a promising mix is found. • Curing at elevated temperature may change results.

Sources for MgO which has been calcined to appropriate consistency (i.e., for reaction slowing; Wagh 2018, personal communication) include Martin-Marietta Magnesia Specialties (MagChem P98 pulverized magnesia, 410/780-5500, www.magnesiaspecialties.com). The production method for KH_2PO_4 is also important; grinding produce angular particles that decrease fluidity. A spray-dried powder form of KH_2PO_4 is recommended (producer ICL Performance Products, distributed by Brenntag North America, Inc., 773/586-2002, www.brenntag.com). Fly ash can be obtained from the supplier identified above, and the plasticizer identified above could work with MKP cements also (Wagh 2018, personal communication). Boric acid is a common laboratory reagent and needed only in small amounts for Phase 1 testing.

Calcium Aluminate-Phosphate Cement (CAPC)

Calcium aluminate-phosphate cement has been formulated for use as wellbore cement, by mixing CAC and sodium polyphosphate (Wagh 2016). Other formulations use concentrated phosphoric acid. After reaction the primary phases are hydroxyapatite ($Ca_5(PO_4)_3(OH)_2$), boehmite (AlOOH), hydrogarnet ($Ca_3Al_2(SiO_4)_x(OH)_{4(3-x)}$), and the zeolite analcime ($NaAlSi_2O_6 \cdot H_2O$).

Hydroxyapatite is stable in sedimentary rock formations (natural analogs), sorbs and sequesters radionuclides (e.g. Moore and Rigali 2015; Rigali et al. 2016) and is a component in sealants for geothermal wells (Sugama 2006). Other naturally occurring secondary Ca-phosphate minerals include monetite and brushite. Natural analogue support for the use of calcium phosphate cements comes from buried vertebrate bones and teeth made of apatite which can remain intact for thousands of years. A complicating factor is that bones and teeth contain organic matter in addition to calcium phosphate, but pure calcium phosphate would be used to fill DPCs. Dental enamel has a lower organic content and is more resistant, and is probably a better analog than bone. Higher calcium phosphate content increases the likelihood of fracture.

Water and acidic conditions ($pH < 5$) *in situ* can sharply decrease the persistence of calcium phosphate, which could be useful because a mildly acidic solution (pH 4) could be used to dissolve and flush calcium phosphate from canisters for intact fuel retrieval. Acidic conditions are not expected to prevail in filled DPCs because: 1) natural waters require particular conditions such as abundance of reduced sulfur, to become acidic, and 2) the contents of DPCs will be selected so as not support acid-generating reactions.

CAPC is used in geothermal wells at high temperature (Sugama 2006). Thermalock® is a CAPC product sold by Haliburton, which is CO_2 and acid resistant. Citric acid is used as a retarder and the material can be foamed using surfactants, though foaming can cause connected, open bubbles, and possibly an undesirable increase in hydraulic permeability. Post-setting cracking in wellbore applications is prevented by the addition of milled carbon microfibers (up to 14 wt %). In practice, Thermalock® is reported to achieve (Sugama 2006):

- Pumpability for at least 3 hours (followed by set).
- Compressive strength > 3.5 MPa (500 psi) at 24 hour-curing time.
- Water permeability $< 10^{-4}$ Darcy.
- Bond strength to steel casing > 0.35 MPa (50 psi).
- Fracture toughness $> 0.008\ MN/m^{3/2}$ at 24 hour-curing time.
- Cost < $15/bag (42.7 kg).
- Slurry density of foamed cement $< 1.3\ g/cm^3$.

The service life of Thermalock® cement in a corrosive geothermal environment is estimated to be ~20 years (Sugama 2006). Its persistence in more benign chemical environments must be verified.

Calcium Phosphate Cement (CPC)

Calcium phosphate cements have been developed for medical/dental repair of bones and teeth (e.g. Meffert et al. 1992; Ong and Chan 2000). A potentially important aspect of dental cements described in the literature is short setting time which would need to be retarded by complexing calcium ions or by dilution with water. The large number of published recipes, the simplicity of the final hydroxyapatite composition, and its similarity to natural analogs make an attractive alternative to CAPC although additional testing will be needed to formulate a self-leveling grout.

To produce stoichiometric hydroxyapatite ($Ca_5(PO_4)_3(OH)_2$, HA) at near-neutral pH the Ca:P ratio should be 1.67. Most Ca-PO_4 salts have lower ratios, with tetracalcium phosphate ($Ca_4(PO_4)_2O$, TTCP) the only higher ratio at 2. TTCP is alkaline and more soluble than dicalcium phosphate anhydrous ($CaHPO_4$, DCPA) which is near-neutral. Using other inorganic, basic Ca-compounds such as CaO as supplemental sources for reaction with acidic phosphate solutions, would be unworkable for DPC fillers because of rapid reaction. Low-solubility compounds of Ca and phosphate in solid form, are used in Ca-phosphate cement (CPC) to prevent flash-setting.

Studies on CPC typically describe combining TTCP with DCPA as dry powders, each ground to fineness (e.g., mean grain size ~15 µm) in equimolar amounts, for biomedical applications. A relatively small amount of $CaCO_3$ (1 µm mean grain size) may be added as a source of free Ca, along with fillers such as silica or fly ash. Setting begins in minutes, and full cure can be complete in 4 hours (Wagh 2016, Chapter 13). Setting is strongly exothermic (on the order of 70 kJ/mol or 10^6 kJ per DPC, using data from Wagh 2016, Appendix A), and the setting reaction is thermally accelerated. Retarders and aggregate fillers would therefore be required to extend setting time significantly, for DPC applications. Increasing the grain size of TTCP and DCPA could also be helpful to slow down setting, and simplify preparation of the powders.

Testing should investigate citric acid as a retarder following Sugama's (2006) work on Ca-aluminate-phosphate cements (discussed below). Citric acid forms a barrier layer on the surfaces of Ca-bearing grains, which can be broken down to a greater or lesser degree as setting progresses. The same effect could occur in a Ca-phosphate mix with Ca contributed by low-solubility solid phases. Sugama's basic ingredient was Ca-aluminate cement (CAC), and a solution of Na-pyrophosphate as the acid ingredient. Thus, a difference with CPC is that the ingredients TTCP and DCPA both contain Ca and phosphate, and citric acid could act on both phases. Citric acid would likely break down slowly at temperature, but the products are other organic molecules for which the effects on corrosion and gas generation in DPCs are not known.

Class F fly ash is recommended, varying the concentration from 30 to 90% of the total weight of all dry ingredients, to slow setting and increase fluidity. The initial water content should be 10% of total weight, or that needed to produce a workable slurry (which may be >10%). The effect of additional water should be evaluated by increasing in steps of 3%. Citric acid should be investigated as a retarder, at concentrations of 2, 4, and 6% of the total powder weight, following Sugama (2006). Ultimately, for DPC filler application setting time will be the major challenge, so testing should focus on retarding and then move on to fluidity and other objectives.

TTCP is commercially available only in small quantities, and is used mainly for bone cements. Kilogram-level quantities might be obtained at some expense from reputable suppliers with effective quality control programs, or it could be synthesized as discussed below. DCPA and citric acid are readily available as laboratory reagents. The relative scarcity of TTCP means that experimental protocols should be designed to minimize batch size (Section 4).

Aluminum Phosphate Cement (APC)

Aluminum complexes with phosphate have been investigated for decades (Wilson and Nicholson 1993, Chapter 6). According to these authors: "…the species present in 50% phosphoric acid solution containing aluminum appear to be H_3PO_4, $H_6P_2O_8$, $H_2PO_4^-$, $H_5P_2O_8^-$, $AlH_3PO_4^{3+}$, $AlH_2PO_4^{2+}$, $Al(H_2PO_4)_2^+$, and $Al(H_3PO_4)_n$ where $n \geq 2$, of unknown protonation." The aluminous complexes generally do not form precipitates at near-neutral or mildly acidic pH and near-ambient temperature. However, aluminum phosphate complexes are apparently polymeric which could affect the flow properties of a cement mix. Note that these statements assume acidic to mildly acidic conditions; as pH becomes alkaline, Al-hydroxide complexes form leading to precipitates such as gibbsite ($Al(OH)_3$).

As Al dissolves, viscosity is reported to increase markedly (Wagh 2018, personal communication). Aluminum oxide (typically α-Al_2O_3, the corundum polymorph) is very slow to dissolve near ambient temperature, so the viscosifying effect would be delayed in a DPC filler slurry subject to gradual heating. One of the effects of heating in thermal-setting aluminum phosphate cement (APC) would be to dissolve Al_2O_3. However, in the design of phosphate cements for use in geothermal boreholes, a recognized problem is that when solubilities of various oxides (SiO_2, Al_2O_3, $CaSiO_3$) increase, flash-setting may result (Wagh 2016, Chapter 16). Alumina solubility reaches a maximum at 118°C in phosphate solution, but for the system Al-PO_4-H_2O, precipitates are not reported in the sparse literature on APC until temperature of 150°C. In a high-temperature water (steam) environment the precipitates are hydrates variscite or metavariscite (polymorphs of $AlPO_4 \cdot 2H_2O$), or wavellite ($Al_3(PO_4)_2(OH)_3 \cdot 5H_2O$). If the set material is then allowed to dry at 150°C, these apparently convert to anhydrous berlinite ($AlPO_4$). The mineral grain density increases with berlinite formation, and the effect on the set cement is not known although shrinkage or cracking have not been reported. By analogy to Mg-K-PO_4 cement discussed below, decrepitation should not occur as the hydrates convert to the anhydrous form. Another option is to heat the Al-PO_4 slurry directly to 150°C in air (i.e., without a pressure vessel), but again, the composition and texture of the final precipitate are not known. These options for heating and dewatering APC should be investigated early in the test series.

Setting via gel behavior has been reported ("aluminum-phosphate gel" described by Wilson and Nicholson 1993, Section 6.5.4). However, this was in a chemically mixed system containing glass, silica, fluoride, etc. Wagh (2016, Chapter 16) suggested that amorphous aluminum hydrophosphate (referred to by the author as $Al(H_3PO_4)_n$) forms in borehole cement at ~100°C, but the result is apparently in a suspension or fine slurry, and readily injectable. Observation of complexation and polymerization behavior will be an important objective for testing.

Orthophosphoric acid (50%, pH 1.5 at ambient temperature) is recommended as the initial liquid in the mix for borehole cement (Wagh 2016, Table 16.2). If too acidic for DPC application (e.g., for Zircaloy cladding) neutralization may be possible without forming precipitates, for example by adding a small amount of finely particulate, microcrystalline or amorphous $Al(OH)_3$. As suggested by Wagh (2016) the $Al(OH)_3$ releases Al ions into solution quicker than the alumina, while not changing the desired cement bonding or temperature behavior discussed above. The amount of $Al(OH)_3$ specified (2.2% w/w or 28 mmol, per 100 g dry powder), is approximately

10% of the molality of H_3PO_4 (48.4 g of 50% solution or 250 mmol, per 100 g dry binder powder including Al_2O_3, $Al(OH)_3$, and boric acid retarder; Wagh 2016, Table 16.2). If much of the $Al(OH)_3$ dissolves at acidic conditions, this may be enough for neutralization. This should be determined from slurry pH measured after mixing. Increased $Al(OH)_3$ may also significantly decrease setting time (Wagh et al. 2006) although this may not be important for DPC application if setting can be controlled by temperature.

The Al:P ratio in the APC binder is approximately 4:1 (Wagh 2016, Section 16). Class F fly ash can be added as a mildly reactive aggregate or conditioner, to control slurry consistency and to impart more strength to the final product. Class F is favored because it contains less Ca (which could react rapidly with phosphate in the mix) than Class C, and contains only moderate amounts of carbon (inert, graphitic, dark in color). APC setting behavior should be tested without fly ash addition, and interaction of 50% H_3PO_4 and fly ash, without alumina, should also be tested to understand the potential effects on pH, setting behavior, and slurry thickening at $T < 150°C$.

A goal of APC mix design should be to limit the amount of water, which forms porosity when anhydrous $AlPO_4$ eventually forms (either during direct heating of slurry under air or by dewatering of previously formed hydrous cement phases). In addition, as the mix is heated to 100°C and higher, pressure curing may be needed to prevent boiling (actually 95°C at the elevation of Albuquerque). The vapor produced by boiling could cause large, irregular macropores to form, and premature dewatering of the mix could degrade the setting behavior. The vapor pressure of water at 150°C is approximately 5 atm (absolute), which is within the internal pressure rating of many DPCs – on the order of 7 bars (gage) (SNL 2017, Table 3). This means that pressure curing in situ is possible for many DPCs.

Plasticizers (typically organic surfactants) may be effective for reducing the amount of water in APC mixes but no results have been reported. Plasticizers such as colloidal clay materials (e.g., inorganic attapulgite – Attagel®) could help to decrease water content in the mix while maintaining fluidity. The possibility of reducing the amount of water using plasticizers should be investigated, although the amount of added organic material should be minimized to inhibit radiolytic gas formation and possible microbial growth. Retarders may not be needed given the temperature-dependent setting behavior of APC.

Literature data on the physical properties of cured APC were not found for this review, but by analogy to MKP cements discussed below, porosity will be up to 35%, and connected micropores can be expected in the paste phase of the final set product if boiling is controlled. Permeability is likely to be significant, possibly enough to allow moisture removal as suggested by SNL (2017, Section 7.2.3).

Ingredients for testing APC (Al_2O_3, $Al(OH)_3$, 50% H_3PO_4, Class F fly ash) are widely available. The purest alumina (~99%) is calcined (> 1,050°C) to drive off chemical water; this is a common industrial commodity (AluChem, Inc. 513/733-8519, www.aluchem.com). Typical industrial product has particle size ranging from 44 to 75 µm, and may be ground (more surface area) or unground. Alumina powder at the finest grade available ("reactive" alumina, mean particle size <10 µm) forms a very smooth and readily pumped slurry (Wagh 2018, personal communication). Reactive grade is recommended for testing, unless it produces undesirable properties or composition in the final cured product, in which case a blend of finer and coarser grades could be used. Fly ash (Class C, Class F, etc.) is available from various sources but previous experience suggests Boral Material Technologies (800/292-5354). A plasticizer that could work with APC

(Wagh 2018, personal communication) is Norlig A, a Ca-lignosulfonate (LignoTech USA, 715/359-6544).

Evolution of Al-PO_4 in the Disposal Environment

Long-term degradation rates for fillers are needed to predict whether the fillers will, over the 20,000 yr (or longer) time frame for postclosure criticality control:

- Hold neutron absorbing components of the DPC basket in place (e.g., B_4C particles encapsulated in aluminum, which corrodes); and/or
- Hold neutron absorbing particles (e.g., pulverized B_4C) in place as constituents of a filler.

In either case, if the aluminum in the basket, or the filler matrix, degrades and does not hold the neutron absorbing material in place, then it will settle to the bottom of the DPC.

The DPC filler degradation (weathering) reaction path must also be understood because, in addition to criticality control, degradation of the filler material should not chemically enhance the release of radionuclides from the package by, for example, raising radionuclide solubilities.

The degradation path will also determine whether the breached DPC is likely to self-seal: a positive reaction ΔV could cause sealing of B_4C in place by higher volume reaction products, such as clays and hydroxide minerals. The pH inside the degrading DPC must be known because solubilities of the cationic radioelements – e.g. U, Pu, Np, Am – are low in the pH range 5 to 8, but increase outside this range. In the absence of DPC filler, the in-package pH would be buffered to near neutral by the presence of alteration phases of the spent fuel, aluminum, and stainless steel. Aluminum metal will corrode first, followed by spent fuel, with the spent fuel degradation being controlled by the integrity of the cladding. Stainless steel corrosion will be slowest of the three. Aluminum will dissolve to gibbsite, $Al(OH)_3$, which has a solubility minimum at pH 6 to 7 at 25°C. Spent fuel under oxidizing conditions will dissolve to form schoepite, $UO_3{:}nH_2O$, which has a solubility minimum at pH 6 to 7. In the absence of filler, any seepage entering a breached DPC would be anchored near pH 6 to 7 by schoepite and gibbsite degradation. This pH range is also the range of minimum solubility for many radioelements. The key question is how degradation of the DPC filler might change this pH, and radioelement solubilities.

After setting of aluminum phosphate cement (APC) filler will initially be an assemblage of Al_2O_3, Class F fly ash, and $AlPO_4$ – berlinite. Al_2O_3 dissolves very slowly in natural waters (Carroll-Webb and Walther 1988) and can probably be assumed to remain stable indefinitely. Class F fly ash, produced from burning of anthracite or bituminous coal, is a glass + mineral mixture containing ~ 40-65% SiO_2; 25% Al_2O_3; 3-30% Fe_2O_3; 3% CaO, with numerous trace metals (e.g., Kim, Kazonich et al. 2003). Fly ash minerals include anhydrite, quartz, aluminosilicates, hematite/magnetite, MgO, calcite, NaCl, KCl, and titanium dioxides. Alkali exchange and dissolution of the CaO and MgO fly ash components will raise the pH of fluids in contact with the fly ash to pH 7 – 9 (Schramke 1992; Roy and Berger 2011). Higher pH is prevented by CO_2 uptake. There are few long-term (> 12 months) dissolution rates for fly ash. The closest natural analogue to fly ash is volcanic glass (Zevenbergen, Bradley et al. 1999) for which measured long-term dissolution rates do exist. Moreover, the long-term degradation path of volcanic glasses in nature is reasonably predictable; leaching of alkalis followed by formation of aluminosilicate clays, and calcite (e.g., Crovisier, Advocat et al. 2003).

Berlinite in contact with low pH groundwater seepage into a breached DPC will dissolve to produce variscite, $AlPO_4{:}2H_2O$, as well as an aluminum hydroxide such as gibbsite, phosphate, and hydrogen ions, the latter causing pH to decrease. More alkaline seepage containing Ca would cause the berlinite to dissolve to form hydroxyapatite. But there are no actual measurements of the kinetics of the berlinite transformation reactions to say how long the process will take. The only published berlinite dissolution rates were carried out at strongly acid pHs not relevant to conditions inside breached DPCs.

There are no known natural occurrences of berlinite that are good analogues for berlinite in a filled DPC buried in a nuclear waste repository. Berlinite is a high-temperature mineral typically found in hydrothermal settings. The only non-hydrothermal berlinite occurrences are caves in Romania (Onac and White 2003), Borneo (McFarlane and Lundberg 2018), and Saudi Arabia where dense P-rich bat guano deposits spontaneously combusted. But because cave temperatures sometimes exceeded 500°C when the berlinite formed, the cave berlinite examples are not useful for projecting long-term stability of berlinite at the lower temperatures of direct DPC disposal.

The in-package pH will depend upon reaction of high-pH fly ash leachate, with berlinite/variscite leachate (pH~4) in the presence of schoepite. But the absence of kinetic measurements and useful natural analogue evidences for long-term berlinite persistence, forces reliance on thermodynamic analyses for quantitative prediction. The geochemical speciation and reaction path code PHREEQC version 2.15.06 (Parkhurst and Appelo 1999), and the llnl.*dat* (thermo.com.V8.R6.230) thermodynamic database, will be used to estimate the in-package DPC seepage pH by: 1) assuming phosphate mineral reactions, such as berlinite dissolution, instantaneously go to equilibrium; 2) using measured glass degradation rates to estimate the weathering rate of the fly ash component; and 3) assuming instantaneous equilibration of schoepite with in-package seepage fluids. Because the amount of schoepite will depend on the amount of exposed fuel (clad failure) and the fuel degradation rate, a range of schoepite masses will be considered in the calculation. Because the surface area and seepage-accessible mass of berlinite and fly ash are uncertain, a range of input values will be considered. The calculation will be done at 25 and 60°C, the higher temperature to reflect in-package pH during the early period of disposal. $AlPO_4$ is less soluble at higher temperature. The input fluid chemistry will be a generic, dilute groundwater under oxidizing conditions (unsaturated scenario).

A second series of calculations will be done assuming reducing conditions. Reducing conditions are favored under saturated conditions. Degradation of spent fuel and steels will consume oxygen and favor reducing conditions inside a breached DPC.

Key outputs of the calculation will be in-package pH, and the volume change of DPC filler as it is weathered under oxidizing and reducing conditions. Again, the calculated in-package pH will be used to consider DPC filler weathering effects on radioelement solubilities. The calculated volume change of DPC filler weathering should set limits on the long-term persistence of the DPC filler and its ability to hold B_4C in place to limit criticality.

Calcium Aluminate Cement (CAC)

Calcium aluminate cement is typically formulated from fused limestone and bauxite, ground to fineness. The manner and temperature of kilning distinguish various commercial products. CAC may contain some silica, but calcium aluminates generally take the place of the calcium silicates in OPC. It may be mixed with OPC to accelerate strength while maintaining self-leveling, and to provide resistance to heat and chemical attack. CAC is considered to be a hydraulic cement and not chemically bonded (Wagh 2016). Calcium and alumina are combined to form Ca-aluminate hydrate as the bonding phase. CSACs have exceptional early strength development and durability.

Calcium Sulfoaluminate Cement (CSAC)

Ca-sulphoaluminate cement is a variant of CAC that includes sulfate from a source such as gypsum, that promotes the growth of crystalline ettringite. CSAC provides similar advantages to CAC with the addition of sulfate resistance. Whereas ettringite is stable, the presence of abundant sulfate in the canister environment could promote microbial activity (e.g., *Desulfovibrio sp.*) and/or the formation of corrosive H_2S. This comparison may not be relevant to filler performance, however, it is considered as a complicating factor in the discussion below. CSAC is also considered to be a hydraulic cement and not chemically bonded, although it derives chemical stability from ettringite.

The foregoing categories of cements are listed in Table 8, which provides compositional information and possible variations for testing. Status of the testing program is presented in Section 8.

5.2.2 Comparison of Cement Slurry Fillers

Qualitative comparison of the cement types discussed above is provided in Table 9. Differences among the candidate types include

Injectability

- All cement types identified are injectable if mixed with enough water (which degrades other properties such as porosity and radiolytic gas generation).
- APC is a highly injectable slurry at temperatures less than approximately 100°C, and solidifies at higher temperature on the order of 150 to 200°C
- CPC probably requires development of a slurry with self-leveling properties and pumpability (the other types have already been developed as grouts).
- Differences in porosity may result from differences in the amount of water needed for injectability.

Void Filling

- All cement types rely on water as a vehicle and will wet the canister and fuel surfaces.
- Void filling will be superior for those recipes that have the least viscosity, and are self-leveling.

Long-Term Chemical Stability

- Chemical stability of CAPC and CPC may be superior because of Ca-phosphate bonds.
- Long-term chemical stability of OPC based formulations may be limited as there are few, if any, natural analogs of the same composition (compared with phosphate minerals).
- Stability of MKP cement has been extensively tested in nuclear waste encapsulation applications (Ceramicrete; Singh et al. 1997; Covill et al. 2011).

Retrievability/Recoverability

- Ca-phosphate and Mg-phosphate bonds can be dissolved with a dilute acid such as HCl.
- Dissolution of Ca-aluminate bonds and solubilization of the products has not yet been tested.
- Similar acidic conditions can attack OPC formulations but may leave insoluble residues.

Material Compatibility

- Material interactions will be examined in the manner of Milestone (2006).
- Material compatibility questions with OPC and CSAC involve the microbial utilization of sulfate.
- Material compatibility questions with CAC and CSAC involve the possible addition of alkaline salts to activate the alumina (cements containing phosphate have circum-neutral pH and may exhibit additional buffering).
- Ca-aluminate and Ca-phosphate, Al-phosphate, or Mg-K-phosphate formulations should not attack stainless steel or Zircaloy if the pH is circum-neutral both before and after set.
- Bonding to metallic surfaces and to previously poured cement, and controlled expansion/shrinkage, have been established for commercial binder products (Table 8).

Moderator Displacement

- Water content will be challenging for all aqueous cement slurry formulations, such that capacity to stabilize a neutron absorbing filler (e.g., B_4C) will be needed.

Gas Generation

- The presence of water and any organic constituents of cements may require measures to control radiolytic gas accumulation (which could build up gas pressure).

Solidification Temperature

- Solidification temperature has been studied for CAPC borehole cement (Wagh 2016) but needs to be evaluated for other formulations to assure that adequate set can be obtained following the temperature-time trajectory anticipated for fillers.

Toxicity

- Toxicity is low for all cement types considered.

Radionuclide Sequestration

- Actinides (U, Pu) are readily immobilized by phosphate in groundwater environments.

Material Cost

- Material cost could be low for OPC-based formulations, but greater for chemically-bonded cements requiring more expensive components.

Given the similarity of the cement types and their availability, representative compositions from each subgroup of cements (Table 8) will be selected for testing and screening.

Table 9. Comparison of slurry cement options on selection criteria (from SNL 2017).

Material	Injectability	Void Filling	Long-Term Chemical Stability	Retrievability/Recoverability[E]	Material Compatibility	Moderator Displacement	Gas Generation	Solidification Temperature	Toxicity	Radionuclide Sequestration	Material Cost	Potential Source
Generic OPC			–	?	–	–		?			+	Use commercially available products (e.g., Sika)
Magnesium potassium phosphate cement (MKP)				+		–		?		+		
Calcium aluminate cement (CAC)			?	?	?	–		?		?		Royal White Cement Co. (binder) Houston, TX 713/676-0000
Calcium sulfoaluminate cement (CSAC)			?	?	?	–		?		?		
Calcium aluminate phosphate cement (CAPC)			?	+		–				+		Halliburton Corp. (mixed cement product) Houston, TX /871-4000
Calcium phosphate cement (CPC)	?		+	+		–		?		+		

Notes:

[A] Boric or citric acid in dry form.

[B] Wagh 2004, Table 15-2.

[C] Wagh 2004, Section 13.4; TTCP is $Ca_4(PO_4)_2O$ and DCPA is $CaHPO_4$, mixed stoichiometrically for hydroxyapatite $Ca_5(PO_4)_3{\cdot}OH$.

[D] This is a qualitative table and the entries are approximate: "+" signifies desirable attributes, "–" signifies undesirable, and no-entry signifies neither.

5.2.3 Low-Melting Point Metal Alloys

Candidate metallic materials with natural analogue evidence of long-term stability include Bronze Age (~5,000 BC) and Iron Age (~1,300 BC) artifacts. Materials suitable for tools and weapons, have strength and thermal properties that may not be amenable to DPC fillers. However, there are a large number of low-melting temperature metals and alloys available, as suggested by the list in Table 10. While various types of glass are abundant in the geologic record and relatively stable, only two low-melting point glasses are included in this preliminary list.

Available Alloys and Sources

Metal/metal-alloy pours should have the following characteristics (e.g., Johnson et al. 1994):

- Possess no major defects, e.g. shrinkage voids.
- React minimally with DPC steels and cladding.

- Have low casting temperature to reduce thermal stresses.
- Wet steel and cladding surfaces to aid void filling.

Eutectic composition is desirable because the liquid-solid transition occurs at a discrete temperature, avoiding a “pasty” temperature band within which the mixture is neither uniformly liquid or solid. Defined melting-solidification temperature also occurs with pure metals. Even with eutectic compositions, a transition occurs whereby the mixture remains both partially liquid and solid, as the latent heat of fusion dissipates (cooling), or is provided externally (melting). Molten metals may exhibit substantial (a few percent) volume increase on solidification.

Metals

Low-melting point metals that can be used as fillers include tin, lead, bismuth, cadmium, and zinc. Melting points for tin, lead, bismuth, and cadmium are below 350°C. Zinc has a melting point of 419°C. Lead and cadmium are regulated materials and in particular lead is toxic, very heavy, and can cause embrittlement of other metal components. In addition, zinc has the potential to interact with fuel cladding. However, for this intended filler application potential cladding interactions may not be critical.

Metal Alloys

Low-melting point eutectics can be formed by combining the above metals in proper ratios. For example, the $Sn_{63}Pb_{37}$ alloy, a solder used in electronics, has a melting point of 183°C. A lead-free or cadmium-free eutectic, e.g., $Sn_{95.6}Ag_{3.5}Cu_{0.9}$ with a melting point of 217°C or $Sn_{91}Zn_{9}$ with a melting point of 199°C, should also be investigated.

Glasses

Glasses are known for their excellent chemical stability and can be a promising candidate as DPC fillers. Borosilicate glass is used extensively in vitrification of high level waste and it has been shown that fission product particulates are immobilized in glass matrix. However, common glasses have very high melting points (>1000°C), i.e., much higher than some canister components such as aluminum. Recently, low-melting point glasses have been formed with melting temperatures in the approximate range 220 to 400°C. For example, Vaneetect® with melting point less than 300°C or solder glass with melting point less than 400°C could be viable candidates.

Comparison of Molten Fillers and Recommendation for Testing

Qualitative comparison of the metal alloy types discussed above is provided in Table 11. This comparison is based on the following assumptions:

- Molten metals/metal alloys are expected to exhibit injectability and void filling performance as long as the canisters and fuel surfaces are wetted by the melt. Glasses may be more viscous and sticky (hence their description in the literature as sealants).
- For molten metal/metal alloy fillers long term chemical stability in the intact canisters is plausible, but remains to be tested for repository conditions after package breach and exposure to groundwater.
- Material compatibility may be questionable for metallic fillers due to possibility of galvanic reactions; on the other hand, metallic fillers may galvanically protect the fuel or waste package. Also, telluric currents in the disposal environment may be important.
- Glass is electrically non-conductive (which limits heating options).

Table 10. Candidate molten metal/metal alloy filler characteristics (from SNL 2017).

Label[A]	Composition	Melting Point (°C)[B]	Ref.
Pure Metals			
Tin	Sn 100%	232	1
Bismuth	Bi 100%	271	
Cadmium	Cd 100%	321	
Lead	Pb 100%	327	
Zinc	Zn 100%	419	
Alloys			
Low 117®	Sn 8.3% Pb 22.6% Bi 44.7% Cd 5.3% In 19.1%	47	2
Low 136®	Sn 12% Pb 18% Bi 49% In 21%	58	
Bend	Sn 13.3% Pb 26.7% Bi 50% Cd 10%	70	
Woods	Sn 12,5% Pb 25% Bi 50% Cd 12,5%	70 – 76	
Safe	Sn 11.3% Pb 37.7% Bi 42.5% Cd 8.5%	71 – 88	
Mellottes	Sn 15.5% Pb 32% Bi 52.5%	95	
Rose	Sn 25% Pb 25% Bi 50%	95 – 115	
Matrix®	Sn 14.5% Pb 28.5% Bi 48% Sb 9%	103 – 227	
Base	Pb 44.5% Bi 55.5%	124	
Pb36A	Sn 62% Pb 36% Ag 2%	179	3
Pb37A	Sn 63% Pb 37%	183	
PB40A	Sn 60% Pb 40%	183 – 191	
Sn10A	Sn 10% Pb 90%	275 – 302	
Sn03A	Sn 3% Pb 97%	314 – 320	
Pb94B	Sn 5% Pb 93.5% Ag 1.5%	296 – 301	
Alloys (lead/cadmium free)			
Tru®	Sn 42% Bi 58%	138	2
Cast®	Sn 60% Bi 40%	138 – 170	
KappAloy9®	Sn 91% Zn 9%	198	1
Tin foil	Sn 92% Zn 8%	199	
Indalloy®	Sn 95.6% Ag 3.5% Cu 0.9%	217	
Sn96A	Sn 96.3% Ag 3.7%	221	3
AG40B	Zn 96% 4% Al	381-387	1
Glasses			
Solder glass	PbO-B_2O_3	320-380	4
Glasses (lead free)			
Vaneetect®	VO-Ag	220-300	5

[A] ANSI/J-STD-006 or other. [B] A single value signifies eutectic composition.

References:

[1] http://www.matweb.com

[2] www.belmontmetals.com/product/eutectic-alloys

[3] www.ami.ac.uk/courses/topics/0128_sm/index.html

[4] www.telux-glas.de/content/en/downloads/solder-glass.pdf

[5] phys.org/news/2012-11-300c-low-melting-glass-hermetic-gold-tin.html

Table 11. Comparison of molten metal/metal alloy and glass options on selection criteria (from SNL 2017).

Material	Injectability	Void Filling	Long-Term Chemical Stability	Retrievability/Recoverability	Material Compatibility	Water Content	Gas Generation	Solidification Temperature	Toxicity	Radionuclide Sequestration	Material Cost	Recipe Guidelines (w/w %)	Potential Source
Pure Metals (Sn, Bi, Cd, Pb, Z)			+	?	?	+	+	–		?			
Metal Alloys			+	?	?	+	+		–	?	–	Sn based alloys: Sn: 3-60% Pb: 15-95% Cd, Bi: as needed Pb based alloys: Pb 44.5% Bi 55.5%	Belmont Metals Inc. 330 Belmont Avenue Brooklyn, NY 11207
Metal Alloys (Pb- and Cd-free)			?	?	?	+	+			?	–	Sn based alloys: Sn: 40-95% Zn, Bi, Ag, Cu: as needed Zn based alloys; Zn: >90% Al: as needed	
Glasses (e.g., solder glass)	?	?	+	?	?	+	?	–	–	?	?	PbO-B_2O_3	TELUX Spezialglas GmbH Weißwasser, Germany
Glasses (lead free)	?	?	?	?	?	+	?			?	?	VO	Hitachi Chemical Co., Ltd.

"+" signifies desirable attributes, "–" signifies undesirable, and no-entry signifies neither.

Notes:

1. This is a qualitative table that lumps together filler materials without distinguishing their differences, so the entries are approximate. For example, material costs for the pure metals shown vary widely and are shown as neither desirable nor undesirable, whereas material costs for metal alloys are shown as undesirable due to the market prices of Sn and Bi which are needed for most low melting temperature alloys.
2. Injectability and void filling could be desirable attributes for metal/metal alloys, depending on wettability as discussed in the text.
3. Retrievability/recoverability is uncertain due to the possibility that remnants of the filler would essentially solder or seal fuel into the basket.
4. Solidification temperature is shown as undesirable, or neither, because of the burden of dealing with higher temperature (compared to cement fillers).
5. Toxicity is shown as undesirable for material categories likely to include Pb, and neither for others.

- Metals will likely not produce gas after solidification and prior to package breach (when gas pressure is important to canister integrity). However, off-gassing of glass from aging and radiation dose may be possible
- Pure metals and typical glasses have higher solidification temperatures than metal alloys, particularly eutectic compositions.
- Metals, alloys and glasses are particularly toxic if they contain Pb or Cd, although not all candidates contain these elements.
- Material cost will be higher if the filler contains much Sn or Ag. Cost of Vaneetect® glass is unknown.
- Some compaction following solidification is likely for metal-based fillers.
- Handling is uncertain due to heating requirements.

Molten metals/metal alloys require development of handling and heating capabilities to avoid premature solidification during filling.

Given the similarity of the molten metal types and their availability, representative compositions from each subgroup identified above will be selected for further investigation.

6. SIMULATION OF DPC FILLING

The following material is excerpted from: *Dual-Purpose Canister Filling Demonstration Project Progress Report*, by Nesrin O. Cetiner, Emilian Popov, Eliott J. Fountain, Venugopal K. Varma, Abiodun I. Adeniyi, and Kaushik Banerjee, all of Oak Ridge National Laboratory (deliverable M4SF-18OR010305017, issued as report ORNL/SPR-2018/906). Minor edits have been included for clarity, and some discussion of work in progress has been omitted. The reader is referred to this document and another recent report (Cetiner et al. 2018b) for more detail.

The objectives of the filling simulations are: 1) to numerically analyze the filling process, initially on ideal surfaces, 2) to determine remaining voids and filling times, and 3) to identify potential problems. Simulations provide the flexibility needed to experiment with different liquids (metals) and surrogates, to explore filling methods based on existing or new canister features, to aid the experiment design by scaling major quantities.

A canister test section was developed and simulated (Figure 10). It represents the lower 16% of a real canister (height 74 cm, diameter 26 cm), and it includes the passages among the assembly shrouds (mouse or limber holes), the support stands (assembly spacers), the assembly lower grids, and the first set of assembly spacer grids. The design uses a 5 × 5 rod array to representative a PWR fuel bundle (which can have a 17 × 17 rod array but has similar spacings between rods). A circular container encloses five 5 × 5 bundles and includes the geometric features important for full-scale canister (Holtec 2010).

The simulation employs a 3D computational fluid dynamics (CFD) method for a two-phase two-component system in isothermal condition. The gas (helium) and the liquid (metals) front propagation is resolved by solving a viscous flow of mixture (CD-Adapco 2015). To implement this approach, the commercial software STAR-CCM+ is selected (https://mdx.plm.automation.siemens.com/star-ccm-plus).

Two types of materials are considered as filler candidates. ORNL is investigating low melting temperature metals and surrogate liquids, and Sandia National Laboratory is studying the use of slurries (concrete mixtures). An initial list of fillers used in numerical simulations is given in Table 12. Note that these are not necessarily candidates for final application but are mainly for numerical simulation in the simple unit test for validation. Two transport properties are important for this phase of the filling evaluation: density and dynamic viscosity. Silicone oils are highly ranked candidates due to their low cost and the large available selection of viscosities.

One half (central symmetry) of the geometry in Figure 10 is initially considered. It has a volume of 11.46 liters, which is about 6.5 less than a full-scale canister. For an estimate of 17 hours for filling a full-scale canister, the scaled filling rate for the half-symmetry model is determined to be 1.26 cm^3/sec (the filling rate for an experiment based on Figure 10 would be 2× greater). The Reynolds numbers (Re) for such filling rates and length scales, which are typical for rod bundles, are in single digits at Re~3, which justifies the laminar flow assumption. The entire geometry was modeled initially, resulting in a computational grid consisting of about six million elements. Liquid was injected into the model at the bottom of the drain pipe (Figure 11). A velocity boundary condition was defined at the drain pipe orifice (area 180 mm^2) with a velocity magnitude of 1.26/180 = 0.007 m/sec. Thus, the filling simulation was separated from the drain pipe simulation. The flow regime in the vertical drain pipe is currently under investigation.

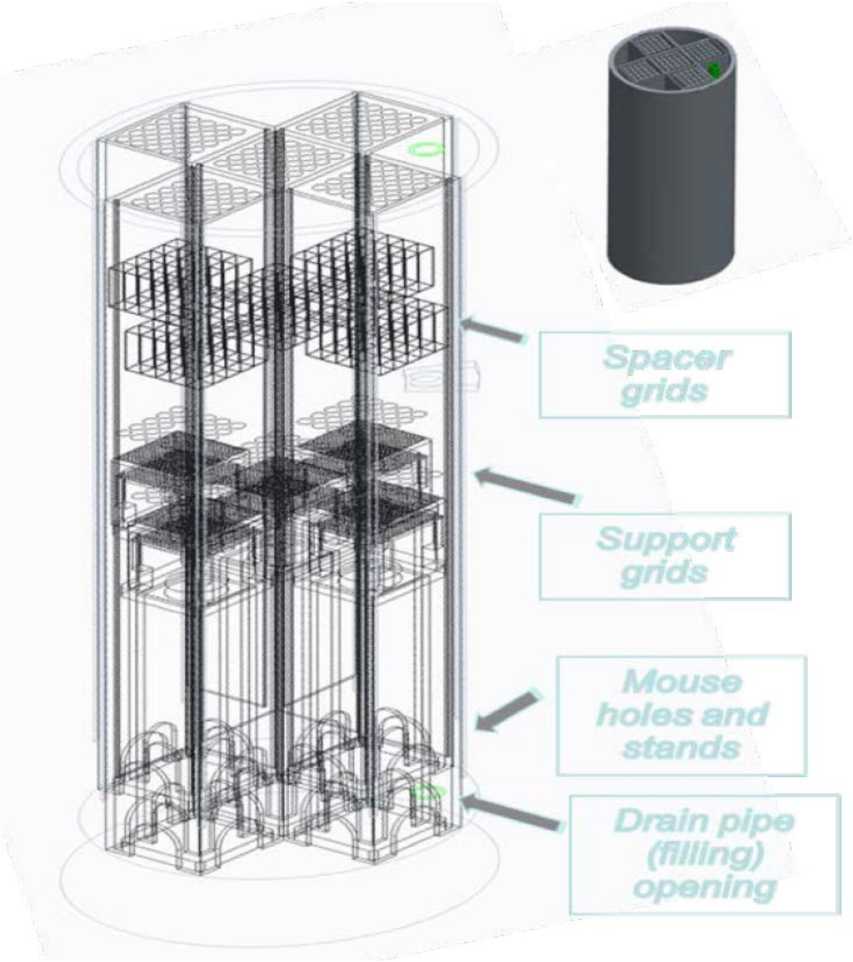

Figure 10. DPC mockup (based on 5 × 5 bundles) of the lower section of the real canister, including mouse holes, supports, lower assembly grid, and one spacer grid (from Cetiner et al. 2018a).

Calculations were run in parallel on 32 to 640 computing processors. To capture the liquid level progression the time step was kept between 1 and 5 msec. The shortest runtime during this preliminary phase was 0.7 hour for one second of the filling simulation. Filling the entire geometry would take days of computing, so the strategy was changed. The major objective of a filling simulation is to predict the level progression and the void removal. Both of these occur near the current level position. The areas of computational domain below and above the level have little-to-no influence on the filling, but they consume computing resources. To reduce the computing burden, the domain was decomposed into smaller regions, and a data mapping algorithm was applied. The regions overlap, and the velocity and the void fraction (liquid) were mapped from one region to another. The canister geometry further facilitates this approach because the area above the mouse holes is composed of parallel channels (bundle region), and only one channel can be modeled. This radically reduced the computing load.

Table 12. Preliminary list of liquids for testing and filling simulations (from Cetiner et al. 2018a).

Material	Melting Temp. (°C)	Density (g/cm^3)	Viscosity (Pa·s)	Reference
Glycerin ($C_3H_8O_3$)	Liquid	1.26@RT^A	0.95@RT^A	www.MatWeb.com
Silicon oil	Liquid	0.96@25C	0.33@25C	www.sigmaaldrich.com
Lead	327 (600K)	10.70 @600K	0.0026@600K	Sobolev (2007)
Lead-bismuth	124 (398K)	10.53 @398K	0.0032@398K	Alchagirov et al. (2003)
Mercury	Liquid	13.53@RT	0.0015@RT	"Thermal Fluids Central"
Water	Liquid	0.997@RT	0.00088@RT	Web (for comparison)
RT = room temperature (~20°C)				

Calculations are run in parallel on 32–640 computing processors. To properly capture the liquid level progression, the time step must be kept between 1–5 msec. The shortest runtime during this preliminary phase was 0.7 hour for one second of the filling process. Filling the entire geometry would take days of computing, so the strategy was changed. The major objective of a filling simulation is to predict the level progression and the void removal. Both of these occur near the current level position. The areas of computational domain below and above the level have little-to-no influence on the filling, but they consume computing resources. To reduce the computing burden, the domain is decomposed into smaller regions, and a data mapping algorithm is applied. The regions overlap, and the velocity and the void fraction (liquid) are mapped from one region to another. The canister geometry further facilitates this approach because the area above the mouse holes is composed of parallel channels (bundle region), and only one channel can be modeled. This radically reduces the computing load.

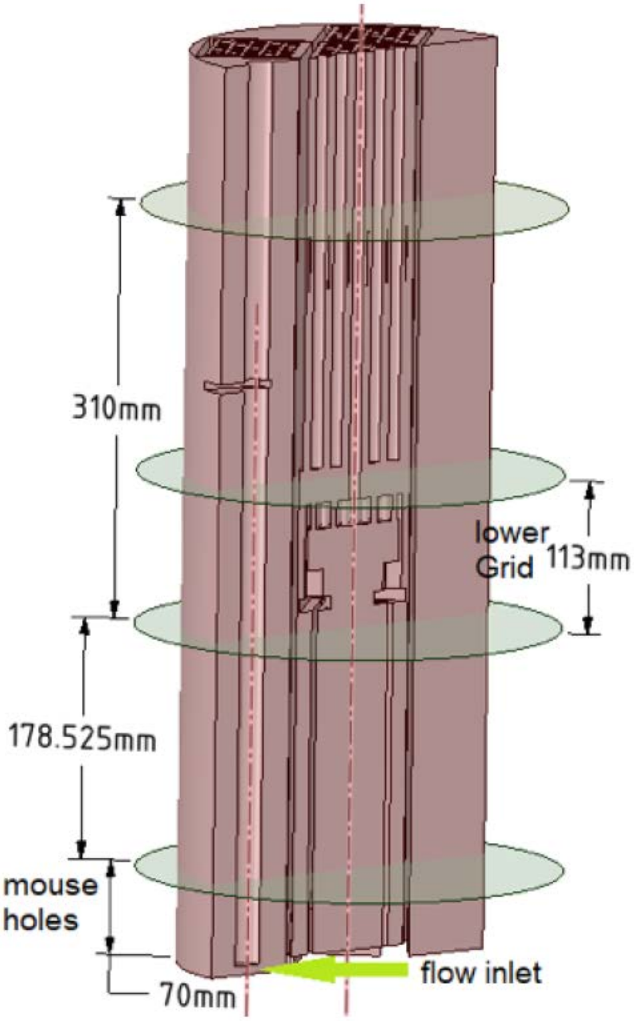

Figure 11. Model split indicating sections of the geometry modeled (from Cetiner et al. 2018a).

6.1 Filling of the Mouse Hole Region

First the mouse hole region was separated and modeled using a polyhedral grid of about 45,000 elements. The objective of this simulation was to demonstrate that the mouse holes can be successfully filled if the drain pipe opening provides a continuous constant flow of 1.26 cm^3/sec. The runs were performed on 32 processors for ~5 days (average runtime is 0.12 hour/sec of transient simulation time) with a time step of 5 msec. Simulations of the following liquids have demonstrated successful filling of voids in the mouse-hole region: glycerin, lead-bismuth, silicone oil, and mercury. Mercury (Hg) is not a practical option for full-scale application, but due to its low viscosity and high density it is a bounding case for the simulation. No noticeable level deformations were observed when different liquids were used. Figure 12 plots sections of the mouse-hole region for two liquids: molten lead-bismuth (Pb-Bi) and silicone oil. Even though the densities of these liquids differ by about 10× and the viscosities differ by about 100×, the filling progressed the same. The plot shows the liquid level at 400 sec and at the end of the simulation

(1020 sec), when the liquid level was at the middle and at the top of the mouse holes, respectively. The volumes of injected liquids at 400 sec are the same: 496.5 cm^3 for silicone oil, and 498.2 cm^3 for Pb-Bi, and no differences in filling are noticeable. Small differences between the results are attributable to local computational inaccuracy; the filling rate is the same for both liquids.

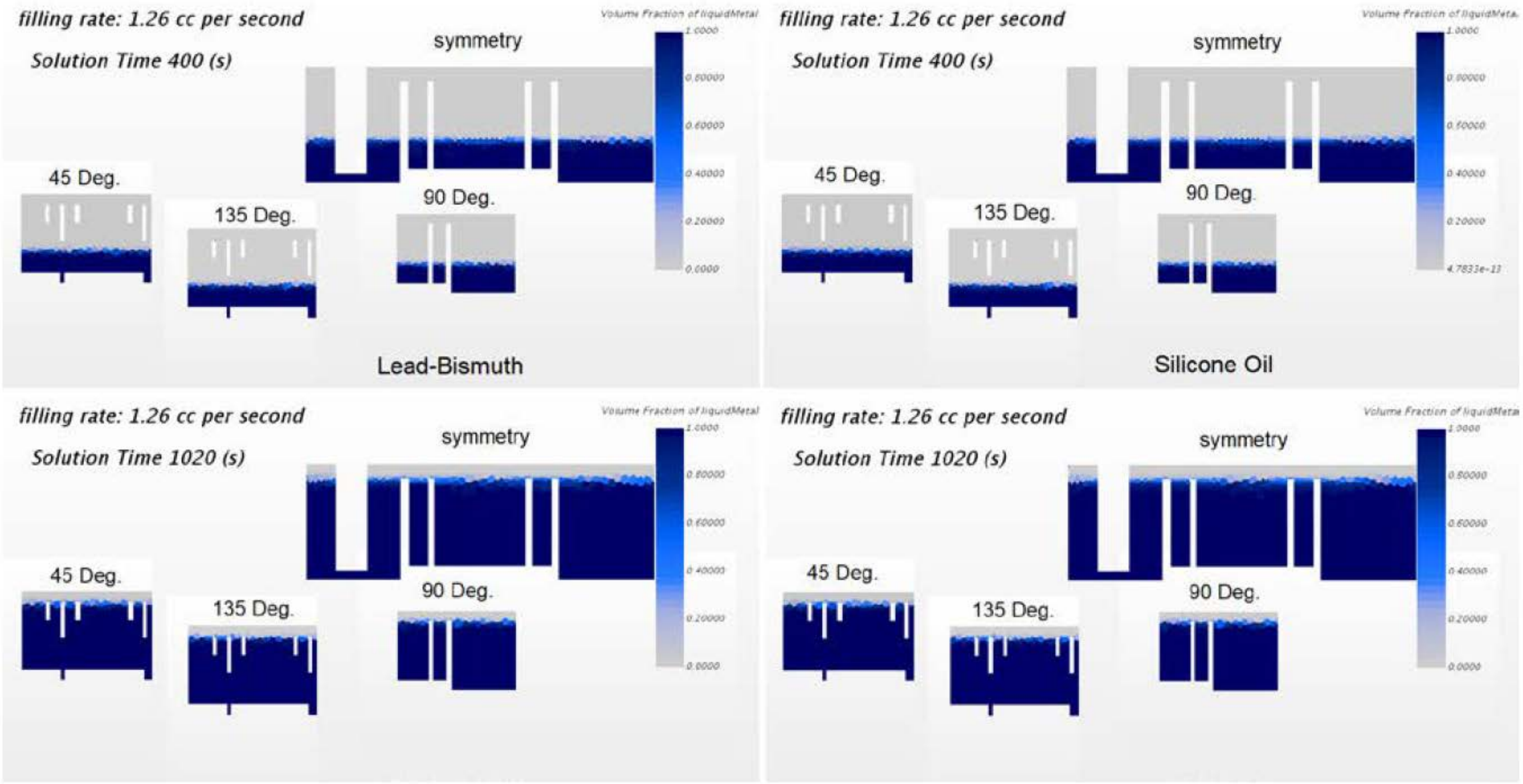

Figure 12. Liquid levels at 400 and 1,020 sec (the ends of two transient from two runs with different liquids). Left: lead-bismuth alloy; and right: silicone oil. Plots show contours of levels at several sections of the mouse hole region with symmetry (45-, 90-, and 135-degree cross-planes) (from Cetiner et al. 2018a).

Even though the silicone oil density was much less, it allowed for the liquid to find its level smoothly cover the entire region. The filling level velocity of 4.2 mm/min is such that the viscosity/density combination of the liquids does not affect the filling process. A detailed examination of the plotted sections does not show the presence of any voids. The same is confirmed by the overall volume balance, which is controlled during the simulation.

An isometric view of the simulated section is shown in Figure 13. The top wall and the symmetry planes are removed for better visibility inside the domain. As represented, each individual fuel assembly is confined in a separate cell, and the cell walls do not allow for cross flow. The parallel cells begin just above the mouse hole region, and the mouse holes are the only flow passage that permits liquid to enter the fuel cells. In order to properly simulate the filling of these individual cells, an extra volume is artificially added on top of this section to connect the parallel cells. This volume is not filled and does not affect the overall filling time or mass balance.

The views in Figure 13 provide another look at the filling process in the mouse hole region of the canister. This is the region where the fuel cells interconnect. The view on the left shows an early stage of filling in which the central part is still not flooded. The liquid initially propagates on the circumference around the outside wall before entering the central area. Even though that space is narrow, the liquid can freely penetrate the space and distribute evenly in the remainder of the domain. The right view in Figure 13 shows a later stage in which the mouse holes are partially filled. By observing the levels in different cells, one can conclude that the level rises evenly in all cells. Although the resolution of the model is low (to limit computation time) the numerical scheme used (high resolution level tracking) maintains the level within 1 to 2 grid elements. No numerical diffusion is observed due to the second order upwind scheme used to run the simulations. Note that the interface between the gas and liquid cannot be sharper than one element (the liquid boundary to match the element boundary) because the numerical method treats the liquid as a fraction of the total fluid, and as the level crosses an element the void fraction increases from 0 to 1 before the element is completely filled. This explains the different color of gradient in the elements near the level.

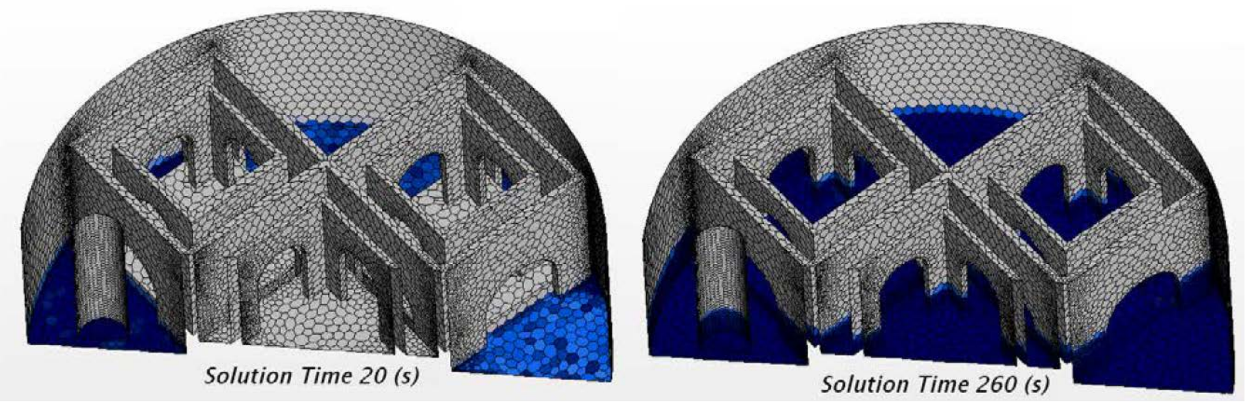

Figure 13. Liquid content during filling of the mouse-hole region at 20 and 260 sec. Total filling time = 1,040 sec; the computational grid is also shown (from Cetiner et al. 2018a).

An important aspect of the filling calculations is the accuracy of the solution, given the relatively coarse domain discretization. To address this question, mass in the system is monitored during the simulation. The result for three test liquids (Pb-Bi, Si-oil, Hg) shows that the error varies within

1.5%. In the simulation, the model fills for 1,040 sec while the actual filling time is 1,024 sec (Figure 14). The error tends to increase toward the second half of the process, and could be due to the grid becoming larger in the space over the mouse holes. Usually element size is driven by the geometric features and to resolve small details more elements are used. Once details such as the mouse holes are gridded, the elements are larger in the spaces over the mouse holes, which increases the error locally but it remains within practical limits. In view of the long filling times, such a small difference could be acceptable.

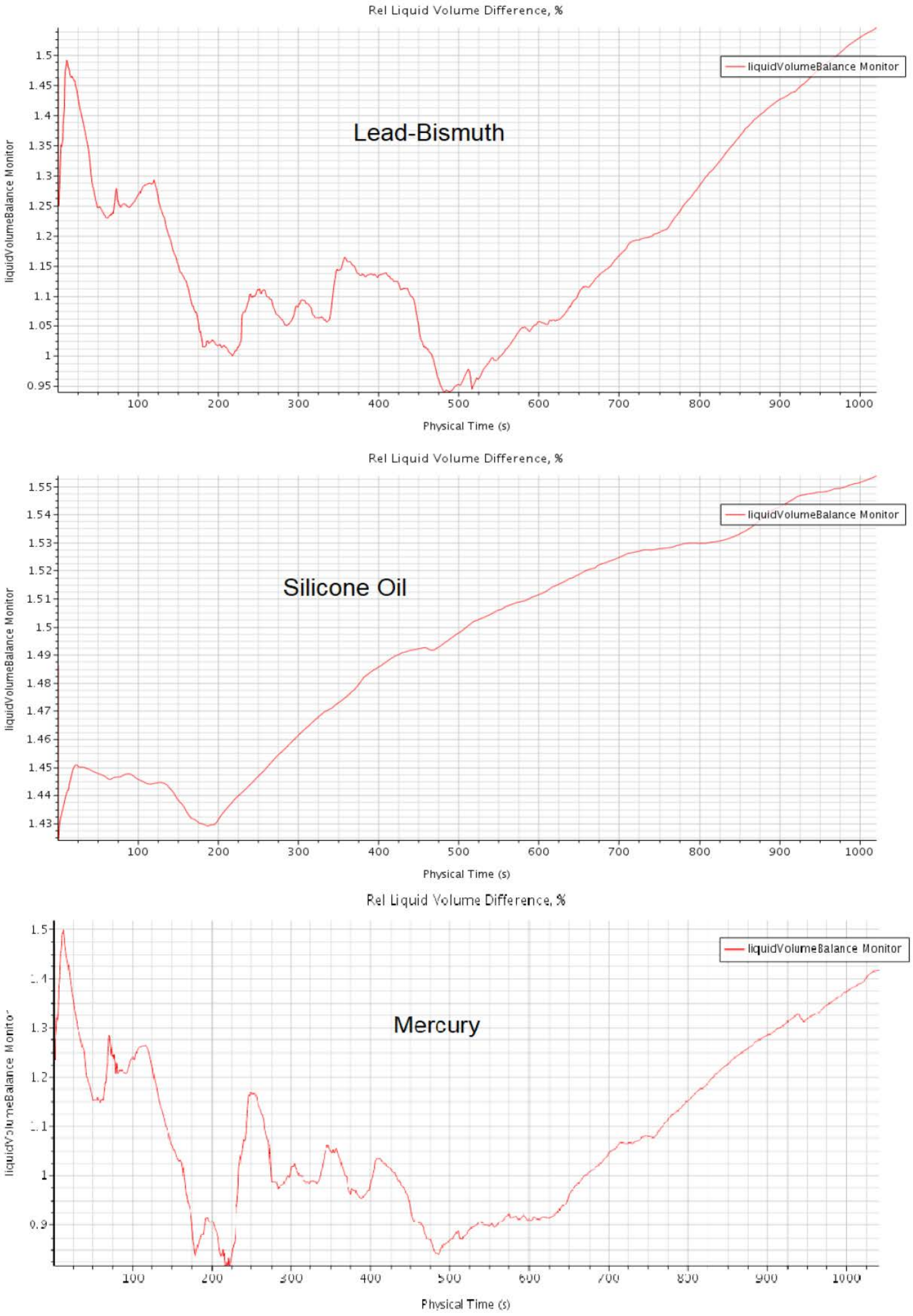

Figure 14. Mass error evolution during filling of the mouse hole region with Pb-Bi (top), silicone oil (middle), and mercury (bottom) (from Cetiner et al. 2018a).

6.2 Lower Grid Filling Simulation

As shown in Figure 15 upstream of the mouse holes there is a section (~180 mm) where the geometry does not change. The fuel assemblies are placed in the canister on rectangular supports that separate them from the canister floor. After filling of the mouse holes has been successfully demonstrated, there is no need to carry the numerical solution in that region because no new geometry features exist. Instead, this section is skipped by shortening the domain to save computing time. The level, which is computed in the region below (mouse holes), is transposed as an input condition, assuming it has the same topology. The rationale is based on the fact that no specific features of the level are observed, like moving or standing waves, substantial radial convection, etc. The liquid front propagates in all cells with the same velocity. Technically, this is accomplished by mapping data between nonconformal domains, which is challenging in CFD computing, but it can be done. This approach is followed in the present analyses.

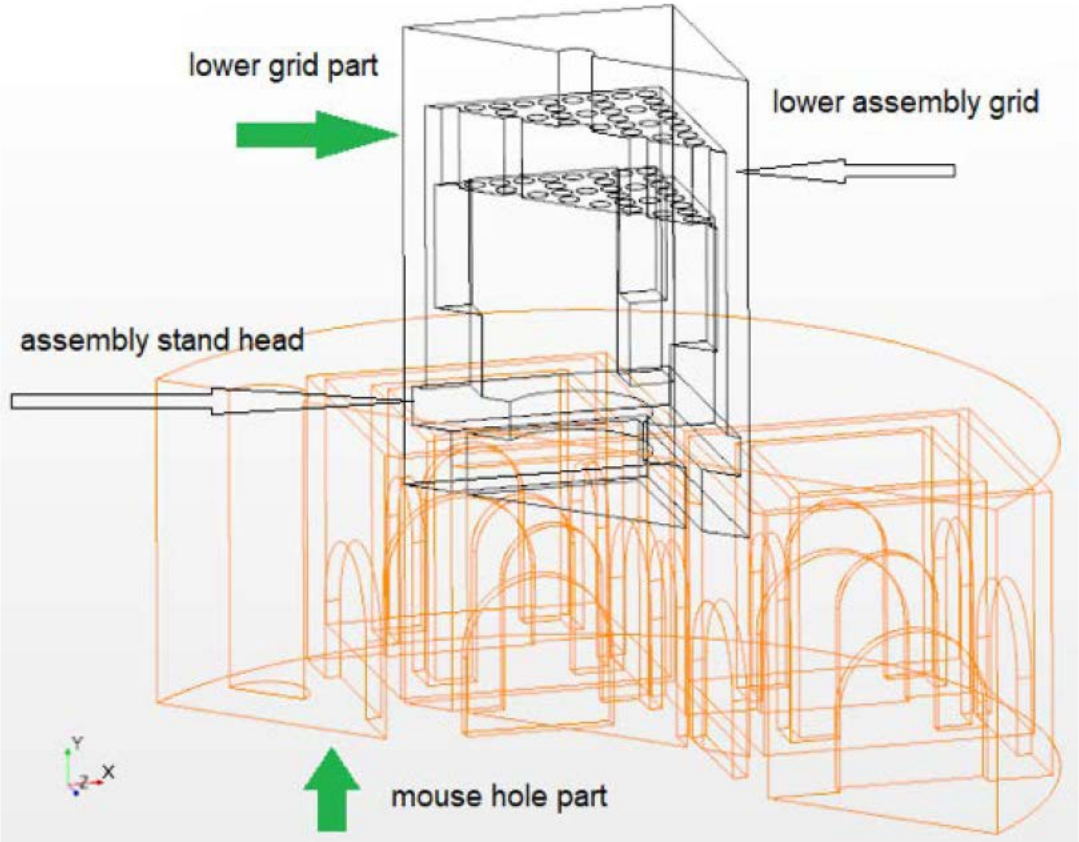

Figure 15. Lower grid and its relative position to the mouse hole region used in the simulation (from Cetiner et al. 2018a).

The simulated section is shown in Figure 15 and is labeled lower grid because the most representative feature of that region is the lower fuel assembly grid. This grid includes several small holes that, in the reactor design, were originally meant to provide more even flow distribution. These holes may pose a problem in the filling process and will require special attention. The modeled section also includes the upper part of the assembly stand and the transition region. It is part of one of the five 5 × 5 bundles, sufficient to study the flow.

More detail about these components and their relative positioning is shown in Figure 15. The mouse hole region is shown with different colors to distinguish the components. The section has an overall height of 113 mm. It is set to overlap the mouse hole region, with 15 mm to allow for data mapping. The overlap is shown in Figure 16. The lower grid section is meshed with about 100,000 elements, which is more than the mouse hole region, because of the holes in the lower assembly grid.

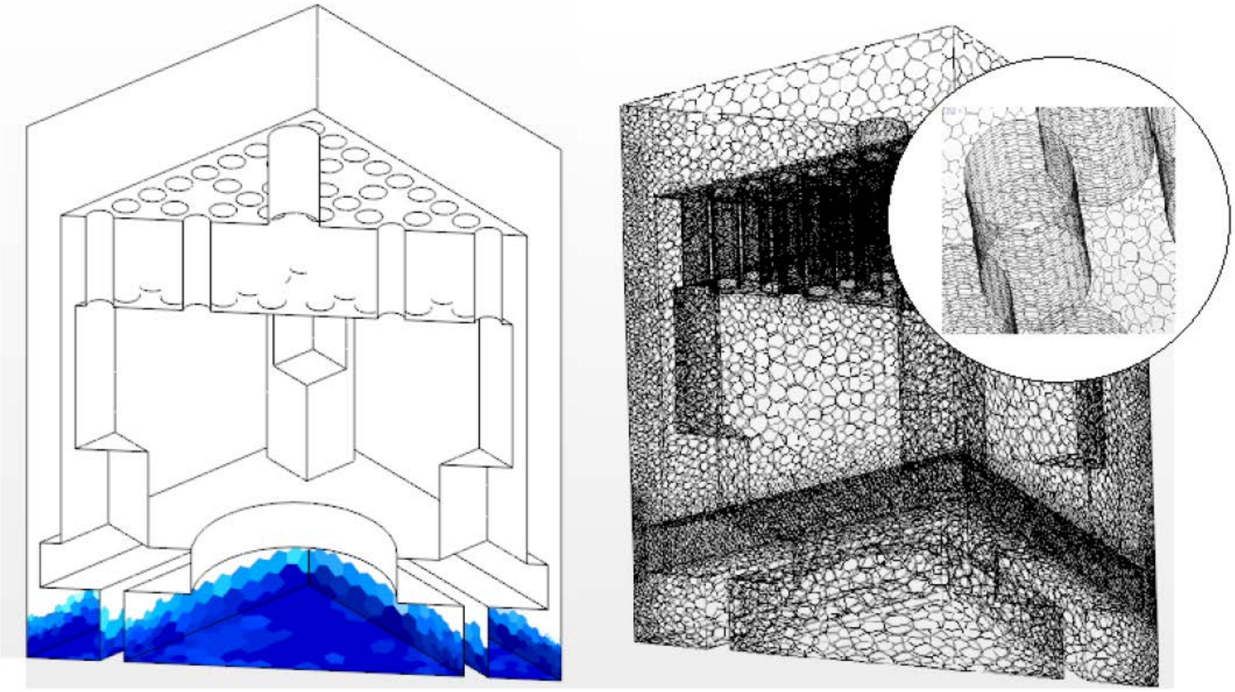

Figure 16. Initial liquid fraction as mapped from the mouse hole region (left), and computational mesh of the lower grid region with a zoom into the hole area mesh (right) (from Cetiner et al. 2018a).

To provide continuity of the filling process, two variables from an existing solution in the mouse hole region must be mapped to the lower grid region. One of them is the current level, expressed as liquid volumetric content (fraction of total fluid). The level is usually spread across at least three layers of elements, which determines the mapped domain. Figure 16 shows the outcome after the mapping is performed. A partial level of data only in the central cell is mapped to the lower grid region. It covers part of the bundle support fluid volume just below the lower grid. The volume of this initial liquid is 15 cm^3, and it must be accounted for in the over-volume balance during the simulation. The computational mesh is demonstrated in Figure 16 with a zoom into the lower grid holes. The geometry is captured in full detail, resulting in an increased element count.

The second variable that must be transferred from the previous solution is the velocity vector at the inlet of the new section. A close examination of velocity vectors in a plane just above the mouse holes (Figure 17) shows a random high frequency distribution of instantaneous velocities. The dominant magnitude is around 0.05 m/s, with no preferential direction. The insert window in Figure 17 enlarges the velocities in the mapped area and shows the computational grid. Such a velocity profile is calculated by the viscous solution when no ensemble time averaging of velocity is performed. The difference between the instantaneous velocity and the axial average velocity (~4mm/min) indicates that a small-scale turbulence is computed in a general laminar flow. Further examination of the velocity contours in the mouse hole region does not indicate formation of eddies, indicating that the flow is not turbulent. The Re numbers for that region, based on the level velocity and typical length scales (~70mm), are ~15. This finding requires more attention and further analysis of the origin of these fluctuations, which are most likely numeric.

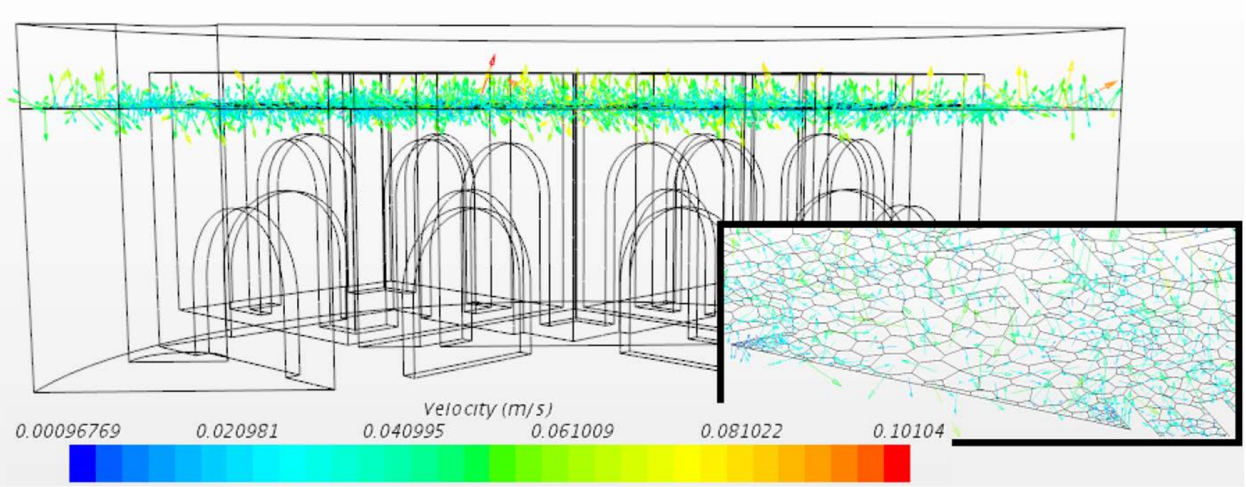

Figure 17. Velocity vectors of the advancing liquid level on a plane just above the mouse holes. The random fluctuation of liquid is noticeable, with no preferential direction. The inset shows the mesh and the velocities in the mapped region (from Cetiner et al. 2018a).

Based on the results discussed above, instantaneous velocities are not suitable as a boundary condition for the lower grid region unless they are time averaged. Instead of time averaging, the velocity at the inlet section of the lower grid region is calculated after the filling rate for the same region is calculated. Additional data are needed to perform this calculation, as summarized in Table 13.

Table 13. Geometry data for the lower grid section and for the entire geometry with the same axial elevations (from Cetiner et al. 2018a).

Parameter	**Value**
Volume of lower grid region	224 cm^3
Axial height of lower grid region	113 mm
Inlet flow are of lower grid region	2137 mm^2
Local volume of entire geometry (113 mm)	2047.8 cm^3
Overall filling rate for the entire model	1.26 cm^3/sec

The approach is based on calculating the overall time for filling a section of the entire geometry with the same axial marks as the lower grid section: 113 mm. The filling time of the entire geometry with 113 mm height = volume (local) of entire geometry / overall filling rate:

$$T_{total} = 2{,}047.8/1.26 = 1{,}625 \text{ sec}$$

If the same filling time is valid for the lower grid section of the geometry, then a part specific filling rate can be calculated:

$$\text{Filling rate (lower grid)} = \text{volume of lower grid} / T_{total} = 224 / 1625 = 0.138 \text{ cm}^3/\text{sec}$$

Once the part-specific filling rate is known, the inlet velocity is calculated:

Inlet velocity for the lower grid section =

Filling rate (lower grid) / inlet flow area =

$$0.138 / 2137 = 6.45\times10^{-5} \text{ m/sec}$$

This velocity is slightly lower than the level advancement velocity of 4.2 mm/min (7.0×10^{-5} m/sec) mentioned before. The difference appears because the flow area in the lower grid section is smaller than the average flow area in the same section of the entire geometry. The inlet velocity is applied to the inlet geometry of the lower grid section together with mapping the level from the mouse hole section. These two initial conditions are sufficient to perform the calculations. The mapping is successfully accomplished following a code-specific procedure, and the analyses runs are planned to be initiated.

6.3 Summary Discussion

The filling simulations that have been performed on the lower region (mouse holes) of a prototypical DPC show successful filling of the inner void space and smooth, uniform liquid level progression, for a wide range of fluid properties. The problem requires intensive computing and is a good candidate for a high-performance computing application. Future work could include filling the upper regions of the canister, assessing options for filling through the drain pipe, and model validation on lab-scale experiments.

7. LABORATORY FILLER DEMONSTRATION CONCEPT

The following material is excerpted from: *Dual-Purpose Canister Filling Demonstration Project Progress Report*, by Nesrin O. Cetiner, Emilian Popov, Eliott J. Fountain, Venugopal K. Varma, Abiodun I. Adeniyi, and Kaushik Banerjee, all of Oak Ridge National Laboratory (deliverable M4SF-18OR010305017, issued as report ORNL/SPR-2018/906). The original report has been abridged for presentation here, and the reader is referred to the source and another report (Cetiner et al. 2018b) for more detail.

ORNL has further developed an experimental design to study filling a DPC through its drain pipe, which can be used with one or more well-characterized liquid materials. The experiment is intended to initially provide integrated data such as filling time and entrapped void fraction. Two experimental setups have been devised for initial testing. The first will represent the computational model described in Section 6, with the exception that certain mechanical features such as spacer grids will be represented in more realistic detail. This setup is also intended to provide supporting data for injectability of various fluids through the drain pipe, identify a sustainable filling rate, and measure filling time and entrapped void space. Fluids used will be similar to those analyzed using CFD (Table 12).

The second experimental setup is intended to provide insight into the formation of voids in intricate geometries, such as the small and irregular spaces between the fuel rods and the springs and dimples in spacer grids. The primary focus of this setup is to provide a flexible experimentation capability while being as close to the real geometric configuration as possible. A salient feature of the second experimental setup is its modular construction and its easy disassembly. This setup will use a surrogate filler material with a low melting point, such as the paraffin wax, which melts at 37°C. This will allow for visual inspection of the filled volume, particularly to understand coalescence of multiple smaller void formations into larger voids.

The DPC filling tests will be scaled down models to expedite testing and minimize cost. The initial phase of testing will involve the use of liquid (water/glycerin) media to test the experimental design and validate CFD simulation results. Three types of spacer grids were procured by ORNL from Westinghouse: 1) a 17 × 17 standard structural grid, 2) a protective (P)-grid, and 3) an intermediate flow mixer (IFM) grid. Custom spacer grids are also being fabricated through a subcontractor to closely match the specifications (Weichselbaum et al. 2018). The custom fabricated spacer grids will be used in initial experiments, while the Westinghouse spacer grids are planned to be used for later tests.

The second experimental apparatus is expected to deviate only slightly from the first. Use of paraffin will allow components of high interest to be removed and disassembled to analyze the filled space. The paraffin will require external heating like any molten filler material. The spacer grids for this experimental setup will be custom fabricated so as to allow complete disassembly for post-experiment visual inspection (and cleaning).

The apparatus for both experimental setups will make use of transparent polycarbonate and acrylic materials to facilitate observation of tests, and for ease of fabrication. An example concept schematic for the second setup is shown in Figure 18. The key quantities of interest for these initial experiments are filler flow rate, filling time, and volume of entrapped gases. Additional details of the experimental apparatus design, including the simulated modular spacer grids, are provided by Cetiner et al. (2018a).

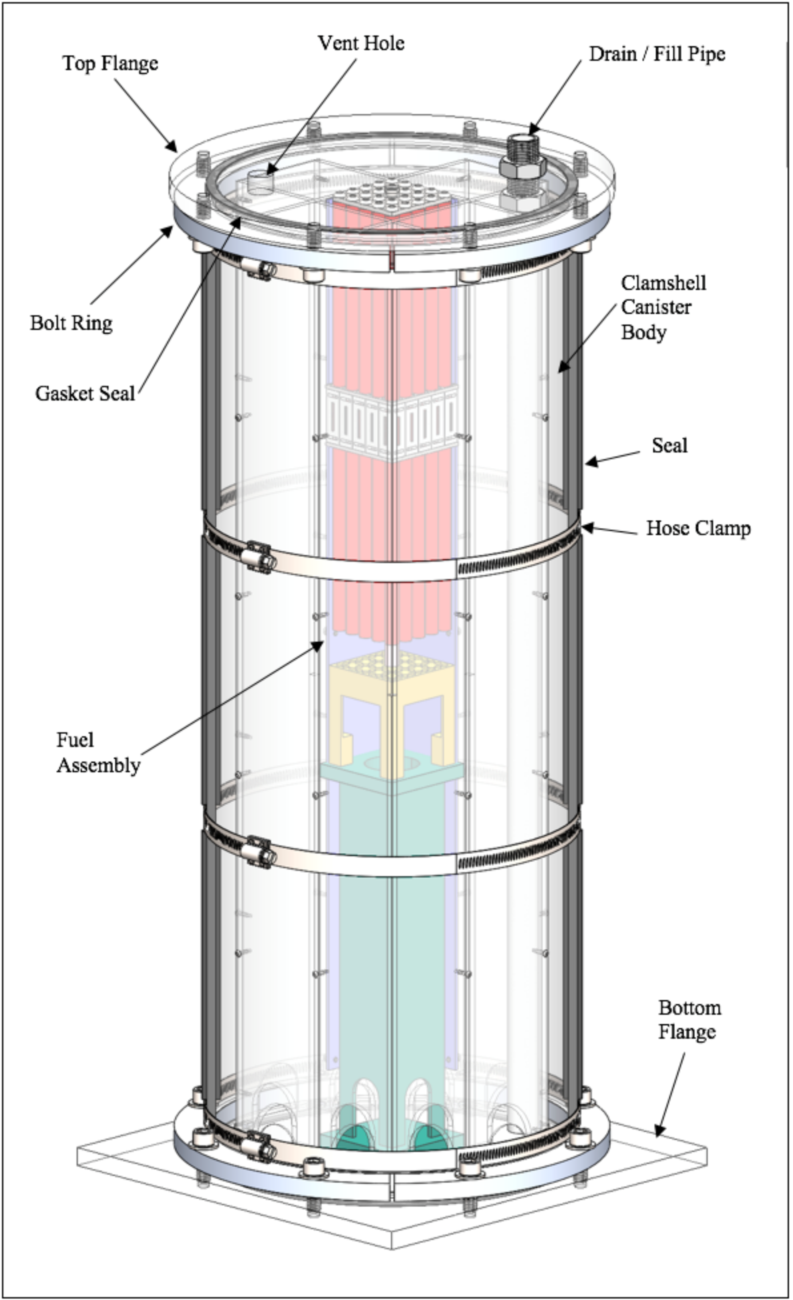

Figure 18. Polycarbonate canister with 5-cell basket for paraffin experiment (from Cetiner et al. 2018a).

8. STATUS OF EXPERIMENTAL PROGRAM FOR CEMENT SLURRIES

8.1 Status of Experimental Program for Cement Slurries

Since its inception in June, 2018 the DPC cement filler experimental program has focused on staff safety training, selection of the initial cement types, experimental equipment and materials purchases to initiate experiments, Job Safety Analysis (JSA) for cementitious filler compositions, and early experimental results.

The cement types selected for the experimental program (Hardin 2018) are discussed below.

JSAs for each cement formulation are under development. The JSA for the Bindan 3.1 binder cement mix has been completed and experiments are underway as described below. A draft of the aluminum phosphate cement (APC) JSA is provided for information (Appendix A). For curing of APC at temperature and pressure, a Pressure Safety Data Package (PSDP) is also under development.

Bindan 3.1 Binder

The experimental core fabrication has been initiated with the use of Bindan 3.1 binder. The binder powder mix consists of the following composition:

- 55% monopotassium phosphate (KH_2PO_4)
- 23% MgO P98, magnesium oxide
- 3.6% TCP, tricalcium phosphate ($Ca_3(PO_4)_2$)
- 9.4% sucrose
- 9% boron carbide
- Water (16% of total dry powders)

In should be noted that the presence of boron carbide (B_4C) with its high neutron absorption cross section, makes it an important material when considering criticality analyses. This cement was developed for nuclear applications involving storage of fissile material.

Aluminum-Phosphate Cement (APC)

The starting APC recipe for screening is based on Wagh (2016) deep/geothermal cement:

- 49% calcined alumina (Al_2O_3, e.g., 10-50 μm)
- 1% aluminum hydroxide ($Al(OH)_3$) as pH buffer and nucleant
- 50% Class F fly ash
- H_3PO_4 solution (50% w/w with water): ~45 mL per 100 g dry alumina
- Water: sufficient for slurry; no more than ~50 mL per 100 g fly ash

Curing will need to be done in a pressure vessel (requiring the special safety considerations described above) placed in an oven in order to expose the samples to a steam environment at 150°C or hotter. Curing at pressure is needed for reasonable reaction time in an aqueous system at elevated temperature, and it is expected to reduce the porosity of the final cement product.

Ceramicrete® (Magnesium Potassium Phosphate Cement (MKPC))

A typical Ceramicrete® recipe (Wagh 2018, personal communication) is:

- 10% calcined P98 MgO, magnesium oxide
- 35% monobasic potassium phosphate (KH_2PO_4)
- 55% Class F fly ash (reactive)
- Water (22 weight % of total dry powders)
- $\geq$ 0.5% boric acid (crystalline; acts as a retarder)

Calcium Phosphate Cement (CPC)

A typical bone cement binder recipe (Wagh 2018, personal communication) is:

- 29.2% tetracalcium phosphate ($Ca_4(PO_4)_2O$)
- 10.8% dicalcium phosphate ($CaHPO_4$)
- 60% Class F fly ash (reactive)
- Water (sufficient to produce pourable slurry)
- 4% citric acid (crystalline; acts as a retarder)

Generic Ordinary Portland Cement (OPC) Grout

A cement recipe reported by Collier et al. (2015):

- 38% Class G oil well cement
- 10% silica fume (submicron)
- 50% Class F fly ash
- 2% Sika ViscoCrete 3011® liquid plasticizer
- Water (100% of the combined weight of cement, fume and plasticizer)

Calcium Aluminum Phosphate Cement (CAPC)

A pre-mixed dry calcium aluminum phosphate cement produced by Haliburton under the tradename Haliburton ThermaLock®.

8.2 Equipment and Laboratory Setup for Fabrication Experiments

Many of the starting materials are extremely fine powders (Bindan 3.1 cement, Class F fly ash, etc.) and represent inhalation hazards. For hazard mitigation the powders are transferred into smaller resealable zipper storage bags in a fume hood. The sealed bags are then transferred to a self-contained glove box where the cement slurries are pre-mixed with their associated liquids to eliminate the presence of dry powder. Figure 19 shows a LABCONCO Precise® HEPA-filtered glove box being used for Bindan 3.1 cement slurry preparation.

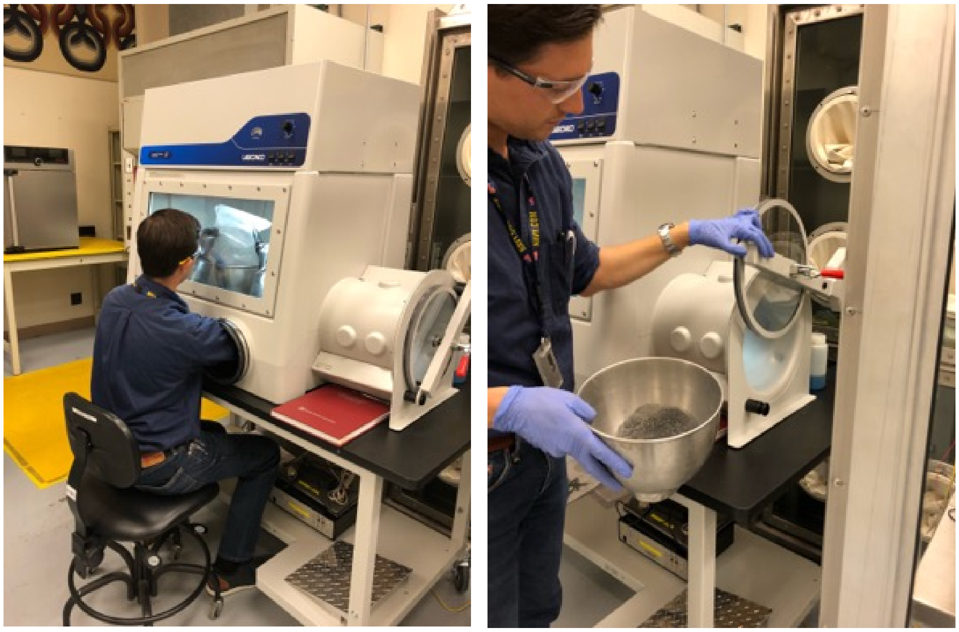

Figure 19. Bindan 3.1 binder powder and water being mixed in a bowl within the glove box (left) then removal of the slurry from the glove box (right) for final mixing.

The pre-mixed slurry is then transferred to a kitchen-type planetary mixer (Figure 20) for final mixing. Mixing time depends on the volume of the mixture and is approximately 2 minutes to produce sufficient volume for two 1” x 3” cement cores.

Figure 20. Bowl containing Bindan 3.1 slurry placed on mixer (left) and the resulting pourable slurry (right).

Once fully mixed, the slurry is poured into cardboard molds (Figure 21).

Figure 21. Pouring Bindan 3.1 slurry into cylindrical molds.

Once the slurry has been poured into the molds, they are placed on the vibrating table for a minute (Figure 22) to release entrained air. The molds are then covered with aluminum foil and placed aside in the laboratory to cure for a minimum of 24 hours. When sufficiently cured the samples are removed from the molds (Figure 23).

Figure 22. Bindan 3.1 slurry-filled molds on the vibrator.

Figure 23. Two Bindan 3.1 binder cement cores fabricated at room temperature (1-inch diameter, 3.25-inch length).

To fabricate APC some additional steps are required. The APC slurry will be poured into Teflon molds, placed in a pressure vessel and heated to 150 to 200 °C in an oven, which will generate steam pressure up to approximately 8.1 MPa. A suitable corrosion-resistant (Hastelloy) pressure vessel was purchased from the Parr Instrument Company (Figure 24), for use in a temperature-controlled oven (Figure 25).

Figure 24. Fully assembled (left) and disassembled (right) Parr vessel.

Figure 25. Memmert UN-55 Plus oven (left) and the Parr vessel within the oven (right).

Planned (FY19) work will focus on: 1) completion of required safety documentation for the fabrication of the APC, MKCP, CPC, and CAPC (ThermaLock®) cements; 2) optimization of these cement formulations for pourability and set time; and 3) cement testing as outlined in Section 5.2.

9. CONTINUING AS-LOADED ANALYSIS OF DUAL PURPOSE CANISTERS

The following material is excerpted from: *Criticality Consequence Analysis Roadmap for a Spent Nuclear Fuel Canister in a Repository,* by Thomas M. Evans, Gregory G. Davidson, Steven P. Hamilton, and Kaushik Banerjee, all of Oak Ridge National Laboratory (deliverable M3SF-18OR0103050111, issued as report ORNL/SPR-2018/951). Minor edits have been included for clarity. The reader is referred to the source document for more detail.

As-loaded criticality analyses of the currently loaded DPCs are being performed using the Used Nuclear Fuel-Storage, Transportation & Disposal Analysis Resource and Data System (UNF-ST&DARDS) (Clarity et al. 2017). As-loaded criticality analysis uses initial fuel characteristics such as assembly type, initial enrichment, and initial uranium mass; reactor irradiation histories such as effective full power day and outage intervals; decay time in the spent fuel pool; and DPC loading maps to calculate the realistic and time-dependent (up to ~22,000 years or second reactivity peak; Wagner et al. 2003) neutron multiplication factor (k_{eff}) of DPCs. As-loaded criticality analysis provides the uncredited criticality margin that is being used to offset postulated DPC degradation scenarios. For criticality analysis, it is important to assume that water enters a waste package at some point over the repository's time frame. While different geologic settings and material degradation mechanisms might yield a large number of potential configurations, two simplified, potentially conservative configurations are being used within UNF-ST&DARDS to assess DPC reactivity changes that may occur over repository time frames:

- Total loss of neutron absorber from unspecified degradation and material transport processes, and
- Loss of the carbon-steel internal basket structure (including the neutron absorber) resulting in elimination of assembly-to-assembly spacing.

To date, UNF-ST&DARDS has completed as-loaded analysis of 616 DPCs (Radulescu and Banerjee 2018). Table 14 and Figure 26 show that even with detailed criticality analysis, a fraction of DPCs have the potential to form critical configurations in a repository time frame. Many of the DPCs that have already been analyzed are of the flux-trap design, which provides a relatively larger criticality margin compared to the modern high-capacity burnup credit DPCs. It is expected that the statistics related to number of DPCs with no criticality potential in a repository time frame presented in Table 14 will deteriorate as UNF-ST&DARDS performs analysis of more and more modern DPC designs. Hence, detailed criticality analysis itself will not be sufficient to support direct disposal of DPCs. Nonetheless, UNF-ST&DARDS detailed criticality analysis will be important in defining the probability of criticality of a particular waste package within a repository performance assessment.

Table 14. Summary of DPC as-loaded criticality analysis in calendar year 12,000 (from Evans et al. 2018).

Description	Value
Total DPCs analyzed	616
Total DPCs below subcritical limit with loss of neutron absorber (design-basis loading)	0 (0%)
Total DPCs below subcritical limit with loss of neutron absorber (as-loaded)	473 (~76%)
Total DPCs below subcritical limit with loss of neutron absorber and carbon-steel structures (as-loaded)	420 (~68%)
Total DPCs below subcritical limit with loss of neutron absorber and carbon-steel structures (as-loaded) considering misload	397 (~64%)
Notes: 1. Misload includes assemblies are placed in wrong location within canister [7]. 2. Subcritical limit is defined by keff = 0.98 [7].	

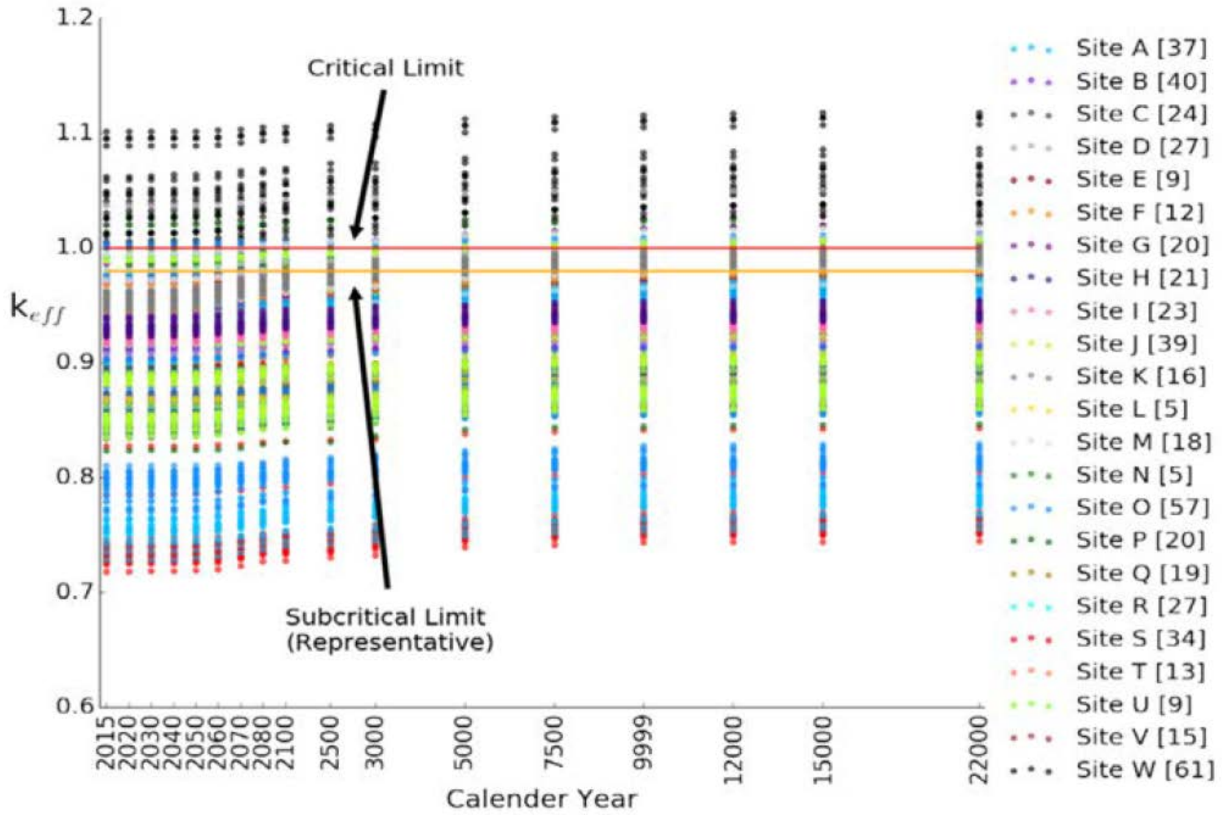

Figure 26. Calculated neutron multiplication factor (k_{eff}) as a function of the calendar year (up to year 22,000) for 551 DPCs loaded at 23 sites (postulated degradation scenario includes loss of neutron absorber panels from basket; from Evans et al. 2018).

Recognizing that as-loaded criticality analysis alone may not be able to demonstrate postclosure criticality control for loaded DPCs in breached waste packages, especially in a disposal environment where ground water composition is fresh (and not saline brine), the DPC disposition

R&D campaign has begun to investigate other options. The two leading options involve canister modifications or investigation of postclosure criticality events in a repository: 1) precondition DPCs with engineered filler materials, and 2) analyze the impact of potential criticality consequence on a generic regulatory performance assessment.

10. INDEPENDENT REVIEWS OF FILLER REQUIREMENTS AND DPC DISPOSITION

The following independent review was provided by Halim Alsaed of EnviroNuclear, under contract to Sandia National Laboratories. The text is excerpted from two reports (Alsaed 2018a,b) including a review of DPC direct disposal feasibility evaluations, and another review on technical and regulatory considerations for using fillers in DPCs to control postclosure criticality. The discussion below focuses on the summaries and recommendations; for more detailed discussion the reader is referred to the original reports.

10.1 Review of Criticality Evaluations for Direct Disposal of SNF in DPCs

10.1.1 Summary

There are currently 2,462 DPCs containing SNF, located across the United States. Repackaging of this SNF into specialized canisters for geologic disposal could be financially and operationally costly with significant radiological risks. Technical feasibility of direct disposal of DPCs has been evaluated by the DOE and industry over the past 15 years. A recent R&D program conducted by the DOE Office of Spent Fuel and Waste Science and Technology (SFWST) looked at technical feasibility of direct disposal of DPCs in various geologies. That work, documented in several reports from 2012 through 2017, was reviewed

The concerted effort by SFWST over the past five years has significantly advanced the viability of direct disposal of DPCs. The effort covered a range of disposal geologies and DPC designs. However, the criticality evaluation approach has been single-faceted and did not significantly advance the overly conservative deterministic analysis bases previously developed for disposal-specialized canisters.

The strengths of the SFWST effort include as-loaded DPC criticality analysis that demonstrates a significant margin, thorough analysis of dissolved species in ground water (especially for salt geologies), a comprehensive criticality analysis process, and a valuable and capable UNF-ST&DARDS database.

The vulnerabilities of the SFWST effort include deterministic misload considerations that are either potentially unjustifiable or significantly penalizing; lack of a thorough evaluation of moderated non-flooded configurations; a deterministic analysis basis configuration with limited margin that may not be suitable as a licensing basis; modeling of “undamaged” fuel as intact in damaged fuel cans; and lack of consideration of source of burnup data including batch averages and uncertainty in assigned burnup values.

Disposal of DPCs is not only viable, but assured from a technical and assumed regulatory perspective (similar to 10 CFR 63). The analysis approach should be multi-faceted to ensure effective implementation of a licensing basis. Recommendations are provided in this report that could enhance the bases for direct disposal of DPCs by exploiting all technically attainable and regulatorily defensible options. The recommendations include the following:

- Pursuing the development of guidance for criticality-oriented loading of DPCs to demonstrate compliance with 10 CFR 72.236(m).
- Probabilistic approach for developing keff distributions that would eliminate the question of whether a DPC is critical or subcritical during disposal and places the emphasis on the probability of criticality.

- Redefining criticality features, events and processes (FEPs) to better align with the assumed regulation and to facilitate a probability-weighted consequence screening (not inclusion) of criticality FEPs from repository performance assessment.

The review objectives, including addressing several questions regarding the value of accumulating as-loaded fuel and DPC design data, suitability of DPC designs for disposal, and reasonable modifications for loading of DPCs that could facilitate eventual disposal, are also addressed in this report.

10.1.2 Recommendations

Disposal of DPCs is not only viable, but assured from a technical and assumed regulatory perspective. The analysis approach should be multi-faceted to ensure effective implementation of a licensing basis. The following is a list of recommendations that enhance the potential for success by exploiting all technically attainable and regulatorily defensible options.

- Regulatory engagement for the development of guidance to address compliance with 10 CFR 72.236(m).
- Probabilistic approach to k_{eff}, which is inherently probabilistic but has been represented by deterministic analyses.
- Probability-weighted consequence screening, which could benefit from defining criticality FEPs to partition the variety of possible criticality events into categories that are readily analyzed and screened.
- Credit for the stable Cs-133. Because the current analysis basis configurations assumed intact fuel pins, there is no path for release of Cs-133 from the fuel. Cs-133 is the highest yield fission product (6.8%) with a cross section of 28.9 b, and is a more valuable burnup credit isotope than most of the currently credited isotopes. Credit for Cs-133 is already accepted for storage and transportation.
- Development of a burnup verification tool. Per ISG-8 Rev. 3 (NRC 2012), burnup confirmation would eliminate the potential for misload consideration for deterministic storage and transportation applications, which is one of the most significant vulnerabilities in the current analysis approach. With a probabilistic approach, a burnup confirmation tool would significantly reduce the probability of a misload.
- Continue the evaluation of the viability of the use of a filler material that would be cost effective and meet the storage, transportation, and disposal structural, thermal, criticality, and retrievability requirements. This option is the subject of a follow-on deliverable and will be discussed in detail.
- Continue to pursue methods for analyzing BWR SNF burnup credit.
- Continue to gather the necessary data for DPCs to support as-loaded modeling.
- Development of overpacks or overpack treatment that would reduce the probability of early failure (e.g., use additive manufacturing), where early failure would be more rigorously defined taking into account appropriate classes of defects and performance-based functions (e.g., maintaining moderator exclusion from the DPC with partial failures).
- Simulate the degradation of DPCs to determine the composition of the water within the DPC, relocation of neutron absorbers and extent of failure.

Further detail on these recommendations is provided in the source report (Alsaed 2018a). They are reflected in the ongoing R&D program described in Section 11.

One of the most important of the recommendations listed above is to investigate low-consequence criticality screening. The basis for concluding that criticality FEPs are inconsequential to repository performance could formed by answering the following questions:

- What is the threshold of mechanical energy (from criticality events) that would impact repository performance?
- What is the threshold of radionuclide concentration increase of those isotopes already considered in the performance assessment that would significantly impact the dose estimate?
- What is the threshold of radionuclide concentration increase for those isotopes that are *not* already considered in the performance assessment (e.g., short-lived fission products)?
- What is the threshold of temperature increase and duration of elevated temperature, that would impact repository performance? (This need not be a large temperature increase given that a criticality event may not increase system temperature by more than a few degrees.)
- What is the radiolysis threshold (mainly from neutrons) that would impact waste package chemistry?

The thresholds referenced in these bullets could be deterministic values or probabilistically developed distributions (or perturbations to distributions) to match the parameters of the performance assessment. Once the above parameters have been established, the threshold of a consequential criticality as opposed to an inconsequential criticality can be determined with only two parameters, power and duration.

In order to evaluate the feasibility of this approach, simplified consequence modeling should be performed to determine the parameter thresholds to initiate a criticality, maintain it, oscillate around it, and shut it down.

10.2 Summary of Technical and Regulatory Considerations for Use of Fillers in DPCs

The concerted effort by SFWST over the past five years has significantly advanced the viability of direct disposal of DPCs. The effort covered a range of disposal geologies and DPC designs. However, the criticality evaluation approach has been single-faceted and did not significantly advance the overly conservative deterministic analysis bases previously developed for disposal-specialized canisters.

The strengths of the SFWST effort include as-loaded DPC criticality analysis that demonstrates a significant margin, thorough analysis of dissolved species in ground water (especially for salt geologies), a comprehensive criticality analysis process, and a valuable and capable UNF-ST&DARDS database.

The vulnerabilities of the SFWST effort include deterministic misload considerations that are either potentially unjustifiable or significantly penalizing; lack of a thorough evaluation of moderated non-flooded configurations; a deterministic analysis basis configuration with limited margin that may not be suitable as a licensing basis; modeling of “undamaged” fuel as intact in damaged fuel cans; and lack of consideration of source of burnup data including batch averages and uncertainty in assigned burnup values.

Disposal of DPCs is not only viable, but assured from a technical and assumed regulatory perspective (similar to 10 CFR 63). The analysis approach should be multi-faceted to ensure effective implementation of a licensing basis. Recommendations are provided in this report that could enhance the bases for direct disposal of DPCs by exploiting all technically attainable and regulatorily defensible options. The recommendations include the following:

- Pursuing the development of guidance for criticality-oriented loading of DPCs to demonstrate compliance with 10 CFR 72.236(m).
- Probabilistic approach for developing keff distributions that would eliminate the question of whether a DPC is critical or subcritical during disposal and places the emphasis on the probability of criticality.
- Redefining criticality features, events and processes (FEPs) to better align with the assumed regulation and to facilitate a probability-weighted consequence screening (not inclusion) of criticality FEPs from repository performance assessment.

The review objectives, including addressing several questions regarding the value of accumulating as-loaded fuel and DPC design data, suitability of DPC designs for disposal, and reasonable modifications for loading of DPCs that could facilitate eventual disposal, are also addressed in this report.

There are several approaches to facilitate direct disposal of DPCs and demonstrate acceptable repository performance. A promising approach is to fill the void space within the DPCs with a material that would significantly limit the potential for criticality through limiting moderation and/or the addition of neutron absorbers in the interstitial spaces within the fuel assemblies and baskets. An acceptable filler would demonstrably show that the probability of criticality in DPCs during the disposal period of interest to be below the probability threshold for inclusion in repository performance assessment. Based on previous work conducted by domestic and international organizations, two approaches were identified as potentially viable for introduction of fillers into DPCs as liquids that would eventually solidify: (1) molten metal fillers introduced at higher temperatures, and (2) resins or cement slurries that solidify at lower temperatures.

The purpose of this report is to document the technical and regulatory considerations for the use of fillers to facilitate direct disposal of DPCs, including addressing effectiveness of filler introduction into different types of DPCs, the functions of filler materials in disposal environments, and impact on storage, transportation and retrieval. The intended use of this report is to support a higher-level concept of operations report that could be used in future interactions with the Nuclear Regulatory Commission (NRC).

The presence of any material interstitial to the fuel assemblies will undoubtedly reduce the potential for criticality. The extent of filler material effectiveness depends on its ability to reduce the moderated volume or moderation effectiveness. A successful filler material need not accomplish both functions. Additionally, a successful filler material need not provide the same function for the entire period of interest. Therefore, the potential presence of void space would not be a showstopper as long as the extent of void space could be statistically quantified or the water filling the void could be adulterated with neutron absorbers. Although relatively small volumes can theoretically form a critical configuration with low enriched fuel, the fact that the fuel is depleted significantly increases the required critical volume. Although some prior analyses estimated criticality potential at various water densities and fuel volumes, these analyses are either overly conservative or not directly applicable to potential disposal configurations. Performing filler-specific analyses based on as-loaded DPCs to determine the minimum critical water density (i.e., maximum acceptable void fraction) and minimum criticality volume in various geometries is essential. It is likely that the results of these analyses could significantly change (make less restrictive) the current perceived expectations regarding acceptable void fractions and void volumes.

The most challenging regulatory aspect for a first-of-a-kind application such as the use of fillers, is to address the potential for “unknown unknowns” (unexpected and unforeseeable conditions). This is often accomplished by a combination of demonstration programs along with monitoring/inspection with remediation capability and defense-in-depth safety systems. Using fillers for disposal is a one-step approach with limited potential for monitoring/inspection or remediation. Implementation of defense-in-depth or backup safety systems during disposal, such as additional barriers to address unknowns, could undermine gains in disposal efficiency from the use of fillers. Therefore, an extensive demonstration program would be needed to demonstrate that the fillers would achieve their primary objective (i.e., uniformly distributed within void spaces interstitial to the fuel and baskets), and to increase confidence that there are no unanticipated modes of failure to perform the intended functions. The demonstration project can start with simulated fuel and baskets to address filling capability. However, to address possible failure modes a combination of modeling, separate-effects tests, and demonstration programs with SNF would have to be conducted.

There may be hundreds of unique combinations of geometries and materials that could impact the flow of fillers in various DPC designs and loadings. However, it is conceivable to design a mockup that would include all potential varieties of fuel designs, basket designs, and loading configurations to cover the range of existing DPCs. Destructive testing of the mockup would then be conducted to evaluate filler properties and the extent of void filling.

Separate-effects tests could focus on the interaction between the filler material and various DPC and SNF materials for a range of storage, transportation, and disposal conditions including the potential presence of impurities and catalysts. The materials subjected to separate-effects tests should be inclusive of all those in the fuel matrix (as modified during reactor depletion), fuel assembly designs and components (as modified during reactor depletion and storage), basket designs and components (as modified by extended storage), DPC shell (as modified by extended storage), and water (due to inadequate drying or water-logged rods). Separate-effects tests should include various groupings of the materials representative of DPC variants, not just individual material interactions.

There are potential advantages beyond criticality control from using fillers in storage, transportation, and disposal designs and their license applications. Fillers could serve as an additional barrier for waste isolation during disposal, which could reduce disposal overpack or drip shield requirements. Successful implementation of fillers could even obviate the need for disposal specialized canisters completely, which would significantly reduce cost and simplify disposal packaging operations. Fillers could also reduce the shielding requirements for neutron radiation (e.g., cementitious materials) or gamma radiation (e.g., molten metals), which could allow for optimizing the size and/or weight of transportation overpacks.

11. SUMMARY AND PATH FORWARD

This report is an update on R&D activities for: 1) injectable fillers that could be used in dual-purpose canisters to prevent postclosure criticality in a geologic repository, and 2) as-loaded DPC data gathering and criticality analysis.

This R&D program, mostly experimental, is now part of a broader R&D program that includes new process modeling and performance assessment of criticality effects to better understand internal criticality in disposal waste packages, and the consequences on radionuclide release from the waste (source term).

Injectable fillers were selected as the objective, to avoid the cost and complexity of cutting lids off of existing DPCs for other criticality-control modifications (e.g., disposal control rod installation, or dry particulate fillers). Fillers investigations were initially conceived to decrease the probability of criticality in a repository, thereby supporting a low-probability risk screening argument for regulatory performance assessment. The new approach also allows low-consequence risk screening, and will consider the overall impact of one or more criticality events in DPC-based waste packages, on repository waste isolation performance. In the context of consequence screening, the use of fillers could be complementary in a mixed screening approach.

Literature research and consultation with cement experts in FY18 identified several potentially effective and workable filler materials (Section 5) including aqueous cement slurries, and molten metals, alloys, and low-temperature glasses. Of particular interest are cement slurries that solidify when heated, and molten materials that solidify when cooled, providing control over when solidification begins (not until the canister is completely filled).

Filler attributes were defined and the preliminary list of materials was compared qualitatively. Further comparative analysis should be done (e.g., cost estimates for filler materials and delivery systems) after experimental screening has narrowed the list of alternatives. Comparisons between cementitious materials and metals/alloys/glasses will be more meaningful then. Presently much of the effort for fillers is focused on getting experimental screening tests underway.

Preliminary scoping calculations (Section 4) were done to frame the challenges with temperature control during filler emplacement, which can be simulated with reasonable accuracy and can likely be managed to keep fuel temperature above or below established limits during filling. Calculations also show the challenges associated with residual moisture in cementitious fillers, specifically gas generation due to corrosion and radiolysis leading to internal canister pressure. This line of investigation will lead to proof-of-concept tests for fillers involving dewatering of cured material, and direct exposure to gamma and neutron radiation.

Physical models for investigation of filling behavior (void filling and compositional consistency) were substantially advanced in FY18 by the ORNL team (Section 7). Fuel and basket mock-ups are available for demonstration testing in FY19. Laboratory capability for cement slurry testing was also advanced at SNL, and testing was begun on MKPC and thermal-setting APC compositions (Sections 5 and 8). All of these testing activities require planning, procurements, and compliance with environment, health and safety requirements extant at the laboratories.

Simulation of DPC conditions during filling has begun, using different simulation approaches for computational fluid dynamics (CFD) and solid-state heat transfer. Some of the CFD work is computationally demanding (Section 7) such that future efforts will find a balance between numerical simulations and physical model demonstrations, that effectively supports the needed filler evaluations and generates validation data.

The compilation and analysis of basket configuration and "as-loaded" burnup for loaded DPCs, continued in FY18 building on work done in FY13 through FY17. The unified database of DPC information is essential to support analysis and future decisions on DPC direct disposal.

Fillers investigations are planned to continue through FY19. An independent expert review of DPC disposal R&D, and fillers in particular (Section 6) was supportive, although alternatives to use of fillers, particularly consequence screening, were also emphasized.

The planned path forward includes continued testing of cement slurry compositions that have been identified, continued development of mock-up physical models, and filling demonstration tests with surrogate materials. Screening of metals/alloys/glasses for testing will be an important step. Compilation of DPC design data and "as-loaded" fuel data will continue.

Recommendations for additional R&D include identifying additional filler materials (e.g., thermal-setting cements and low-temperature glasses), testing the pourability and self-leveling behavior of potential filler materials, and engaging outside contractors and university collaboration to make exploratory filler testing more cost effective and to encourage new ideas.

REFERENCES

Agrenius, L. 1993. *SFL-Specifikation av kriticitetsberäkningar för slutförvaringskapseln*. SKB Rapport 20.152. Svensk Kärnbränslehantering AB, Stockholm, Sweden.

Akiyama, M. and S. Kawasaki 2012. “Novel grout material comprised of calcium phosphate compounds: In vitro evaluation of crystal precipitation and strength reinforcement.” *Engineering Geology*. V.125, pp. 119-128.

Alchagirov, B.B., T.M. Shamparov and A.G. Mozgovoi 2003. “Experimental Investigation of the Density of Molten Lead–Bismuth Eutectic.” *High Temperature*, **41**(2), 210 (Transl. from *Teplofizika Vysokikh Temperatur*, Vol. 41, No. 2, pp. 247-253).

Alsaed, A. 2018a. *Review of Criticality Evaluations for Direct Disposal of DPCs and Recommendations*. SFWD-SFWST-2018-000491 Rev. 0. U.S. Department of Energy, Office of Spent Fuel and Waste Science and Technology. April 20, 2018.

Alsaed, A. 2018b. *Technical and Regulatory Considerations for Use of Fillers in DPCs*. SFWD-SFWST-2018-000495 Rev. 0. U.S. Department of Energy, Office of Spent Fuel and Waste Science and Technology. July 31, 2018.

Arthur, S. 2000. *EQ6 Calculation for Chemical Degradation of Shippingport LWBR (TH/U Oxide) Spent Nuclear Fuel Waste Packages*. CAL-EDC-MD-000008 Rev. 0. Office of Civilian Radioactive Waste Management, U.S. Department of Energy.

Anderson, K.J. 1981. *Use of Filler Materials to Aid Spent Nuclear Fuel Dry Storage*. Allied-General Nuclear Services, Barnwell, SC.

Armijo, J.S., P. Kar, and M. Misra 2006. “Second Generation Waste Package Design and Storage Concept for the Yucca Mountain Repository.” *Nuclear Engineering and Design*. 236: 2589-2598.

Bennett, D. and R. Gens 2008. “Overview of European concepts for high-level waste and spent fuel disposal with special reference waste container corrosion.” *Journal of Nuclear Materials*. V.379, pp. 1-8.

BSC (Bechtel-SAIC Company) 2003. *The Potential of using Commercial Dual Purpose Canisters for Direct Disposal*. TDR-CRW-SE-000030, Rev 0. Las Vegas, NV: Bechtel SAIC Company.

BSC (Bechtel-SAIC Company) 2005. *Cladding Degradation Summary for LA*. ANL-WIS-MD-000021 Rev. 3. Las Vegas, NV: Bechtel SAIC Company.

Carroll-Webb, S. and J.V. Walther 1988. "A surface complex reaction model for the pH-dependence of corundum and kaolinite dissolution." *Geochim. Cosmochim. Acta* 52: 2609-2623.

Carter, J., A. Luptak, J. Gastelum, C. Stockman and A. Miller 2012. *Fuel Cycle Potential Waste Inventory for Disposition*. FCR&D-USED-2010-000031 Rev. 5. U.S. Department of Energy, Used Fuel Disposition R&D Campaign. July, 2012.

CD-Adapco, STAR-CCM+ 13.02 Theory Guide, 2015.

Cetiner, N.O., E. Popov, E.J. Fountain, V.K. Varma, A.I. Adeniyi and K. Banerjee 2018. *Dual-Purpose Canister Filling Demonstration Project Progress Report*. ORNL/SPR-2018/906. Oak Ridge National Laboratory (DOE deliverable M4SF-18OR010305017).

Cetiner, N.O., E. Popov, E.J. Fountain, V.K. Varma, E. Dominguez-Ontiveros, A.I. Adeniyi and K. Banerjee 2018. *Dual-Purpose Canister Filling Demonstration Project Progress Report*. ORNL/SPR-2018/973. Oak Ridge National Laboratory (DOE deliverable M4SF-18OR010305015 Rev. 1). September 10, 2018.

Clarity, J.B., K. Banerjee, H. K. Liljenfeldt and W. J. Marshall 2017. “As-Loaded Criticality Margin Assessment of Dual-Purpose Canisters Using UNF-ST&DARDS.” *Nuclear Technology*. 199(3), 245–275.

Cogar, J. 1996a. *Waste Package Filler Material Testing Report*. BBA000000-01717-2500-00008 Rev 01. Office of Civilian Radioactive Waste Management, U.S. Department of Energy.

Cogar, J. 1996b. *Spent Nuclear Fuel Waste Package Filler Testing Guidelines Document*. BBA000000-01717-2500-00003 Rev. 03. Office of Civilian Radioactive Waste Management, U.S. Department of Energy.

Covill, A., N. Hyatt, J. Hill and N. Collier 2011. “Development of magnesium phosphate cements for encapsulation of radioactive waste.” *Advances in Applied Ceramics.* V.110, pp. 151-156.

Crovisier, J.-L., et al. 2003. "Nature and role of natural alteration gels formed on the surface of ancient volcanic glasses (Natural analogs of waste containment glasses)." *Journal of Nuclear Materials* 321(1): 91-109.

DOE (U.S. Department of Energy). 2003. *Disposal Criticality Analysis Methodology Topical Report*. YMP/TR-004Q, Revision 2. Las Vegas, NV: U.S. Department of Energy, Office of Civilian Radioactive Waste Management.

DOE (U.S. Department of Energy) 2008. *Transportation, Aging and Disposal Canister System Performance Specification*. WMO-TADCS-000001. Office of Civilian Radioactive Waste Management.

EIA (Energy Information Adminstration) 2012. *Nuclear Fuel Data Survey Form GC-859*. U.S. Department of Energy, Washington, DC. July, 2012.

Elliott, A.J., M.P. Chenier and D.C. Ouellette 1990. “g-Values for γ-irradiated water as a function of temperature.” *Canadian Journal of Chemistry*. V.68, pp. 712-719.

EPRI (Electric Power Research Institute). 2008. *Feasibility of Direct Disposal of Dual-Purpose Canisters: Options for Assuring Criticality Control*. Palo Alto, CA: Electric Power Research Institute. #1016629.

EPRI (Electric Power Research Institute) 2009. *Handbook of Neutron Absorber Materials for Spent Nuclear Fuel Transportation and Storage Applications*. Palo Alto, CA. #1019110.

Evans, T.M., G.G. Davidson, S.P. Hamilton and K. Banerjee 2018. Criticality Consequence Analysis Roadmap for a Spent Nuclear Fuel Canister in a Repository. ORNL/SPR-2018/951. Oak Ridge National Laboratory. (DOE deliverable M3SF-18OR0103050111)

Fish, R., N. Wynhoff and V. Ferrell 1982. *Spent LWR-Fuel Waste-Package-Stabilizer Recommendations*. HEDL-7204. Hanford Engineering Development Laboratory, Richland, Washington.

Forsberg, C.W., R.B. Pope, R.C. Ashline, M.D. DeHart, K.W. Childs and J.S. Tang 1995. *DUSCOBS – A Depleted-Uranium Silicate Backfill for Transport, Storage, and Disposal of Spent Nuclear Fuel*. ORNL/TM-13045. Oak Ridge National Laboratory, Oak Ridge, TN.

Forsberg, C.W. 1997. Description of the Canadian Particulate-Fill Waste Package (WP) System for Spent Nuclear Fuel (SNF) and its Applicability to Light-Water Reactor SNF WPs with Depleted Uranium Dioxide Fill. ORNL/TM-13502. Oak Ridge National Laboratory, Oak Ridge, TN. October 20, 1997.

Forsberg, C.W. 2000. “Effect of Depleted-Uranium Dioxide Particulate Fill on Spent Nuclear Fuel Waste Packages.” *Nuclear Technology*. 131:337–353.

Forsberg C.W., S.N. Storch and K.W. Childs 2001. “Depleted-Uranium Dioxide as SNF Waste Package Particulate Fill: Engineering Properties.” 2001 International High-Level Radioactive Waste Management Conference. American Nuclear Society, La Grange Park, IL.

Forsberg, C.W. 2002. “Repository Applications for Depleted Uranium (DU) (Potential Use of the Entire DU Inventory).” Presentation at DU Uses R&D Program Review, Oak Ridge, TN.

Greene, S. R., J. S. Medford and S. A. Macy 2013. *Storage and Transport Cask Data for Used Commercial Nuclear Fuel*. ATI-TR-13047. Energx. Oak Ridge, TN.

Grundfelt, B. and J. Crawford 2014. *The deep borehole concept: A conceptual model for gas generation and gas transport*. Report P-13-11. Svensk Kärnbränslehantering AB (SKB).

Hardin, E. and R. Howard 2013. *Assumptions for Evaluating Feasibility of Direct Geologic Disposal of Existing Dual-Purpose Canisters*. FCRD-UFD-2012-000352 Rev. 1. U.S. Department of Energy, Used Fuel Disposition R&D Campaign. November, 2013.

Hardin, E., L. Price, E. Kalinina, T. Hadgu, A. Ilgen, C. Bryan, J. Scaglione, K. Banerjee, J. Clarity, R. Jubin, V. Sobes, R. Howard, J. Carter and T. Severynse 2015. *Summary of Investigations on Technical Feasibility of Direct Disposal of Dual-Purpose Canisters.* FCRD-UFD-2015-000129 Rev. 0. U.S. Department of Energy, Used Fuel Disposition R&D Campaign. May, 2015.

Hardin, E.L. and P.V. Brady 2018. *Recommendations for Filler Material Composition and Delivery Method for Bench- Scale Testing*. SFWD-SFWST-2018-000490 Rev. 0. U.S. Department of Energy, Office of Spent Fuel and Waste Science and Technology. March, 2018.

Hariprakashk, B., P. Bera, S.K. Martha, S.A. Gaffoor, M.S. Hegde and A.K. Shukla 2001. “Ceria-Supported Platinum as Hydrogen-Oxygen Recombinant Catalyst for Sealed Lead-Acid Batteries.” *Electrochemical and Solid-State Letters*. V.4, No.3, pp. A23-A26.

Holtec International 2010. *Final Safety Analyses Report for the HI-STORM 100 Cask System*.

Hsue, S.T., J.E. Steward, K. Kaieda, J.K Halgiv, J.R. Phillips, D.M. Lee and C.R. Hatcher 1979. *Passive Neutron Assay of Irradiated Nuclear Fuels.* LA-7645-MS. Los Alamos Scientific Laboratory. February, 1979.

IAEA (International Atomic Energy Agency) 2008. *Thermophysical Properties of Materials For Nuclear Engineering: A Tutorial and Collection of Data*. IAEA-THPH. Nuclear Power Technology Development Section. Vienna, Austria.

Itasca (Itasca Consulting Group) 2011. *FLAC Version 7.00 User’s Guide*. Minneapolis, MN.

Johnson, L., J. Tait, D. Shoesmith, J. Crosthwaite and M. Gray 1994. *The Disposal of Canada's Nuclear Fuel Waste: Engineered Barriers Alternatives*. AECL-10718. Atomic Energy of Canada, Ltd.

Jubin, R., K. Banerjee and T. Severynse 2014. *Potential Dual-Purpose Canister (DPC) Filler Materials*. FCRD-UFD-2014-000521 Rev. 0. U.S. Department of Energy, Office of Used Nuclear Fuel Disposition.

Kessler, J., A. Sowder and M. Kozak 2008. *Feasibility of Direct Disposal of Dual-Purpose Canisters in a High-Level Waste Repository*. Palo Alto, CA: Electric Power Research Institute. #1018051.

Kim, A.G., et al. 2003. "Relative solubility of cations in class F fly ash." *Environmental Science & Technology* 37(19): 4507-4511.

Liljenfeldt, H., K, Banerjee, J, Clarity, J, Scaglione, R, Jubin, V, Sobes, R. Howard, E. Hardin, L. Price, E. Kalinina, T. Hadgu, A. Ilgen, C. Bryan, J. Carter, T. Severynse and F. Perry 2016. *Summary of Investigations on Technical Feasibility of Direct Disposal of Dual-Purpose Canisters*. SFWD-SFWST-2017-000045. U.S. Department of Energy, Office of Spent Fuel and Waste Science and Technology. September, 2017 (calculations update to Hardin et al. 2015).

Maheras, S.J., R.E. Best, S.B. Ross, E.A. Lahi and D.J. Richmond 2012. *A Preliminary Evaluation of Using Fill Materials to Stabilize Used Nuclear Fuel During Storage and Transportation*. FCRD-UFD-2012-000243. U.S. Department of Energy, Office of Used Nuclear Fuel Disposition. August, 2012.

Massari, J.R. 1999. *License Application Design Selection Feature Report: Additives and Fillers, Design Feature 19*. B00000000-01717-2200-00212 REV 01. Office of Civilian Radioactive Waste Management, U.S. Department of Energy.

McDonell, W.R. 1954. *Radiation Chemistry of Normal and Heavy Water Solutions. II. Decomposition of Hydrogen Peroxide by Gamma Radiation.* ANL-5207. Argonne National Laboratory for the U.S. Atomic Energy Commission.

McFarlane, D.A. and J. Lundberg 2018. "New records of guano-associated minerals from caves in northwestern Borneo." *International Journal of Speleology* 47(2): 1.

Meffert, R.M., B. Langer and M.E. Fritz 1992. “Dental implants: a review.” *Journal of Periodontology*. V.63, pp. 859-870.

Michener, T.E., D.R. Rector, J.M. Cuta and H.E. Adkins, Jr. 2015. *COBRA-SFS: A Thermalhydraulic Analysis Code for Spent Fuel Storage and Transportation Casks, Cycle 4*. PNNL-24841. Pacific Northwest National Laboratory.

Milestone, N.B. 2006. “Reactions in cement encapsulated nuclear wastes: need for toolbox of different cement types.” *Advances in Applied Ceramics*. V.105, No.1, pp. 13-20.

Mobasheran, A. 1999. *Enrico Fermi Fast Reactor Spent Nuclear Fuel Criticality Calculations: Intact Mode*. BBA000000·01717-0210-00037 Rev. 0. Office of Civilian Radioactive Waste Management, U.S. Department of Energy.

Montierth, L.M. 2000. *Intact and Degraded Criticality Calculations for the Codisposal of Shippingport LWBR Spent Nuclear Fuel in a Waste Package*. CAL-EDC-NU-000004 Rev. 0. Office of Civilian Radioactive Waste Management, U.S. Department of Energy.

Moore, R.C. and M.J. Rigali 2015. *In Situ Formation of Apatite in Sediment For Construction of Permeable Reactive Barriers for Immobilization of Radionuclides*. Sandia National Laboratories, Albuquerque, NM.

Moscalu, D., L. Angers, J. Monroe-Ramsey and H. Radulescu 2000. *Enrico Fermi Fast Reactor Spent Nuclear Fuel Criticality Calculations: Degraded Mode*. CAL-EDC-NU-000001 Rev. 0. Office of Civilian Radioactive Waste Management, U.S. Department of Energy.

NRC (U.S. Nuclear Regulatory Commission) 2003. *Issue: Cladding Considerations for the Transportation and Storage of Spent Fuel*. Interim Staff Guidance – 11, Revision 3. Spent Fuel Project Office.

NRC (U.S. Nuclear Regulatory Commission) 2012. Burnup Credit in the Criticality Safety Analyses of PWR Spent Fuel in Transport and Storage Casks. Interim Staff Guidance – 8, Revision 3. Spent Fuel Project Office.

Onac, B.P. and W.B. White 2003. "First reported sedimentary occurrence of berlinite (AlPO4) in phosphate-bearing sediments from Cioclovina Cave, Romania." *American Mineralogist* 88(8-9): 1395-1397.

ONDRAF/NIRAS. 2001. “SAFIR 2: Safety Assessment and Feasibility Interim Report 2.” Report No. NIROND 2001-06 E. Belgian Agency for Radioactive Waste and Enriched Fissile Materials.

Ong, J.L. and D.C. Chan 2000. “Hydroxyapatite and their use as coatings in dental implants: a review.” *Critical Reviews in Biomedical Engineering*. V.28.

Oversby, V.M. and L.O. Werme 1995. “Canister Filling Materials – Design Requirements and Evaluation of Candidate Materials.” *Scientific Basis for Nuclear Waste Management XVIII*. Materials Research Society Symposium Proceedings 353:743–750 (October 23–27, 1994).

Parkhurst, D.L. and C.A.J. Appelo 1999. *User's guide to PHREEQC (Version 2) - A computer program for speciation, batch-reaction, one-dimensional transport, and inverse geochemical calculations*. Water-Resources Investigations Report 99-4259. U.S. GEOLOGICAL SURVEY. Reston, VA.

Pope, R.B., C.W. Forsberg, R.C. Ashline, M.D. DeHart, K.W. Childs and J.S. Tang 1996. “Benefits/Impacts of Utilizing Depleted Uranium Silicate Glass as Backfill for Spent Fuel Waste Packages.” In: *High Level Radioactive Waste Management, Proceedings of the 7th Annual International Conference*. April 29–May 3, 1996, Las Vegas, Nevada. pp. 369–371.

Puig, F., J. Dies, J. de Pablo and A. Martínez-Esparza 2008a. “Spent fuel canister for geological repository: Inner material requirements and candidates evaluation.” *Journal of Nuclear Materials*, 376, pp. 181–191.

Puig, F., J Dies, M. Savilla, J. de Pablo, J.J. Pueyo, L. Miralles and A. Martinez-Esparza 2008b. “Inner Material Requirements and Candidates Screening for Spent Fuel Disposal Canister.” *Scientific Basis for Nuclear Waste Management XXXI*. Materials Research Society Symposium Proceedings V.1107, pp. 67–74, September16–21, 2007.

Raddatz, M.G. and M.D. Waters 1996. *Information Handbook on Independent Spent Fuel Storage Installations*. NUREG-1571. Office of Nuclear Material Safety and Safeguards, U.S. Nuclear Regulatory Commission.

Radulescu, H.R. 2001. *Evaluation of Codisposal Viability for Th/U Carbide (Fort Saint Vrain HTGR) DOE-Owned Fuel*. TDR-EDC-NU-000007 REV 00. Las Vegas, NV: Bechtel SAIC Company.

Radulescu, G. and K. Banerjee 2018. *Dual-Purpose Canister Reactivity and Groundwater Absorption Analyses*. FCRD-UFD-2014-000520. U.S. Department of Energy, Office of Spent Fuel and Waste Science and Technology. May, 2018.

Rechard, R.P., M.S. Tierney, L.C. Sanchez and M.-A. Martell. 1996. *Consideration of Criticality when Directly Disposing Highly Enriched Spent Nuclear Fuel in Unsaturated Tuff: Bounding Estimates*. SAND96-0866. Albuquerque, NM: Sandia National Laboratories.

Rigali, M.J., Brady, P.V., Moore, R.C., 2016. “Radionuclide removal by apatite.” *American Mineralogist.* V.101, pp. 2611-2619.

Risenmark, S. 1993. *Preliminär Kriticitetsberäkning av slutförvaringskapsel*. BR 93-150. ABB Atom AB, Västerås, Sweden.

Robb, K. 2018. *Thermal Analysis of DPC Fillers – Phase I*. ORNL/SPR-2018/799. Oak Ridge National Laboratory (DOE deliverable M4SF-18OR010305016).

Roy, W.R. and P.M. Berger 2011. "Geochemical controls of coal fly ash leachate pH." *Coal Combustion and Gasification Products* 3: 63-66.

Russo, V., L. Protasova, R. Turco, M.H.J.M. de Croon, V. Hessel and E. Santacesaria 2013. “Hydrogen Peroxide Decomposition on Manganese Oxide Supported Catalyst: From Batch Reactor to Continuous Microreactor.” *Industrial & Engineering Chemistry Research*. V.52, pp. 7668−7676.

Schramke, J.A. 1992. "Neutralization of alkaline coal fly ash leachates by CO_2 (g)." *Applied Geochemistry* 7(5): 481-492.

Shelson, K.N. 1983. *Particulate Packings for Irradiated Fuel Disposal Containers*. Report No. 83085. Ontario Hydro Design and Development Division, Ontario Hydro Technologies, Toronto, Canada.

Singh, D., A.S. Wagh, J.C. Cunnane and J.L. Mayberry 1997. “Chemically bonded phosphate ceramics for low-level mixed-waste stabilization.” *Journal of Environmental Science & Health Part A*. V.32, pp. 527-541.

SNL (Sandia National Laboratories) 2017. *Joint Workplan on Filler Investigations for DPCs*. SFWD-SFWST-2018-000481 Rev. 0. U.S. Department of Energy, Office of Spent Fuel and Waste Science and Technology. December, 2017.

Sobolev, V. 2007. “Thermophysical properties of lead and lead–bismuth eutectic.” *Journal of Nuclear Mater*ials, 362: 235-247.

Stefanko, D.B., C.A. Langton and D. Singh 2011. *Magnesium Mono Potassium Phosphate Grout for P-Reactor Vessel In-Situ Decommissioning (U).* SRNL-STI-2010-00333 Rev. 0. Savannah River National Laboratory, Aiken, SC.

Sugama, T. 2006. *Advanced Cements for Geothermal Wells*. Report BNL-77901-2007-IR. Brookhaven National Laboratory. July, 2006.

Teper, B. 1987a. *Test Program of Granular Materials for the Thin-Walled Particulate-Packed Container*. 87-154-K, Ontario Hydro Research Division, Ontario Hydro Technologies, Toronto, Canada.

Teper, B. 1987b. *Test Program of the Prototype of the Thin-Wall Particulate-Packed (TWPP) Container: 1—Hydrostatic Tests*. TR-369-1, Chalk River Laboratories, Atomic Energy of Canada Limited (also Ontario Hydro Research Division Report 84-293-K).

Wagh, A.S. 2004. *Chemically Bonded Phosphate Ceramics: 21st Century Materials with Diverse Applications (1st Edition)*. Elsevier Science.

Wagh, A.S. 2016. *Chemically Bonded Phosphate Ceramics: Twenty-First Century Materials with Diverse Applications (2nd edition)*. Elsevier.

Wagner, J.C., et al. 2003. *Recommendations on the Credit for Cooling Time in PWR Burnup Credit Analyses*. NUREG/CR-6781 (ORNL/TM-2001/272). Prepared for the US Nuclear Regulatory Commission by Oak Ridge National Laboratory, Oak Ridge, Tenn., January 2003.

Wallin, W.E. 1996. *Analysis of MPC Access Requirements for Addition of Filler Materials*. BB0000000-01717-0200-0010, Revision 0. Office of Civilian Radioactive Waste Management, U.S. Department of Energy.

Weichselbaum, N.A. et al. 2018. *Surrogate Spacer Grid Design for Fluid-Structure Interactions Studies in Fuel Bundles*. The George Washington University, Washington, DC.

Wilson, A.D. and J.W. Nicholson 2007. *Acid-Base Cements: Their Biomedical and Industrial Applications (Chemistry of Solid State Materials) (1st Edition)*. Cambridge University Press.

Wynhoff, N., S. Girault and R. Fish 1982. *Spent Fuel Stabilizer Material Characterization and Screening*. HEDL-7210. Hanford Engineering Development Laboratory, Richland, Washington.

Zevenbergen, C., et al. 1999. "Clay formation and metal fixation during weathering of coal fly ash." *Environmental Science & Technology* 33(19): 3405-3409.

Zhang, J.T., F. Tancret and J.M Bouler 2011. “Fabrication and mechanical properties of calcium phosphate cements (CPC) for bone substitution.” *Materials Science and Engineering C*. V.31, pp. 740-747.

APPENDIX A – JOB SAFETY ANALYSIS FOR ALUMINUM PHOSPHATE CORE FABRICATION

JOB SAFETY ANALYSIS

(3-Column Format)

JSA ID No. and Revision No.: 12018-08-03

Page 1 of 3

Job/Title
Aluminum-Phosphate Cement Core Fabrication

Effective Date

Expiration Date (3 years chem. 1 year rad) 08/2021

Applicable PHS(s) and NEPA documents:

PHS- SNL11A00004
NEPA- NM18-0171

Facility
823/B59B

PI
Mark J. Rigali
Eduardo Basurto
Joseph Mohagheghi

Department
8842, 8844 & 8864

Department Manager
Robert MacKinnon and Kevin McMahon

Describe The Job Scope of Work and Expected Result(s)

Core fabrication of Aluminum-Phosphate Cement (APC), $AlPO_4$, will measure 3 inches in length and 1 inch in diameter using 3D printed flexible photoreactive resin cylinder molds. This involves making an acid base cement slurry in a HEPA filtered glove box and then pouring it into molds. The cement filled molds will be placed within a Parr vessel, which will be placed in a programmable oven and allowed to cure for several days. The oven will then be powered down and allowed to cool for 24 hours before the vessel is removed from the oven. After cooling, the vessel will be removed from the oven and opened. The cement casts will be removed from the vessel and placed in a storage container which will be sent out for prep work and testing.

Analysis Performed By and Date
Mark J. Rigali, Joseph Mohaghehi and Eduardo Basurto
Name **Date** **Review Completion Date**

SME OR SAFETY COMMITTEE CONCURRENCE (A "Yes" response requires a review by SME or Safety Committee concurrence signature or equivalent.)

No	Yes	SME	Concurrence Initials/Date	No	Yes	SME	Concurrence Initials/Date
☐	☐	Industrial Safety		☐	☐	Env. Protection	
☐	☒	Industrial Hygiene	Tracy Altrock	☐	☐	Quality Assurance	
☐	☐	Fire Protection		☐	☐	Engineering	
☐	☐	Radiation Protection		☐	☐	Safety Committee	
☐	☐	Explosives Safety		☐	☒	JSA Team Lead	Kevin McMahon
☐	☒	Other (SME/Worker)	Jessica Kruichak	☐	☐	Line Manager	
☐	☒	Other (SME/Worker)	ES&H coordinator	☐	☐	Other (SME/Worker)	

Line Manager Approval and Date
Robert MacKinnon
Printed Name/Signature **Date**

Lab Owning Manager Approval and Date
Kevin McMahon
Printed Name/Signature **Date**

ES&H Coordinator concurrence
Chuck Atwood
Printed Name/Signature **Date**

Required Job Training/Required Personal Protective Equipment
All required training in 823/B59 TWD.

Feedback, as desired

Page 2 of 3

Sequence of Basic Job Steps	Potential Hazards	Controls/PPE
➢ Within fume hood: • Place large material containers and equipment into the hood: ○ Class F fly ash bucket ○ Small re-sealable plastic bags ○ Scooper ○ Funnel • Close fume hood sash ¾ of the way • Open the Class F fly ash bucket and transfer material to the smaller re-sealable plastic bags with the use of the scooper and funnel • Reseal all containers once the transfer is complete. • Remove all containers from fume hood, label and store in designated area • Make sure fume hood lining is clean	• Could drop materials and/or fly ash container • Class F fly is fine powder and inhalation of dust should be avoided	• Wear splash goggles, acid resistant gloves, and lab • Fume hood ventilation • Eye wash station • Line the fume hood with paper or cardboard.
➢ Within fume hood: • Place large chemical containers and equipment into the hood: ○ 2.5 L glass bottle of phosphoric acid (H_3PO_4) 85% ○ 1 L of Deionized water ○ Erlenmeyer flask ○ Beaker, 2 L ○ Graduated pipette ○ Glass stirring rod ○ 1-liter polypropylene bottle ○ pH test strips • Close fume hood sash ¾ of the way • Perform a 1 L dilution of H_3PO_4 at 50% • Reseal all containers once the dilution is complete • Remove all containers from fume hood, label and store in designated area • Make sure fume hood lining is clean	• Could drop materials and/or phosphoric acid • H_3PO_4 exposure by inhalation, skin, eyes, and/or ingestion can be hazardous.	• Wear splash goggles, acid resistant gloves (compatible with H_3PO_4) and a lab apron. • Fume hood ventilation • Eye wash station • Line the fume hood with paper or cardboard • Always add acid to water (in small quantities) and never the reverse. • Acid spill clean-up kit available for spill mitigation. Read through Amphomag® "Simple Spill Cleanup Guide" step-by-step instructions provided below before handling acids: 1. Alert ▪ Communicate the presence of a spill to people in the immediate area 2. Prepare ▪ Wear appropriate PPE such as mask, googles, gloves, and acid-resistant apron ▪ Gather supplies such as a broom, plastic dust pan and Amphomag® 3. Confine ▪ Use Amphomag® to set up an absorbent barrier around the minor spill preventing the chemical from spreading 4. Neutralize and absorb ▪ Pour Amphomag® slowly and directly onto the spill to contain and neutralize ▪ Amphomag® will initially turn red to indicate an acid or blue to indicate the spill is a baseabsorb the spill and reduce harmful vapors ▪ Continue to add Amphomag® until the spilled material turns a yellow/green color to indicate it is fully neutralized. **NOTE: Reactions with acids and some aqueous solutions will generate some heat** 5. Dispose ▪ Sweep up neutralized material with a broom and plastic dust pan ▪ Properly dispose of materials 6. Sanitize ▪ Ensure all traces of the chemical spill are removed from the affected area ▪ Wash spill area with soap and water or specific cleaning solvent 7. Report ▪ Communicate spill cleanup to people in the immediate area ▪ Follow established lab safety procedures to document occurrence of spill and actions taken

Sequence of Basic Job Steps	Potential Hazards	Controls/PPE
➢ Open the glove box to the lab space atmosphere ➢ Place cement forming component materials and equipment into the chamber: • Calcined/reactive alumina powder (Al2O3) • Aluminum hydroxide nucleant • Class F fly ash • Distilled water • 50% H_3PO_4 solution • Mixing bowl ➢ Reseal the chamber	• Could drop materials and/or cement container • Calcined alumina is fine powder and inhalation of dust should be avoided • Reactive alumina is fine powder and inhalation of dust should be avoided • Aluminum hydroxide can be slightly hazardous in case of skin contact (irritant), of eye contact (irritant), of ingestion, and of inhalation • Class F fly is fine powder and inhalation of dust should be avoided • H_3PO_4 exposure by inhalation, skin, eyes, and/or ingestion can be hazardous. • Spilling phosphoric acid inside glovebox.	• Wear safety glasses, acid resistant gloves (compatible with H_3PO_4) and lab apron. • Glovebox with acid resistant gloves (compatible with H_3PO_4) / HEPA filtration on its air intake and out take is a control for handling and mixing of cement component materials. • Acid spill clean-up kit will be available for spill mitigation; will work with smallest volumes of acid possible.
➢ According to a specific recipe* within the glove box, use a scale to weigh out: • X grams of alumina powder • X grams of aluminum hydroxide nucleant • X grams of fly ash • X mL of distilled water • X mL of 50% H_3PO_4 ➢ Mix dry powders in a Teflon beaker ➢ Mix water into dry powders and stir ➢ Slowly add acid to water-powder mixture ➢ Stir slowly until a cement slurry has been made ***Note: several recipes will be prepared using varying ratios of the components listed above.**	• Could spill materials inside the glove box. • When adding H_3PO_4 to the mixture, the solution may react in a vigorous exothermic reaction, releasing heat, sometimes boiling the liquid if not done correctly.	• Wear safety glasses, acid resistant gloves (compatible with H_3PO_4) and lab apron. • Glovebox with acid resistant gloves (compatible with H_3PO_4) and HEPA filtration on its air intake and out take is a control. • Always add acid to water, and never the reverse. • Acid spill clean-up kit will be available for spill mitigation; will work with smallest volumes of acid possible.
➢ Open the glove box to the lab atmosphere and take out the mixing bowl containing the cement slurry ➢ Leave on impeller for 5 – 10 min at 50-100% speed after work in glove box. This is done to purge the interior of any contaminants. ➢ Make sure to close the chamber after taking out the bowl.	• Could drop the mixing bowl. Might spill some loose powder. • Could drop the mixing bowl. Might spill some unmixed acid at low pH.	• Wear safety glasses, acid resistant gloves (compatible with H_3PO_4) and lab apron. • Make sure all contents in the bowl are mixed thoroughly before taking the bowl out of the glove box. • Acid spill clean-up kit will be available for spill mitigation.
➢ Within fume hood: • Take the bowl to the Kitchen Aid mixer and mix the slurry at speed one for one minute and then at speed two for another minute. • The cement slurry is now ready to be poured into the mold(s)	• Some of the cement slurry may drip out of the bowl and onto the fume hood.	• Wear safety glasses, acid resistant gloves (compatible with H_3PO_4) and lab apron. • Acid spill clean-up kit will be available for spill mitigation. • Line the fume hood with paper or cardboard.

Sequence of Basic Job Steps	Potential Hazards	Controls/PPE
➢ Within fume hood, using a funnel, fill the mold(s) to ~1/2 inch of the top with the cement slurry	• Some cement slurry could drip out of the mold(s) and onto the fume hood.	• Wear safety glasses, acid resistant gloves (compatible with H_3PO_4) and lab apron. • Acid spill clean-up kit will be available for spill mitigation. • Line the fume hood with paper or cardboard.
➢ Within fume hood: • Place mold(s) into the Parr pressure vessel • Make sure the vessel is securely sealed	• Could drop mold(s) or vessel • If vessel is not correctly sealed it will not pressurize	• Wear safety glasses, acid resistant gloves (compatible with H_3PO_4) and lab apron. • PSDP has been done for this operation
➢ Oven – located outside of fume hood on work bench • Open oven door and place vessel on the rack in a vertical position. • Close the oven door • Set the oven temperature to 150℃ for 1hour ➢ Place warning sign on oven stating it is currently in use and hot.	• Vessel might tilt and fall inside the oven if not placed correctly thus possibly causing cement slurry to spill from within • Temperature might be set incorrectly • Cure time might be set incorrectly • Burn from oven heat	• Wear safety glasses, acid resistant gloves (compatible with H_3PO_4) and lab apron. • Vessel base holder • Vessel MAWP Rating: 3000 psi at up to 350℃ • Vessel safety rupture disc of Alloy C276, rated to 3000 psi • Oven temperature range of 20℃ to 300℃ • PSDP • Hot temperature gloves and signage
➢ Within fume hood: • Rinse mixing bowl and funnel with distilled water and collect effluent for proper disposal	• Spilling low pH effluent within the fume hood.	• Wear safety glasses, acid resistant gloves (compatible with H_3PO_4) and lab apron. • Acid spill clean-up kit will be available for spill mitigation. • ENV112- required to learn the steps to dispose of hazardous waste
➢ After 1 hour, power oven off and leave samples to cool for 24 hours	• Oven might be left on and not allowed to cool	• Wear safety glasses, oven mitts, and lab apron. • Double check oven is turned off
➢ After 24 hours of cool time, remove vessel from oven ➢ Open vessel and remove molds	• Samples may still be warm • Vessel might be dropped	• Wear safety glasses, oven mitts, and lab apron. • Make sure to hold vessel with both hands
➢ Place cement casts in storage container.	• May drop core or sample container.	• Wear safety glasses, acid resistant gloves (compatible with H_3PO_4) and lab apron.